Development of sulfonated carbon catalysts for integrated biodiesel production

by

Jidon Adrian Bin Janaun

M.Sc. in Chemical Engineering, Universiti Malaysia Sabah, 2001
B.Eng. in Chemical and Process Engineering, Universiti Kebangsaan Malaysia, 1997

A thesis submitted in partial fulfillment of the requirement for the degree of

Doctor of Philosophy

in
THE FACULTY OF GRADUATE STUDIES
(Chemical and Biological Engineering)

The University of British Columbia
(Vancouver)

August 2012

Abstract

The issues of energy security, climate change, and environmental protection attract the use of biodiesel as an alternative fuel worldwide despite several potential setbacks such as deforestation and escalating food prices. A better biodiesel production scheme is needed to reduce the setbacks, to increase the economical value, and to have a safer production process. The use of waste oil and fat as feedstock, and conversion of glycerol into fuel oxygenates are the key solutions in this scheme. Motivated by the high activity of the sugar catalyst, a low surface area and non-porous carbon-based catalyst, this study investigates the synthesis of mesoporous, high surface area and acidity carbon-based catalysts that are active for the conversion of oleic acid and glycerol into biodiesel and fuel oxygenates, respectively. The results showed that a silica templating technique, prepared via confined activation process, was effective for synthesizing mesoporous and high surface area catalyst, but low in total acidity. The technique of catalyst functionalization in liquid fuming sulfuric acid was effective, but destroyed the internal pores of the char. The activity of the mesoporous catalyst was lower than the sugar catalyst in esterification of oleic acid. The catalyst activity was dependant on the total acidity, but independent of surface area and porosity. Further investigation showed that multiple vapour phase sulfonation was effective in synthesizing higher acidity catalyst while maintaining the mesoporous and high surface area structure. Vapour phase sulfonation caused less pore destruction in the char compared with liquid phase sulfonation. Repeated vapour phase sulfonation was effective in loading increased functional groups on the catalyst at the expense of its surface area. Evaluation of the activities of carbon-based catalysts on esterification of oleic acid showed that it depended on density and accessibility of active sites, and catalyst deactivation. Evaluation of etherification of glycerol showed that all catalysts, despite having huge differences in surface area, had comparable activity per unit mass. The carbon-based catalysts had a high selectivity to di- and tri- glyceryl ethers. In conclusion, the carbon-based catalysts synthesized through multiple vapour phase sulfonation processes are promising catalysts for a better biodiesel production process.

Preface

This dissertation consists of five manuscripts which are included in Chapters 1 to 5. This doctorate work including experimental design and set-up, sample and data analysis, preparation of manuscript for publication, and preparation of the dissertation have been performed by Jidon Adrian Bin Janaun under the supervision of Professor Naoko Ellis in the Department of Chemical and Biological Engineering at the University of British Columbia. During the absence of Professor Naoko Ellis for her sabbatical leave in January to May 2011, Professor Kevin J. Smith acted as the co-supervisor. The manuscripts included in this dissertation are listed below. For manuscripts with co-authors, the contributions of Jidon Adrian Bin Janaun have been described in detail.

1. Jidon Janaun and Naoko Ellis. Perspectives on biodiesel as a sustainable fuel, *Renewable Sustainable Energy Rev.* 14 (2010), 1312–1320. A version of this manuscript is included in Chapter 1.

   The preparation and writing of the manuscript was done by Jidon Adrian Bin Janaun under direct supervision and final approval of Professor Naoko Ellis.

2. Jidon Janaun and Naoko Ellis. Role of silica template in the preparation of sulfonated mesoporous carbon catalysts, *Appl. Catal., A* 394 (2011), 25–31. A version of this manuscript is included in Chapter 2.

   The catalyst preparation and characterization, design and experimental setup, performing esterification of oleic acid with methanol experiments, sample and data analysis have been done by Jidon Adrian Bin Janaun under direct supervision of Professor Naoko Ellis. The preparation and writing of the manuscript was done by Jidon Adrian Bin Janaun under direct supervision and final approval of Professor Naoko Ellis.

3. Jidon Janaun and Naoko Ellis. Glycerol etherification by *tert*-butanol catalyzed by sulfonated carbon catalyst, *Journal of Applied Sciences* 10 (2010), 2633-2637. Sections of this manuscript are included in Chapter 5.

   The catalyst preparation and characterization, design and experimental setup, performing etherification of glycerol with *tert*-butanol experiments, sample and data analysis have been done by Jidon Adrian Bin Janaun under direct supervision of Professor Naoko Ellis. The preparation and writing of the manuscript was done by Jidon Adrian Bin Janaun under direct supervision and final approval of Professor Naoko Ellis.

4. Jidon Janaun, Naoko Ellis, and Kevin J. Smith. Controlled functionalization of amorphous carbon using multiple vapour phase sulfonation, to be submitted for publication. Sections of this manuscript are included in Chapters 3 and 4.

   The catalyst preparation and characterization, design and experimental setup, performing esterification of oleic acid with methanol experiments, sample and data analysis have been done by Jidon Adrian Bin Janaun under direct supervision of Professor Kevin J. Smith. The preparation and writing of the manuscript was done by Jidon Adrian Bin Janaun under direct supervision and final approval of Professors Naoko Ellis and Kevin J Smith.

5. Jidon Janaun, Naoko Ellis, and Kevin J. Smith. New carbon-based catalysts for esterification and etherification reactions, to be submitted for publication. Sections of this manuscript are included in Chapters 4 and 5.

   The catalyst preparation and characterization, design and experimental setup, performing esterification of oleic acid with methanol experiments and etherification of glycerol with isobutylene, sample and data analysis have been done by Jidon Adrian Bin Janaun under direct supervision of Professors Naoko Ellis and Kevin J. Smith. The preparation and writing of the manuscript was done by Jidon Adrian Bin Janaun under direct supervision and final approval of Professors Naoko Ellis and Kevin J Smith.

Table of contents

List of tables

List of figures

Nomenclature

a(t)	Catalyst deactivation activity (Dimensionless)
C	Constant (Dimensionless)
C_A	Concentration of oleic acid at any time (mol/L).
C_{AO}	Initial concentration of oleic acid (mol/L)
C_{As}	Concentration of A at the surface (mol/L)
C_G	Concentration of glycerol at any time (mol/L).
C_{GO}	Initial concentration of glycerol (mol/L),
C_{WP}	Weisz – Prater criterion (m^{-3})
C_y	Product concentration (mol/L)
D	Diameter (mm)
D^o_{AB}	Mutual diffusivity at infinite dilution of A in B (m^2/s or cm^2/s)
D_{AB}	Mutual diffusivity (m^2/s or cm^2/s)
D_e	Effective diffusivity (m^2/s)
$\triangle G^o$	Gibbs free energy of formation (kJ/mol)
H	Height (mm)
k'	Reaction constant (L^2/mol.min.g)
k	Reaction constant (min^{-1})
k_d	Deactivation constant (min^{-1})
K_e	Equilibrium constant (Dimensionless)
M_i	Molecular weight of species i (kg/kmol or g/mol)
n	Number of moles (mole)
N	Number of moles (mole)
N_{AO}	Initial number of moles of reactant A (mole)
P	Pressure (mmHg or kPa)
P_c	Critical pressure (Pa)
P_o	Saturation vapour pressure of adsorbate gas or vapour (mmHg)
P_1, P_2	Pressure (kPa)
r	Radius of the droplet (m)
r_A'	Rate of reaction (mol/g.min)
r' (obs)	Rate of reaction observed (M/s.gcat)
r_d	Rate of catalyst deactivation (min^{-1})
R	The universal constant (8.314 J/Kmol) or catalyst particle radius (m)
S_y	Selectivity (mole %)
t	Time (s)
T	Temperature (K)

T_c	Critical temperature (K)
V	Reaction volume (L) or total volume adsorbed (STP) at pressure P (cm^3)
V_A	Molar volume of A at its normal boiling point (m^3/kmol or cm^3/mol)
V_c	Cup volume (cm^3)
V_m	Molar volume (m^3/mol)
V_p	Volume of particulate sample (cm^3)
V_{pore}	Total volume of pores (cm^3/g)
V_r	Reference volume (cm^3)
W	Catalyst weight (g)
X	Conversion (%)
X_e	Equilibrium conversion (Dimensionless)
X_G	Glycerol conversion (%)
x_A	Mole fraction of component A (kmole A/kmole fluid)
β_A	$M_A^{1/2} P_c^{1/3}/T_c^{5/6}$ (Dimensionless)
γ	Surface tension (N/m)
ρ_c	Solid density of catalyst (kg/m^3)
ρ_s	Catalyst specific density (g/cm^3)
σ_c	Constriction factor (Dimensionless)
ϕ_p	Catalyst porosity (Dimensionless)
$\tilde{\tau}$	Tortuosity (Dimensionless)
μ_i	Viscosity of pure i (cP)

Abbreviations

Ar-OH	Aryl-hydroxyl
ATR	Attenuated total reflectance
B	Base catalyst
BET	Brunaeur-Emmett-Teller
BH^+	Intermediate base catalyst
BJH	Barrett-Joyner-Halenda
CMK	Mesoporous char containing silica template
CMK – w	Silica template-removed mesoporous char
CMK-SO_3H-w	A catalyst prepared by sulfonating the mesoporous char before the removal of silica template
CMK-w-SO_3H	A catalyst prepared by sulfonating the mesoporous char after the removal of silica template
CMK-3-873-SO_3H	A catalyst prepared by sulfonating the mesoporous char pyrolyzed at 873 K.
CN	Cetane number
CPS	Count per second
C_{WP}	Weisz – Prater criterion
DF	Dilution factor
DNA	Deoxyribonucleic acid
DIB	Di-isobutylene
DSC	Differential scanning calorimetry
DTA	Derivative thermal analysis
DTBGs	Di-*tert*-butylglycerol ethers
EI	Electron ionization
FAO	Food and Agriculture Organization of the United Nations
FFA	Free fatty acid
FT-IR	Fourier transform – infrared spectroscopy
GC-MS	Gas chromatography – mass spectrophotometer
GHG	Greenhouse gas
HC	Hydrocarbon
$H_4PNbW_{11}O_{40}/WO_3$-Nb_2O_5	Heteropolyacid derived catalyst
IR	Infrared
IS	Internal standard
MO	Methyl oleate
MR	Molar ratio
MSDS	Material safety data sheets

MSTFA	N-methy-N-(trimethylsilyl) trifluoroacetamide
MTBE	Methyl-*tert*-butyl ether
MTBGs	Mono-*tert*-butylglycerol ethers
MW	Molecular weight
m/z	The ration of the mass number and the charge number, z.
NaOH	Sodium hydroxide
NGO	Non-governmental organization
NO_x	NO and NO_2
ON	Octane number
PAHs	Polycyclic aromatic hydrocarbons
P.D.	Pore diameter
PM	Particulate matters
PSA	1-pyrenesulfonic acid
P/Si	Phosphoric acid to tetraethyl orthosilicate molar ratio
P.V.	Pore volume
R	Carbon chain of the fatty acids or alkyl group of the alcohol
RO^-	Active species
RSPO	The roundtable on sustainable palm oil
SA	Specific surface area
SC	Sugar catalyst
SEM	Scanning electron microscopy
Si	Silica
SO_3	Sulfur trioxide
SO_3H	Sulfonic acid
Std Err	Standard error
STO	Sulphated tin oxide
STP	Standard temperature and pressure
SZA	Sulphated zirconia-alumina
T.A.	Total acidity
TBA	*Tert*-butyl alcohol
TEM	Transmission electron microscopy
TGA	Thermo-gravimetric analysis
TGs	Triglycerides
TiO_2/ZrO_2,	Titanium dioxide/Zirconium dioxide
TTBG	Tri-*tert*-butylglycerol ether
UDR	Undersampling ratio
VPS1	A catalyst prepared by single sulfonation in vapour phase sulfonation technique

VPS2	A catalyst prepared by double sulfonation in vapour phase sulfonation technique
VPS3	A catalyst prepared by triple sulfonation in vapour phase sulfonation technique
wt.%	Weight percent
WZA	Tungstated zirconia-alumina
XPS	X-ray photoelectron spectroscopy

Acknowledgements

First and foremost, I thank God for His grace, love, and protection, without which I would not be able to complete my program and survive in a foreign land. I am also indebted to the generosity of the Government of Malaysia through the Ministry of Higher Education for providing the scholarship that covers the University Fees and living allowance, and through Universiti Malaysia Sabah, for granting me a study leave. This certainly will be my encouragement and motivation to serve my beloved country to the fullest. I am thankful to the Department of Chemical and Biological Engineering, University of British Columbia (UBC) and Canada for giving me the opportunity to gain an education in state of the art research facilities and a very conducive learning environment. I will certainly be an "ambassador" of UBC and Canada wherever I go.

I am grateful for the dedication and patience of Professor Naoko Ellis as she guided me in my research, manuscript and thesis writing. The freedom given to me to carry out all the experiments with full financial support enabled me to explore my scientific potential and trained me to be an effective independent researcher. I am also grateful for Professor Kevin J. Smith, and his effective analysis of my experimental results which enabled me to understand and go deeper in my research. His assistance goes above and beyond his role as an examination committee member. I thank Professor Jennifer Ann Love for being an effective examination committee member, and in fact the discovery of multiple vapour phase sulfonation originated from her idea of running multiple liquid phase sulfonation to increase the acidity of the catalyst.

I treasure the friendship, help, and useful discussion shared with my fellow graduate students – Farnaz Satoodeh, Masakazu Sakaguchi, Amir Mehdi Dehkhoda, Soojin Lee, Nagu Daraboina, Victoria Whiffen, Mehdi Bazri, Fahimeh Yazdanpanah, Steve Reaume, Hooman Rezaei, Xingxing Cheng, Shahin Goodarznia, Alexander Dauth and many more. Special thanks to Farnaz Satoodeh for helping on the molecule size simulation and Andrew Knight for helping on the Mastersizer analysis. Often times our discussions helped me to solve my research problems, knowing and working with you guys was a life enriching experience for me. I also thank Timothy Ma and Rob Christian for their kind assistance in GCMS analysis and troubleshooting, Dr. Ken Wong at AMPLE for XPS analysis, Dr. Mary Fletcher at the Department of Material Engineering for SEM analysis assistance, and Derrick Horne at UBC BioImaging Facility for TEM analysis. The courtesy of Igor N. Filimonov of GS Caltex Corporation, Republic of Korea for donating mono-, di- and tri- glyceryl ethers is gratefully acknowledged. I would like to thank Dana and Justin Glessner, Maria Linda Torio, and Sandeep Jadhav for doing the proofreading of my thesis draft. The comments and suggestions by anonymous reviewers for Chapter 2 are greatly appreciated.

I am indebted to the spiritual and community support provided by University Chapel, especially through the Acadia Park Home Group, that gives my family and I a sense of belonging to

the local community. This immensely helped to keep my mind peaceful and enabled me to concentrate on my research.

Last but not least, I am indebted to my beloved wife Maria Wong Janaun, for taking care of the family while I worked on my studies. Without you, I am sure to fail! I especially express my deepest love to my children – Mark, Grace, and Rick. Your understanding of my duty to study and finish my degree is a blessing from God!

Dedication

To my beloved wife, Maria and my children Mark Alysn, Alyssa Grace, and Rick Gynorie

and

in loving memory of my parents, Janaun and Ranchumi

Chapter 1 Introduction

1.1 Perspectives on biodiesel as a sustainable fuel

Biodiesel (fatty acid alkyl esters) is an alternative diesel fuel derived from the reaction of vegetable oils or lipids and alcohol with or without a catalyst. Despite the invention of the vegetable oil fuelled engine by Rudolf Diesel dating back to the early 1900s, full exploration of vegetable oil based fuel such as biodiesel only came into light in the nineteen eighties as a result of renewed interest in renewable energy sources for reducing greenhouse gas (GHG) emissions, and alleviating the depletion of fossil fuel reserves (Pahl 2008; Sorrell et al. 2010). Since then, biodiesel has penetrated the market in Europe, especially in Germany and France, as a blend to petro diesel. Commercially, these blends are named as B5, B20 or B100 to represent the volume % of biodiesel in the blend with petro diesel as 5, 20 and 100 vol.%, respectively. Currently, many countries around the world have explored and commercially used biodiesel blends for their vehicles, such as the US, Japan, Brazil, Canada, and India.

Esterification (Figure 1-1) and transesterification (Figure 1-2) reactions are currently the most favoured reaction pathways to produce biodiesel or alkyl esters. Any type of feedstock that contains free fatty acids and/or triglycerides such as vegetable oils, waste oils, animal fats, and waste greases can be converted into biodiesel. However, the final product must meet stringent quality requirements before it can be accepted as biodiesel (EN14214 for European standard; ASTM D6751 for US). The fuel properties of B5, B20, B100 and No. 2 Diesel, according to the standards, are well established in the literature (Ali and Hanna 1994; Mittelbach 1996; Altin et al. 2001; Canakci and Sanli 2008). A number of processing technologies for the production of biodiesel have been reported as the feedstock conversion depends on the type of feedstock used.

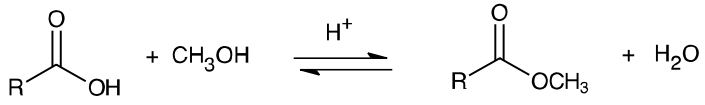

R: carbon chain of the fatty acids

Figure 1–1 Esterification reaction of free fatty acid (FFA) with methanol.

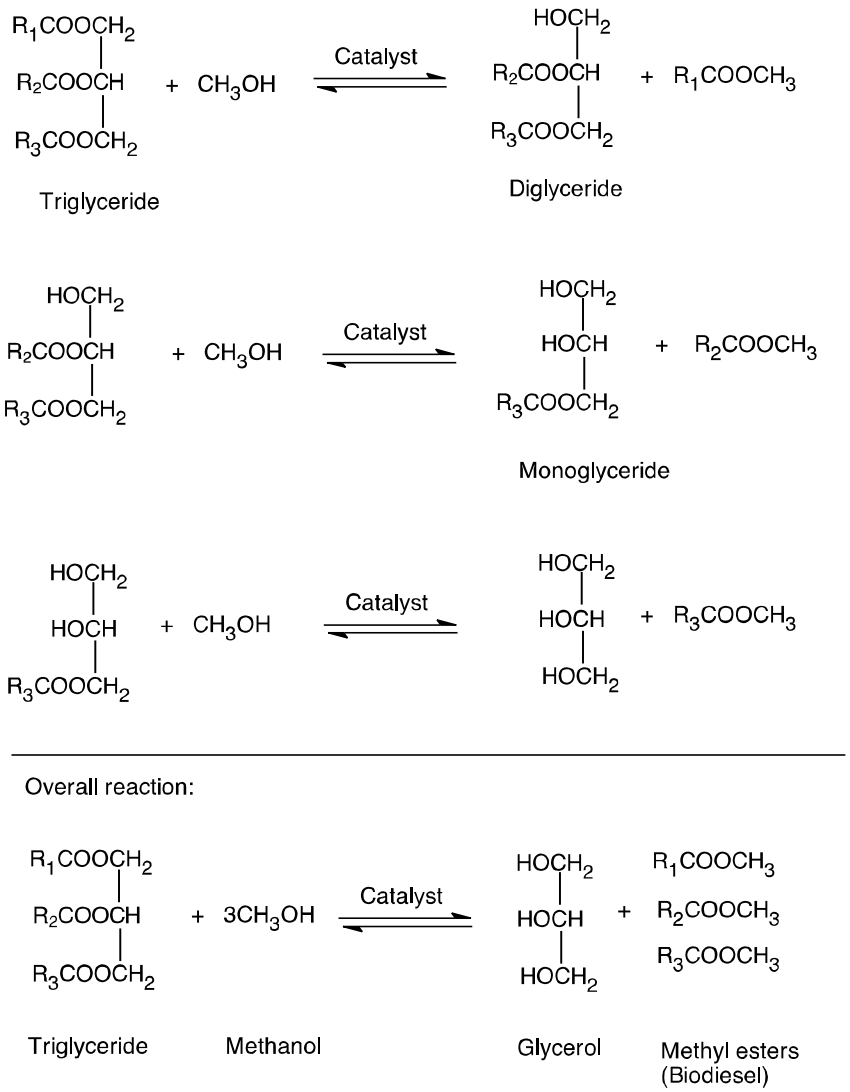

Figure 1–2 Transesterification reactions of glycerides with methanol.

While the biodiesel industry is being established in many countries, it has also been hit by the recent global economic crisis. In order to overcome the adversities of the economic background, it is critical for the biodiesel industry to continuously improve on aspects that will strengthen the prospects of better market penetration. There are numerous review papers recently published focusing on the specific issues related to production processes (Balat 2009; Fjerbaek et al. 2009; Hanna and Isom 2009; Shahid and Jamal 2011; Sharma et al. 2011; Chouhan and Sarma 2011; Santori et al. 2012), feedstock (Ju and Rayat 2009; Meher et al. 2009; Abdulla et al. 2011; Ahmad et al. 2011; Koh and Mohd. Ghazi 2011), engine testing and emission (Kalam et al. 2009; Murugesan et al. 2009; Bakeas et al. 2011; Karavalakis et al. 2011; Basha and Raja Gopal 2012), and social, economy and policy (Pinzi et al. 2009; Sharma and Singh 2009; Tan et al. 2009a; Brian J. 2011; de Gorter et al. 2011; Hassan et al. 2011; Perdiguero and Jimenez 2011; Kumar et al. 2012). In this chapter, important aspects of the biodiesel, which will strengthen the prospect as the next generation green fuel, are discussed through four major topics:

(i) cost and environmental impact of conversion processes;

(ii) efforts towards environmentally benign and cleaner emissions;

(iii) diversification of products derived from biodiesel glycerol;

(iv) policy and government incentives.

Some points require further advancement of research, while others may be controlled by regional policies. Nevertheless, these points are critically discussed in the following.

1.1.1 Cost and environmental impact of conversion process

For a sustainable future of the planet, we must look into renewable energy sources which implicitly include sustainable fuel sources. Based on the positive energy balance or life cycle analysis, biodiesel is shown to be sustainable (Kaltschmitt et al. 1997; Varanda et al. 2011). However, competition of feed source with food, and destruction of natural habitats resulting from energy crop plantation are some inevitable issues which require attention. Furthermore, various aspects in increasing the economic perspectives of the biodiesel are examined.

1.1.1.1 Efficient processes

One of the benefits of biodiesel is that it can be produced from a wide range of feedstock types, ranging from controversial neat vegetable oils to environmentally-polluting waste oils. As discussed in detail in Section 1.1.1.2, the use of neat vegetable oils as feedstock is controversial because it is associated with the increase of food prices, as well as deforestation resulting from of expansions of vegetable oil plantation. However, waste oils contains unfavourable components such as high particulates, free fatty acids (FFAs) and water content requiring a suitable pre-treatment process. Table 1-1 shows typical FFA and water contents of fresh and waste oils. Typically the pretreatment includes esterification with an acid catalyst to convert free fatty acids into biodiesel, followed by transesterification with a base catalyst to convert triglycerides into biodiesel (Gui et al. 2008). Transesterification of waste oils containing high FFAs using a base catalyst without the pretreatment would cause the formation of soap, which require a large amount of water for removing them in the product separation stage. In addition, the formation of soap also deactivates the base catalyst (Figure 1-3) (Lotero et al. 2005). For neat vegetable oils (containing less than 0.5 wt.% FFAs), the process is relatively simple using alkaline homogeneous transesterification, with conversion efficiency of more than 98% (Canakci and Sanli 2008). However, the homogeneous transesterification has disadvantages, as it consumes large amounts of water for wet washing to remove the salts produced from the neutralization process, and the residual acid or base catalyst. In spite of this, there are many companies commercializing this technology, such as MPOB, Lurgi, EsterFIP, owing to the high conversion efficiency, cost effective reactants and catalyst, and relatively lower energy use compared with the heterogeneous transesterification process (Canakci and Van Gerpen 2003; Bloch et al. 2008; Chew and Bhatia 2008). In order for this process to reduce the environmental impact, improvements on the efficiency of the washing and effluent treatment steps are warranted. There is a considerable

amount of research on dry washing which selectively absorbs impurities from the product (Shvets 2003; Bertram et al. 2005; Berrios and Skelton 2008). Investigations are focusing on finding suitable adsorbents (Anderson 2008; Sohling et al. 2008; Predojević 2008). An excellent review on biodiesel separation and purification was recently published (Atadashi et al. 2011).

Table 1-1 Typical vegetable oil properties and methyl ester yields through alkaline- and acid-catalyzed, and supercritical methanol conversion.

Raw Material	FFA content (wt.%)	Water content (wt.%)	Yields of methyl esters (wt.%)		
			Alkaline-catalyzed	Acid-Catalyzed	Supercritical methanol
Rapeseed oil	2.0	0.02	97.0	98.4	98.5
Palm oil	5.3	2.1	94.4	97.8	98.9
Frying oil	5.6	0.2	94.1	97.8	96.9
Waste palm oil	> 20.0	> 61.0	-	-	95.8

(Source: Kusdiana and Saka (2004))

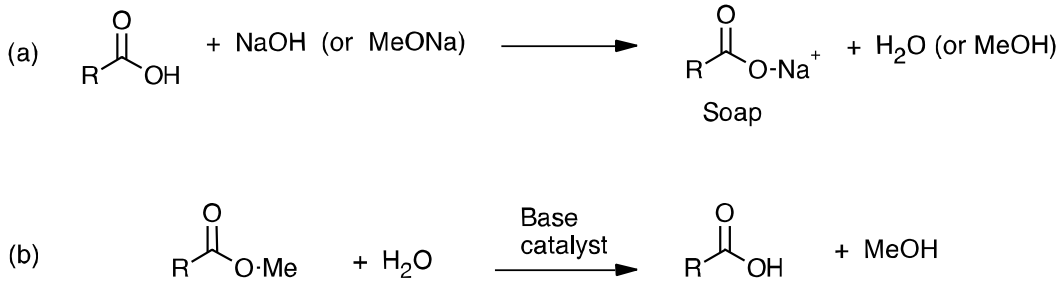

Figure 1–3 (a) Base catalyst reaction with FFAs to produce soap and water, both undesirable byproducts; (b) Water promotes the formation of FFAs. These, then, can deactivate the catalyst and produce soap, as in (a). Adapted from Lotero et al. (2005).

Concerns over the downstream processing of the homogeneous transesterification processes have motivated intense research on the heterogeneous transesterification method (Di Serio et al. 2007; Arzamendi et al. 2007; Di Serio et al. 2008; Zabeti et al. 2009; Hara 2009). In general, the heterogeneous biodiesel production processes have fewer unit operations, with simpler separation and purification steps of products as there are no neutralization steps required. In contrast, a typical homogeneous acid-catalyzed process require neutralization step, as shown in Figure 1-4 (Lotero et al. 2005). The effectiveness of the heterogeneous catalyst conversion depends on the effectiveness of the solid catalyst used (Chouhan and Sarma 2011). There are three types of solid catalysts: acid, base and enzyme. Solid base catalysts such as alkaline-earth metal hydroxide, oxides, and alkoxides like $Ca(OH)_2$, CaO, and $Ca(CH_3O)_2$ function as effective catalysts for the transesterification of triglycerides (Hara 2009). The mechanism of triglycerides (TGs) transesterification using homogeneous base and acid catalysts are shown in Figures 1-5 and 1-6, respectively (Lotero et al. 2005). The surface area and basicity determines the reactivity of the alkaline-earth metals. So far, the

catalytic activity of alkali hydroxide catalyst is found to be higher than those of the alkaline-earth metal. In addition, alkali- and alkaline earth metal cations are prone to dissolve in solvents, including biodiesel, while the base catalyst is readily poisoned by water (Hara 2009).

In general, solid base catalysts are more reactive than solid acid catalysts, requiring relatively shorter reaction time and lower reaction temperature (Hara 2009). However, solid acid catalysts have several advantages over solid base catalysts; the reaction is less affected by the presence of water and free fatty acids (Lotero et al. 2005). The main advantage of solid acid catalysts is their ability to carry out the esterification of free fatty acids and transesterification of triglycerides simultaneously (Gao 2007; Di Serio et al. 2008; Zabeti et al. 2009). Hence, a solid acid catalyst is ideal for low-quality feedstock thereby lowering the overall production costs. Low-quality feedstock, in the context of this thesis, is a term used for oils, fats or greases that contain high amount of free fatty acids, water and impurities.

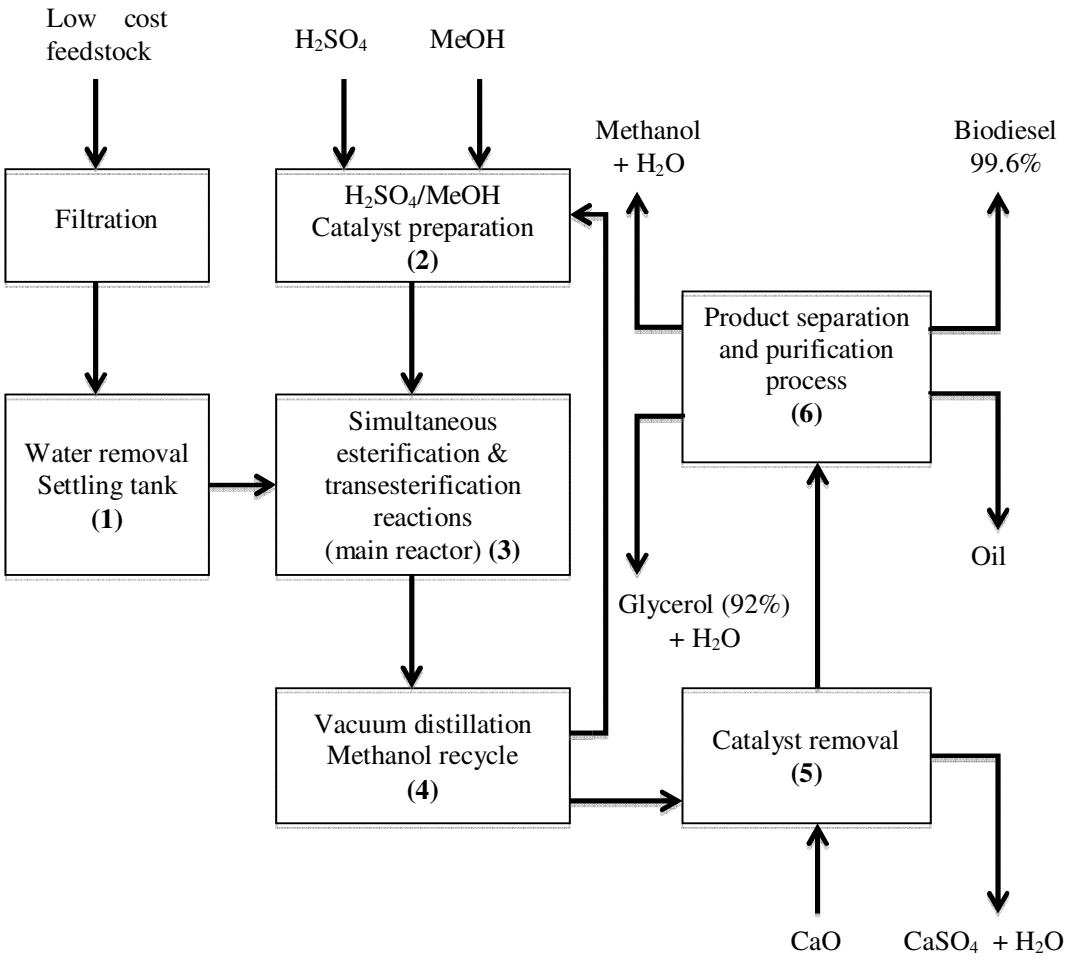

Figure 1–4 Simplified block flow diagram of the acid-catalyzed process including: (1) feedstock pretreatment; (2) catalyst preparation; (3) transesterification and esterification; (4) alcohol recycle; (5) acid catalyst removal; and (6) biodiesel separation and purification process. Adapted from Lotero et al. (2005).

Among the solid acid catalysts, tungstated zirconia-alumina (WZA), sulphated zirconia-alumina (SZA), sulphated tin oxide (STO), Amberlyst-15 (Sulfonated polystyrene-based resin), nafion NR50 (perfluorinated alkane sulfonic acid resin), and metal compounds such as TiO_2/ZrO_2, Al_2O_3/ZrO_2, ferric sulphate and ZnO are most widely studied (Di Serio et al. 2008; Hara 2009). Furuta et al. (2004) evaluated WZA, SZA, STO, TiO_2/ZrO_2, and Al_2O_3/ZrO_2 in the transesterification of soybean oil with methanol at 200 – 300°C and esterification of n-octanoic acid with methanol at 175-200°C, using a packed bed reactor. WZA shows potential as it gives high conversion in esterification and transesterification reactions and is stable at relatively higher temperature (250°C).

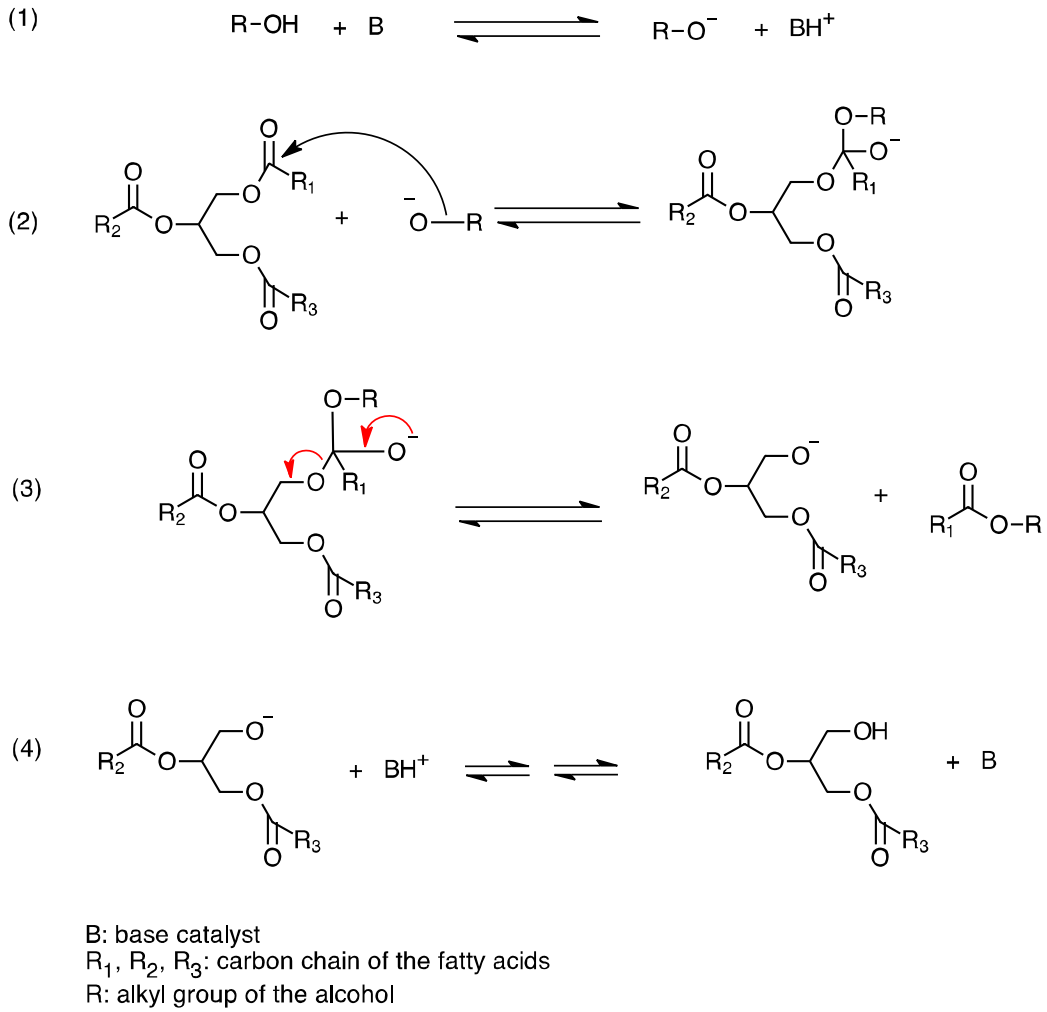

Figure 1–5 Homogeneous base-catalyzed reaction mechanism for the transesterification of TGs: (1) production of the active species, RO-; (2) nucleophilic attack of RO- to carbonyl group on TG, forming of a tetrahedral intermediate; (3) intermediate breakdown; (4) regeneration of the RO- active species. The sequence is repeated twice. Adapted from Lotero et al. (2005).

The discovery of the sugar catalyst (also known as sulfonated carbon catalyst) by Toda et al. (2005) also contributes to the development of solid acid catalysis for biodiesel production. Sugar

catalyst made from sulfonating the pyrolized sugar is inexpensive and is prepared from an environmentally benign, renewable catalyst support. It is shown to be very stable with comparable acidity to sulphuric acid, and higher catalytic activity than all the typical solid acid catalysts (Toda et al. 2005; Zong et al. 2007; Nakajima et al. 2007). Moreover, it is reactive on both esterification and transesterification reactions at relatively low temperature (i.e., 80°C). However, more trials and experiments are needed to validate the application of this catalyst. Mo et al. (2008a) have shown that the sugar catalyst is not as stable as claimed by Toda et al. (2005). Other more recently reported solid acid catalysts reactive at relatively lower temperature are $H_4PNbW_{11}O_{40}/WO_3$-Nb_2O_5, a novel heteropolyacid derived catalyst (Hara 2009), and sulfated zirconia materials functionalized by alkyl-bridged organosilica moieties (Li et al. 2011). A new promising catalyst for a fast microwave biodiesel production is reported by Jin et al. (2011). This heterogeneous catalyst, a $ZnO/La_2O_2CO_3$, has a higher reaction rate than the homogeneous KOH catalyst with the assistance of microwave irradiation. Furthermore, there are several excellent reviews on heterogeneous catalysis for biodiesel production available in the literature (Lotero et al. 2006; Sarma et al. 2008; Hara 2009; Sharma et al. 2011; Chouhan and Sarma 2011).

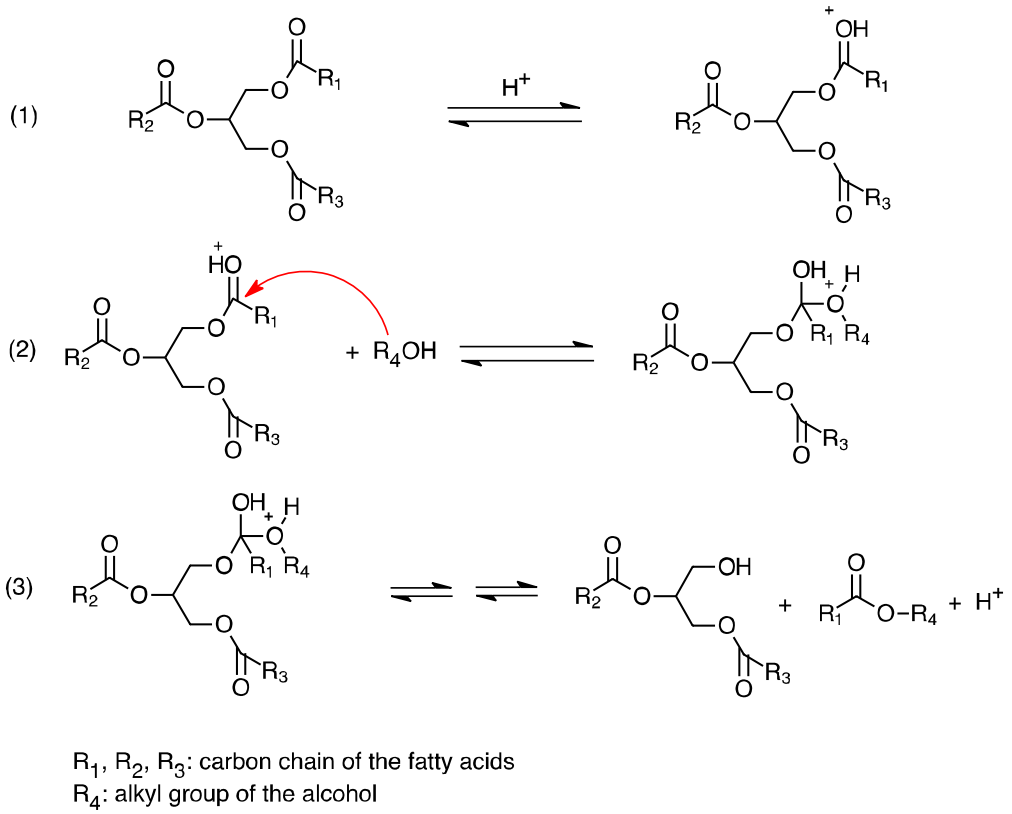

Figure 1–6 Homogeneous acid-catalyzed reaction mechanism for the transesterification of triglycerides: (1) protonation of the carbonyl group by the acid catalyst; (2) nucleophilic attack of the alcohol, forming a tetrahedral intermediate; (3) proton migration and breakdown of the intermediate. The sequence is repeated twice. Adapted from Lotero et al. (2005).

Enzyme-catalyzed transesterification is another way to achieve biodiesel production. Lipase has shown to have high catalytic activity to produce high quality biodiesel (Ognjanovic et al. 2008; Haldar and Nag 2008). Enzyme production is a renewable process, but is currently more costly than the production of conventional solid catalysts, owing to the higher cost of enzyme production requiring more complicated and high technology instrumentations (Enweremadu and Mbarawa 2009). One of the challenges in using enzymes, as a biocatalyst is its reusability as enzymes can leach out. Thus, lipase immobilized on solid material such as porous kaolinite functions as a reusable heterogeneous catalyst (Hara 2009). Another problem with the use of lipase is its deactivation by glycerol which blocks the active sites of lipase, requiring efficient product separation to maintain the activity of lipase. The use of methanol in the triglycerides transesterification catalyzed by the lipase is limited to only a maximum methanol-to-oil molar ratio of 1:1, above which it seriously inactivates the enzyme (Du et al. 2004a). Published findings show that an alternative acyl acceptor such as methyl acetate to replace methanol can attain up to 92% methyl ester yield. In addition, the by-product of triacetylglycerol has a more expansive market than glycerol, and does not deactivate the lipase (Du et al. 2004b; Parawira 2009). A recent review by Tan et al. (2010) provides an overview of the latest enzyme immobilization techniques. As a result of continuous development, a large-scale biodiesel production via enzymatic process is now feasible (Nielsen and Rancke-Madsen 2011).

Supercritical methanol is another way of making biodiesel via transesterification reaction at high temperature and pressure (e.g., 350^{o}C, 43 MPa) without any catalyst (Saka and Dadan 1999; Kusdiana and Saka 2001; Demirbas 2002). The reaction requires a very high methanol-to-oil molar ratio (42:1), but is completed in less than 4 minutes (Saka et al. 2006; Demirbas 2006; He et al. 2007). As shown in Table 1-1 (Kusdiana and Saka 2004), the supercritical methanol process can tolerate higher FFA and water contents with less reaction time compared to the alkaline- and acid-catalyzed conversion processes (Kusdiana and Saka 2003; Warabi et al. 2003; Demirbas 2007; Tan et al. 2009b). However, higher production cost due to the extreme reaction conditions, and the negative environmental impact due to the use of large amount of methanol albeit recycled, hinder the commercialization of supercritical methanol process (Enweremadu and Mbarawa 2009).

An economic comparison between different conversion methods is reported using HYSYS simulator (Zhang et al. 2003; West et al. 2008). A study by West et al. (2007) shows that for a 8000 tonne/yr biodiesel production capacity, the total manufacturing cost for pre-treated alkali-catalyzed, acid-catalyzed, heterogeneous acid-catalyzed, and supercritical using waste vegetable oil processes are US$ 5.20, US$ 4.76, US$ 3.88, and US$ 4.59 million dollars, respectively. A heterogeneous acid-catalyzed has the lowest total manufacturing cost, owing to the relatively small sizes and carbon steel construction of most of the process equipment. However, for a larger production capacity, i.e., 40,000 tonne/yr, Lee et al. (2011) also using HYSYS simulator, show a contrary result. The total manufacturing cost for alkali-catalyzed using fresh vegetable oil, alkali-catalyzed using waste vegetable oil with acid catalyzed pre-treatment, and supercritical using waste vegetable oil processes are US$ 45.8, US$ 35.0, and US$ 29.0 million dollars, respectively. Supercritical process using waste

vegetable oil as the feedstock is the most economically feasible. Nevertheless, both studies are in agreement regarding the feedstock cost being the most significant variable affecting the production cost, comprising 64–84% of the biodiesel manufacturing costs.

1.1.1.2 Feedstocks

While various biodiesel feedstocks are renewable, its competition with food source is a major concern. The increase in staple food prices may be linked with the use of edible oil for biodiesel production (FAO 2008). An interesting perspective lies in the argument that the amount of vegetable oil produced in the world can meet the demand for consumption and for consumer product (Corley 2009). However, the issue goes beyond the supply – encompassing the complex balance of the ecosystem. For instance, the mass plantation of monoculture plants could benefit the economy of rural populations while negatively affecting the water resources and the biodiversity (FAO 2008).

1.1.1.2 (a) Non-edible oil

One of the ways to reduce the dependency on edible oil to make biodiesel is to use non-edible oils, such as jatropha, castor, *Pongamia pinnata*, rubber seed, and sea mango (Gui et al. 2008). Table 1-2 shows oil yield for major non-edible oil sources, including those that have been commercialized to produce biodiesel (Gui et al. 2008). Conversion of these types of oil into biodiesel is comparable in the process and quality to other edible oils (Pinzi et al. 2009).

Table 1-2 Oil yield for major non edible oil resources.

Oil source	Oil yield (kg oil/ha)	Oil yield (wt.%)
Jatropha	1590	Seed (35 - 40); Kernel (50 - 60)
Rubber seed	80 – 120	40 – 50
Castor	1188	53
Pongamia pinnata	225 - 2250	30 – 40
Sea mango	N/A	54

(Source: Gui et al. (2008))

Jatropha curcas in particular has an extra advantage over other oil sources because it is a drought-resistant plant capable of surviving in abandoned and fallowed agricultural land (Achten et al. 2008; Achten et al. 2010). This will potentially provide extra source of income for the local farmers without sacrificing the fertile land that is used for other crops. However, further research is needed to fully commercialize jatropha oil as feedstock for biodiesel for information such as basic agronomic characteristics of *Jatropha Curcas* is still scarce (FAO 2008). The latest development in the production of biodiesel from jatropha are reported (Abdulla et al. 2011; Koh and Mohd. Ghazi 2011; Kumar et al. 2012).

1.1.1.2 (b) Algae-based biodiesel

There is a growing interest in algae-based biodiesel for its higher yield non-edible oil production, and non-competition for land with food production (Chisti 2008; Li et al. 2008; Cheng et al. 2009). Table 1-3 shows the comparison of the biodiesel production from algae and oil plants (Li et al. 2008). Algae-based biodiesel has a superior yield per hectare over conventional oil crops. This is because algae can be grown on farms or in bioreactors (Goh and Lee 2010). Studies indicate that algae for biodiesel production can grow on flue gas, giving opportunities in consuming greenhouse gas as feedstock (Vunjak-Novakovic et al. 2005; Li et al. 2008; Rhodes 2009). This gives additional benefit in reducing the carbon footprint. Furthermore, algae can be genetically modified to increase its growth rate, biomass production, and lipid content (Tabatabaei et al. 2011; Costa and de Morais 2011). The main obstacles for the commercialization of algae-based biodiesel include its high production cost from requiring high-oil-yielding algae strains and effective large-scale bioreactors, inconsistent and insufficient algal productivities, uncertain capital and operating costs, volatile market prices, and unknown levels of government support (Vasudevan and Briggs 2008; Mata et al. 2010; Brian 2011). Hence, continuous research and development is needed before algae-based biodiesel production can be fully commercialized.

Table 1-3 Comparison of biodiesel production from algae and oil plants.

	Biodiesel produced from algae	**Biodiesel produced from plants**
Technology	Cell bioengineering, automatically produced in pilot plant	Agriculture in farm
Production period	5–7 days for a batch cultivation	Several months or years
Oil content	More than 40–50% in whole cells	Less than 20 % in seeds or fruits
Land occupied	0.010–0.013 hectare for producing $1x10^3$ L oil[a]	2.24 hectare for producing $1x10^3$ L oil[b]
Cost performance	$2.4 per liter microalgal oil	$0.6–0.8 per liter plant oil
Further technical development	Unlimited (work just beginning)	Limited (many works have been done)

(Source: Li et al. (2008))

[a]Based on projected area of bioreactor in pilot plant.
[b]Based on soybean cultivation in farmland.

1.1.1.2 (c) Waste oils, grease, and animal fats

Waste vegetable oils, greases, and animal fats have been used as feedstock for biodiesel production. The use of these types of feedstock eliminates the need for disposal, and more importantly contributes to the supply of biodiesel. However, some of the major challenges, especially for waste stream feedstock, such as waste cooking oil and grease, are the collection infrastructure and logistics. For example, the collection system for the waste cooking oil could be a hurdle as the sources are generally scattered and without any quality control. The city of Kyoto has taken this challenge and reported on

producing enough biodiesel to fuel their city buses from waste vegetable oils collected from general households, restaurants and cafeterias (Takahashi 2009). A study in a city of Langkawi, Malaysia showed that an estimated 100,000 – 400,000 kg waste cooking oil can be collected annually, which could provide 1.6% of transport diesel demand in Langkawi (Kumaran et al. 2011). In certain remote or seasonal communities, it may be feasible for this type of model to work. However, further public awareness, education and acceptance become key importance for successful implementation.

Meanwhile, animal fats are more readily available as the slaughter industry is generally well managed for product control and handling procedure (Mata et al. 2011). However, there is a biosafety issue related to animal fats that could come from the contaminated animals. Future research needs for ensuring biosafety of biodiesel produced from animal waste through cradle to grave life cycle studies have been highlighted (Greene et al. 2005).

1.1.1.2 (d) Edible oil from sustainable plantation

The use of edible vegetable oil as a feedstock for biodiesel production warrants a discussion. Despite the fact that neat edible oil competes with food supply, it is the feedstock that allows the simplest conversion method. Furthermore, for many, the edible oil crop plantation has already been well established, with some crops producing high quality oil that gives highest conversion through the transesterification reaction. The central issue is the proper management on the oil supply so that oil for food consumption and for consumer products are guaranteed, with the remaining oil being converted into biodiesel. Sustainable plantation scheme includes comprehensive practices that maintain the benefits to the environment (planet), people, and profitability (Basiron 2007). To illustrate the practise of sustainable plantation, a case study is presented from the palm oil plantation in Malaysia.

1.1.1.2 (e) Sustainable plantation: A case study of palm oil plantation in Malaysia

Palm oil is currently the largest supply of edible oil in the world with Malaysia and Indonesia being the largest producers (Santosa 2008; Sumathi et al. 2008; McCarthy et al. 2011). Palm oil has dominated the world's vegetable oil demand because of its versatile applications ranging from food to consumer products, and now as biodiesel. The large supply of palm oil can be attributed to the superiority of palm oil in terms of oil yield, shown in Table 1-4 (Sumathi et al. 2008), requiring a smaller area of land to produce oil. Furthermore, palm oil has the highest fossil energy balance, i.e., energy produced over energy consumed, as defined in Table 1-5 (FAO 2008), and the lowest cost relative to other energy crops (Figure 1-7). The success of the palm oil industry in Malaysia is achieved based on the highly desirable properties of the palm oil trees, careful management by Malaysian Palm Oil Board (MPOB), and more importantly sustainable practices in palm oil farming (Basiron 2007; Sumathi et al. 2008; Lam et al. 2009).

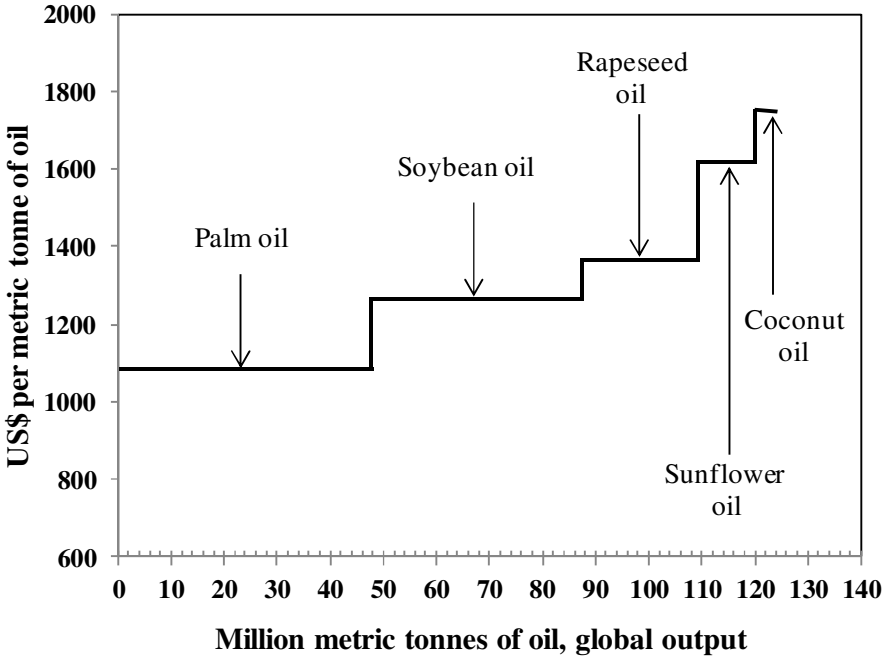

Sources:
Global oil output (United States Department of Agriculture (USDA) 2012)
Commodity prices (Index Mundi 2012)

Figure 1–7 Average cost and quantity of vegetable oil production, 2010/2011.

Table 1-4 Oil production and yield of major oil crop in the world in 2006.

Oil crop	Average oil yield (ton/Ha/yr)	Planted area (million Ha)
Soybean	0.40	94.15
Sunflower	0.46	23.91
Rapeseed	0.68	27.22
Oil Palm (mesocarp[1])	3.62	10.55

(Source: Sumathi et al. (2008))

Oil palm cultivation in Malaysia has long advocated sustainable practices. It has struck a balance between economic needs and preservation of the environment. Laws including the Protection of Wildlife Act 1972 were already in place when the industry saw a surge in planted area from the 1980s (Basiron 2007). The oil palms were originally forest species which have been domesticated to maximize the yield of their respective products. It is estimated that palm oil crop emits eight to ten times more oxygen and absorbs up to ten times more CO_2 per hectare per year compared to annual crops grown in temperate countries (Basiron 2007). In addition, while oil palm plantations never

[1] Mesocarp (a pulp) is the outer layer of palm fruit containing the palm oil in a fibrous matrix.

regain the microclimate or vegetation structure of forests, specific habitat could evolve creating a heterogeneous habitat through time (Koh and Wilcove 2007; Luskin and Potts 2011).

Table 1-5 Estimated ranges of fossil energy balance of biodiesel and diesel.

Fuel	Feedstock	Fossil energy balance (ratio)[a]
Biodiesel	Soybean	1.4 – 3.4
	Rapeseed	1.2 – 3.6
	Waste vegetable oil	4.8 – 5.8
	Palm oil	8.6 – 9.6
Diesel	Crude oil	0.8 – 0.9

(Source: FAO (2008))

[a] The fossil energy balance = [Energy contained in the fuel]/[Fossil energy used in its production]

However, there are many issues concerning the oil palm cultivation in Malaysia such as deforestation, Orangutan extinction, and peatland destruction, addressed in several publications (Chuah et al. 2006; Basiron 2007; Sumathi et al. 2008; Wicke et al. 2008; Yee et al. 2009; Lam et al. 2009). In summary, Malaysia has been practicing the use of the roundtable on sustainable palm oil (RSPO) to involve NGOs in an effort to be transparent and to maintain best management practices.

In general, palm oil derived biodiesel meets the EN14214 and D6751 standards with exception to the cold flow properties (Crabbe et al. 2001; Kalam and Masjuki 2002; May et al. 2005; Kinoshita et al. 2007). Palm oil biodiesel is typically associated with high cloud point and pour point limiting its usage in warmer climates (May et al. 2004). However, there are several treatments such as winterization, additives and blending with other oils which could alleviate the limitations (Soriano Jr. et al. 2006; Shudo et al. 2006; Liang et al. 2006; Sern et al. 2007; Sarin et al. 2007; Sarin et al. 2009).

1.1.1.3 Genetically engineered plants

Genetically engineered plants can be used to enhance the plant's oil yield (e.g., increased protein and oil content in corn), incorporate noble attributes (i.e., plants resistant to drought and diseases), and suppress undesirable properties (Sticklen 2006; Sticklen 2008; Du et al. 2008; Gressel 2008). For example, oilseed rape (canola oil) is a naturally producing methyl bromide, an ozone-depleting chemical. Suppression of the methyl bromide-producing gene was achieved by a transfer DNA disruptive insertion into the gene, resulting in plants that produced less than 1% the amount of methyl bromide as the wild type (Rhew et al. 2003). This field is expected to grow in achieving sustainable biodiesel or biofuel production, especially to create new bioenergy crops that are not associated with food crops. Examples of such crops are poplar, switchgrass, miscanthus and big bluestem which are considered to have energetic, economic and environmental advantages over food crops (Stewart 2007). However, precaution on biosafety must always be considered for genetically engineered crops (Gressel 2008).

1.1.2 Cleaner emissions

One of the attractions to biodiesel is its biodegradability and being more environmentally benign than fossil fuels, resulting in less environmental impact upon accidental release to the environment. However, as a vehicular fuel, there are numerous studies on the safety, health and environmental effects of biodiesel emissions (Gaffney and Marley 2009; Huo et al. 2009; Karavalakis et al. 2009; Liu et al. 2009; MacPherson et al. 2009).

Five methyl ester biodiesel samples (palm oil, soybean, rapeseed, cottonseed, and waste cooking oil methyl esters) were run on a Cummins ISBe6 direct injection engine, comparable with the Euro III diesel engine standards, and tested for emissions (Wu et al. 2009). Results are comparable to previous studies (Chincholkar et al. 2005; Lapuerta et al. 2008) showing the reductions in particulate matter ranging from 53 to 69%; dry soot ranging from 79 to 83%; hydrocarbons ranging from 45 to 67%; and carbon monoxide ranging from 4 to 16% compared to petroleum diesel. However, nitric oxides (NO_x) show slight increase ranging from 10 to 23%. Reasons for the variations of the emission performance of each methyl ester are associated with the oxygen content and viscosity of the methyl esters, resulting from the properties of the feedstock.

There are many efforts in further improving the quality of emissions from biodiesel-containing fuels. Blending biodiesel, ethanol, and diesel known as diesterol has been investigated (Shi et al. 2005; Chen et al. 2008; Rahimi et al. 2009). Ethanol works as a fuel oxygenate – to increase the oxygen content, which is desirable to increase the Octane Number[2] of the fuels; however, addition of ethanol reduces the heat content (gross heat content of ethanol, diesel (No. 2), and methyl soyate are 27.0, 42.5, and 38.0 MJ/kg, respectively) (Shi et al. 2005; Chen et al. 2008). Addition of biodiesel compensates the heating value loss due to the addition of ethanol, and increases the fuel stability and the cold flow properties (Shi et al. 2005; Rahimi et al. 2009). In general, the torque of engine almost reduces linearly with the addition of ethanol to diesel fuel due to the low heating value of the ethanol. Biodiesel-ethanol-diesel blends reduce smoke and PM significantly, while NO_x remain the same or slightly increased. Nevertheless, the reductions of HC and CO emissions vary with the operating conditions.

Lin et al.(2008) reported the use of emulsified biosolution – biodiesel/diesel blends to increase energy saving and to reduce pollution from diesel engines. The biosolution is prepared from natural organic enzyme-7F (96.5 wt.%) and water (3.5 wt.%), a blend that is stabilized with surfactant, and results in reduction of PM and polycyclic aromatic hydrocarbons (PAHs) emissions from diesel engines compared to diesel and biodiesel-diesel blends. Further investigations are required, especially on the economics of using enzymes.

[2] Octane number (ON) is a rating for gasoline, where higher values of ON indicate greater resistance to autoignition and therefore lower potential to experience engine knock. Whereas, diesel fuel ignition is rated by its cetane number (CN), where fuels with higher values of CN ignite more readily than fuels with lower CN values (Westbrook et al. 2011).

It is known that fuel oxygenates reduce hazardous emissions from diesel engines. Jaecker-Voirol et al. (2008) reported an emission performance test for various biodiesel formulations including di- and tri-glyceryl ethers-biodiesel blends releasing less regulated and toxic air pollutants compared with biodiesel alone. The detailed mechanism as to why the di- and tri-glyceryl ethers-biodiesel blends have better emission quality, however, is not clearly understood. Glycerol has long been known to produce mono-, di-, and tri-*tert*-butylglycerol ethers via etherification reaction using isobutylene or *tert*-butanol in the presence of solid acid catalyst such as Amberlyst-15 (Klepacova et al. 2003; 2005; 2006; 2007). Blending di-, and tri-*tert*-butylglycerol ethers with biodiesel improve the cloud point and pour point of biodiesel (Noureddini 2001). Moreover, they can replace the banned methyl *tert*-butyl ether (MTBE) as fuel oxygenates. MTBE was found to be recalcitrant and harmful to humans (Mehlman 1995; Borak et al. 1998; Ahmed 2001; Mehlman 2002), and has been fully banned as fuel oxygenate in the US since 2006 due to contamination in the surface and ground waters (Siminiceanu 2007). However, the use of isobutylene to produce di- and tri-glyceryl ethers from glycerol needs further research as isobutylene is expensive, as is currently made from non-renewable source and requires high pressure for the glycerol etherification reaction. Several other fuel additives as fuel oxygenates have been reported such as dimethoxymethane, butyl methyl ether, 1,2-dimethoxyethane, 2-methoxyethyl acetate, 2-ethoxyethyl acetate, and diethylene glycol dimethyl ether (Bruno et al. 2011).

A recent study by Theinnoi et al. (2012) showed that emissions can be reduced by the diesel particulate filter via addition of H_2 with a diesel oxidation catalyst. A H_2-assisted diesel oxidation catalyst upstream of the diesel particulate filter improved the regeneration activity by promoting the oxidation of the engine-out NO into NO_x. However, further investigation needs to be done to understand the actual function of H_2 over the diesel oxidation catalyst and its ability to promote the NO-NO_x oxidation reaction.

1.1.3 Diversification of products derived from biodiesel glycerol

With the increase in biodiesel production world-wide, the market saturation of glycerol, a by-product of biodiesel production, is inevitable (Johnson and Taconi 2007). Besides the application to produce glyceryl ethers discussed previously, there are many other applications for use of crude glycerol as listed below, albeit not exhaustive:

(i) Catalytic conversion: Propylene glycol, propionic acid, acrylic acid, propanol, acrolein, propanediol, etc. (Holser 2008; Zheng et al. 2008; Zhou et al. 2008).

(ii) Biological conversion: Citric acid, sophorolipids, 1,3-propanediol, etc. (Bergman et al. 2008; Goetsch et al. 2008; Gu et al. 2008).

(iii) Fuel oxygenates: Acetal (2,2-dimethyl-1,3-dioxolan-4-yl) (Garcia et al. 2008).

(iv) Production of H_2 and syngas via steam gasification of glycerol (Iriondo et al. 2006; Adhikari et al. 2008).

(v) As carbon source for bioreactors treating Acid Mine Drainage (Zamzow et al. 2006).

(vi) Agricultural usage: Broiler feed (Cerrate et al. 2006); pig feed (Della Casa et al. 2009).

1.1.4 Policy and government incentives

The energy policy may include international treaties, legislation on commercial energy activities (trading, transport, storage, etc.), incentives for investment, guidelines for energy production, conversion, and use (efficiency and emission standards), taxation and other public techniques, energy-related research and development, energy economy, general international trade agreements and marketing energy diversity (Demirbas 2009). Globally, current energy policies reflect environmental issues including developing environmentally friendly technologies, and increasing energy security and clean energy supplies (Hammond et al. 2008; Monni and Raes 2008; Hoekman 2009; Sawyer 2009). In targeting reductions in GHGs, EU, Brazil, Canada and others have mandated the use of biofuels in recent years (Mabee 2007; FAO 2008). For instance, the establishment of the Directive on the promotion of the use of biofuels for transport in the EU (Directive 2003/30/EC) mandates an increasing share of biofuels from 2% of total fuel supply in 2005 to 5.75% of total supply in 2010 (based on energy content) (Mabee 2007). The implementation of this directive triggers a huge demand for biodiesel, not to mention the target by other large countries like the US and Canada. This type of policy is crucial for the establishment of the biodiesel industry. However, the target of 2% by 2005 was not achieved in all EU countries, and the share of biofuels in fuel consumption amounted to 1.06% in 2005 in the EU-27 and to 2.6% in 2007. Only Germany and Sweden exceeded the 2005 target with 3.86% and 2.11% biofuels use in total fuel consumption, respectively (Ziolkowska et al. 2010). Despite a steady increase in biofuels consumption, and stagnate use of fossil fuels, the EU did not achieve its Directive 2003/30 target in 2010 (Flach et al. 2011).

Government incentives play an important role in sustaining the biodiesel industry especially during the economic crisis. There are many incentives that can be offered by a government to spur the industry and maintain its sustainability, such as crop plantation in abandoned and fallowed agricultural lands, and lands that currently sequester little carbon, and subsidies such as discounted soil fertilizers and financial aid to the local farmers (Wassell Jr. and Dittmer 2006; Ewing and Msangi 2009). Incentives can be in the form of improved water management and conservation practices, or to compensate the financial disadvantages if compared with the cultivation of good agricultural land. Implementation of carbon tax that rewards the use of renewable fuels including biodiesel and its blends (i.e., less tax or tax free fuel) over fossil diesel can catalyze the biodiesel industry (Kahn and Franceschi 2006; de Gorter et al. 2011).

One of the issues that can inhibit the development of the biodiesel industry is the various levels of commitment from the global community towards the reduction of GHG emissions, especially during the economic recession. As the GHG emission is closely related to the industrial activity of a country, not all countries agree on the target to reduce their GHGs emissions. There must be a mechanism to encourage wider participation of the global community, such as flexible GHGs

emissions reduction target, to cultivate a ground which will further promote the use of renewable fuels (Patz et al. 2007).

1.1.5 Conclusions

Biodiesel is gradually gaining acceptance in the market as an environmentally friendly alternative diesel fuel. However, for biodiesel to establish and continue to mature in the market, various aspects must be examined and overcome. Some of the key issues such as improving the efficiency of the production process, using low cost feedstock, developing cost effective catalysts, and managing agricultural land have been reviewed. As with any new technology or products, biodiesel will require continuous production efficiency and market penetration especially in producing cleaner emissions and having less impact on the environment. Further development on the use of the by-product will enhance the economic viability of the overall biodiesel production process. Finally, the incentives posed by the government resulting in the promotion of the biodiesel production and usage will assist in establishing biodiesel as a renewable, alternative fuel.

1.2 Research motivation

As discussed earlier, two ways to improve biodiesel processes are through the effective conversions of free fatty acids and triglycerides into fatty acid alkyl esters, and efficient conversion of glycerol into fuel oxygenates. These improvements may be achieved with an effective solid acid catalyst.

The discovery of sugar catalyst, a carbon-based catalyst, discussed previously, paves the way for the development of effective solid acid catalyst. Sugar catalyst can potentially be a substitute for sulfuric acid as the catalyst in the esterification and transesterification of waste oil. Hence, further improvement of the carbon-based catalyst would potentially contribute to the improvement of biodiesel processes. Carbon-based solid acid catalyst has many advantages including renewable carbon precursors, inexpensive, and a well-researched material. Therefore, the ability to enhance the surface area, porosity, and total acidity of the sugar catalyst allows a deeper understanding on the carbon-based catalyst catalytic performance with respect to its physical structure and chemical functionalization.

Hence, the aim of this study is to develop effective carbon-based catalysts for esterification of free fatty acids, and etherification of glycerol reactions.

1.3 Hypothesis and research objectives

The hypothesis of this study is that a catalyst with higher surface area, mesoporosity, and total acidity may performs better compared to non-porous sugar catalyst with low surface area towards esterification, transesterification and etherification reactions. Since sugar catalyst is nonporous and has a very low surface area, enhancement of its surface area and porosity is anticipated to increase its catalytic activity and applicability to a wider reaction.

In order to prove these hypotheses, this study is carried out to achieve the following objectives:

1. To synthesize a high surface area, mesoporous, and high acidity carbon-based catalyst.

2. To characterize the carbon-based catalyst, chemically and physically.
3. To evaluate the catalytic activity of the carbon-based catalyst for the esterification of oleic acid, and the etherification of glycerol reactions.

Chapter 2 Role of silica template in the preparation of sulfonated mesoporous carbon catalysts

2.1 Introduction

Since the discovery of sugar catalyst (Toda et al. 2005), also known as sulfonated carbon catalyst (Mo et al. 2008a), the progress of carbon-based catalyst development has increased rapidly especially for biodiesel production. An acid sugar catalyst is prepared by incomplete carbonization of sugar, followed by sulfonation. The resulting catalyst has the activity comparable to sulfuric acid in esterification of oleic acid (Nakajima et al. 2007), and is more active than sulfated zirconia, Amberlyst-15 and niobic acid in transesterification of waste vegetable oil (Zong et al. 2007).

Carbon-based catalysts have several advantages as solid catalysts because of the unique properties of carbon possessing sp, sp^2 and sp^3 hybridized atoms resulting in the ability to make different structures, such as layers, tubes and spheres. Carbon can be in amorphous to crystalline structures – easily functionalized especially in the amorphous form. Furthermore, it can be activated to produce high surface area and large porosity material with hydrophobic surface – an important property especially for functional group such as sulfonic acid as it is easily deactivated by water. Because of these advantages, research using carbon as a catalyst has increased: renewable and inexpensive carbon precursors based on sugars (Toda et al. 2005; Budarin et al. 2006; Budarin et al. 2007), wood (Kitano et al. 2009), vegetable oil asphalt (Shu et al. 2009), glycerol (Prabhavathi Devi et al. 2009); carbon composites (Mo et al. 2008b; Liu et al. 2009), as a solid basic catalysts (Villa et al. 2009); as sulfonated-multiwalled carbon nanotubes (Shu et al. 2009); and as ordered mesoporous catalysts (Tanaka et al. 2005; Wang et al. 2007; Xing et al. 2007a; Liu et al. 2008; Peng et al. 2010).

Considerable attention has been directed towards synthesizing mesoporous and high surface area carbon-based catalysts owing to their potential for higher activity and wider application compared with the low surface area sugar catalyst (Liu et al. 2008; Liu et al. 2009; Peng et al. 2010). Several methods have been reported to synthesize sulfonated mesoporous carbon such as the use of silica template (Xing et al. 2007b; Peng et al. 2010), and chemical activation (Kitano et al. 2009). Silica template is a popular approach because of its tunable porosity. Researchers reported the similar observation that silica template prevented the internal porosity from collapsing during the sulfonation process (Xing et al. 2007b; Peng et al. 2010). However, there are no data reported on the activity of the internal porosity-collapsed catalysts. This leaves a gap in understanding the role of the silica template during the sulfonation step. As a result, the effects of the surface area, pore size, total acidity, and density of SO_3H groups on the activity of a carbon-based catalyst are not well understood. In addition, previous papers overlook the relative importance of surface area vs. acidity on the activity of the carbon-based catalysts.

In this chapter, mesoporous carbon catalysts preparation using the silica templating method via the confined activation process is presented. Moreover, the role of the silica template on the effectiveness of sulfonation process in the synthesis of mesoporous carbon catalysts is investigated. The resulting catalyst characterized by the surface area, porosity, total acidity, and sulfur content is tested for the activity on esterification of oleic acid.

2.2 Experimental

2.2.1 Preparation of carbon-based catalysts

The sugar catalyst was prepared according to the procedure reported by Toda et al. (2005). Mesoporous carbon was prepared with modification to the confined activation process (Hu et al. 2006). A typical confined activation process consists of three preparation steps: (1) the formation of silica/sucrose nanocomposites that contain phosphoric acid, an activation agent often used in the production of commercial activated carbons; (2) carbonization of the nanocomposites in an inert atmosphere; and (3) dissolution of the silica/phosphoric templates (Hu et al. 2006). The modification done in this study consisted of the use of D-glucose as carbon precursor with the molar ratio of phosphoric acid to tetraethyl orthosilicate (P/Si) as 0.31 and the pyrolysis temperature of 400^{o}C under nitrogen for 4 h. The use of D-glucose and the pyrolysis temperature of 400^{o}C were to produce incomplete carbonized carbon, a core material in the preparation of the sugar catalyst. The resultant black solids were ground using a mortar and pestle and then sieved to contain < 250 μm size particles. The particles were then divided into two: one was washed with 20 wt.% HF and deionized water to remove silica and phosphoric components, followed by sulfonation with the loading of 323 mmol fuming sulfuric acid (20 wt.% free SO_3) in 1 g washed char at 150^{o}C under nitrogen for 15 h - denoted as CMK-w-SO_3H; and the other half was sulfonated (similar procedure to the preparation of CMK-w-SO_3H), followed by the removal of silica and phosphoric components - denoted as CMK-SO_3H-w, where 'CMK' refers to the mesoporous char, 'w' refers to the removal of silica template step, and 'SO_3H' refers to the acid functionalization. The removal of the silica template was confirmed by X-ray Photoelectron Spectroscopy (XPS) analysis, and the final CMK-SO_3H-w and CMK-w-SO_3H were washed repeatedly with hot distilled water until the pH of the washed water became neutral and no sulfur ion was detected (Details of the procedure for sulfate ions detection are given in Appendix **A.1**). The catalysts were dried in an oven at 110^{o}C overnight and stored in a desiccator until use. Sugar catalyst, CMK-w-SO_3H, and CMK-SO_3H-w are all referred to as carbon-based catalysts.

2.2.2 Characterization of the carbon-based catalysts

The specific surface area, pore size, and pore size distribution of the samples were analyzed based on the nitrogen adsorption isotherm measured at -196^{o}C using a Porosimeter Micromeritics ASAP2020. Samples were degassed at 120^{o}C for 3 h prior to analysis (Details of the procedure are given in Appendix **A.2**). Total acidity was measured using the acid-base back titration method on an automatic

titrator (Metrohm Titrator Model 794 titrino) (The procedure and a sample calculation are given in Appendix **A.3**). Sulfur content was determined by elemental analysis performed by Canadian Microanalytical Service Ltd. (Delta, British Columbia). The analysis of elements on the external surfaces of the samples was done using X-ray Photoelectron Spectroscopy (XPS) (Model Leybold MAX200 XPS). The X-ray was an Al K-alpha X-ray (15 kV, 20 mA emission current) with the pass energy for survey scan and narrow scans were 192 and 48 eV, respectively. (A sample calculation of SO_3H concentration is given in Appendix **A.4**). Infrared (IR) spectra were recorded using the Varian FT-IR spectrometer (3100 spectrometer) equipped with attenuated total reflectance (ATR). Approximately 10 mg of sample was used in the measurement done under ambient conditions. The FT-IR settings were: speed at 5 kHz; filter of 1.2; resolution at 4 cm^{-1}; sensitivity of 1; aperture of 0.25 cm^{-1}; undersampling ratio (UDR) of 2. The thermal stability of the carbon-based catalysts was examined on a thermo-gravimetric analyzer (TGA), an instrument that capable for simultaneous TGA/DSC (TA Instruments). In a typical thermo-gravimetric analysis, approximately 20 mg of sample was placed in a crucible and purged with nitrogen at 30°C for 30 min at the flow rate of 100 mL/min, then the heating was ramped at 10°C/min to 400°C under the flow of nitrogen at 100 mL/min.

2.2.3 Catalyst activity

The activity of the carbon-based catalysts and sulfuric acid towards esterification of oleic acid with methanol was tested in a batch reactor (STEM-OMNI Reacto Station 6100), at 80±2°C under reflux, stirred at 800 rpm. The molar ratio of methanol to oleic acid was 10 to 1, and the amount of catalyst was 7 wt.% based on oleic acid. 250 mmol of methanol, and 25 mmol of oleic acid were used as reactants. Sampling was performed at 4, 10, and 24 h into the reaction. In a typical sampling procedure, 60 µL of sample was taken from the reaction mixture, diluted with heptane, then centrifuged at 10,000 rpm for 10 min. The supernatant was then further diluted with heptane and analyzed on a GC-MS (Varian) using a VF-5ms column. The temperature program was 150°C ramped at 20°C/min to 280°C, using helium as the carrier gas with a column flow of 2 mL/min.

2.3 Results and discussion

2.3.1 Preparation of the carbon-based catalysts

The information on chemical elements on the surface of the sample was studied using X-ray photoelectron spectroscopy (XPS). XPS spectra are obtained by irradiating a material with a beam of X-rays while simultaneously measuring the kinetic energy and number of electrons that escape from the top 1 to 10 nm of the material surface. Argon gas was used to sputter the material surface. Figures 2-1 to 2-3 show the XPS analysis of the CMK char, CMK-w-SO_3H, and CMK-SO_3H-w. The main purpose of the XPS analysis is to verify the removal of the silica template used during the preparation of the carbon-based catalysts. Figure 2-1 shows the detection of P and Si at binding energies of 134 eV and 104 eV, respectively, while carbon is detected at 284 eV. This indicates that the D-glucose is

effectively carbonized at 400°C using the confined activation process. Figures 2-2 and 2-3 show no detection of Si confirming the Si template being completely removed from the samples. The detection of peak at 168 eV in Figures 2-2 and 2-3 was attributed the energy of electron ejected of S 2p orbital, this corresponds to the oxidation state of -SO_3H (Takagaki et al. 2006). Since there is only a single peak associated to S, this suggests that all S atoms are contained in SO_3H groups.

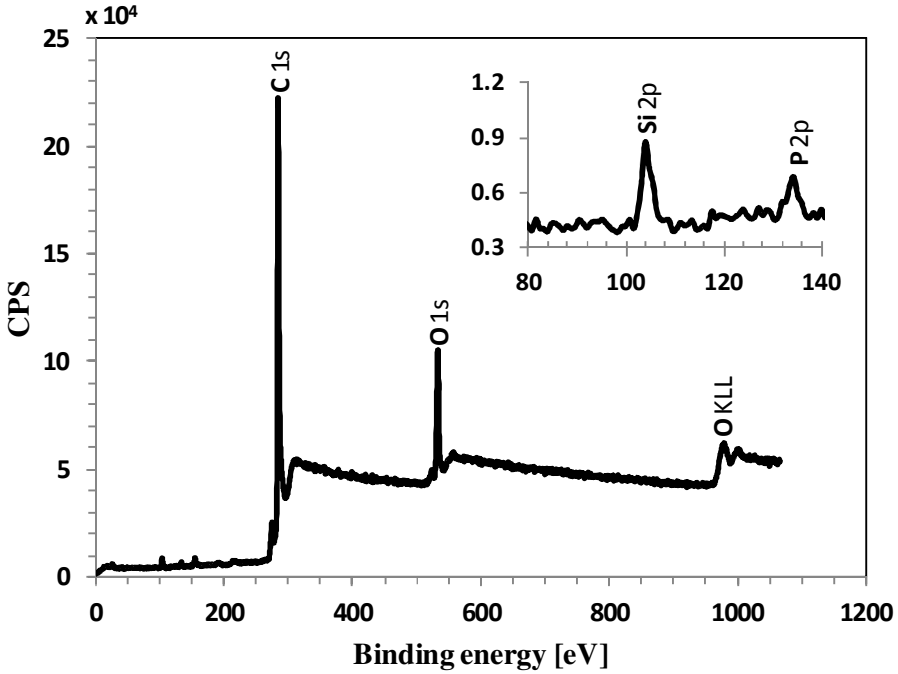

Figure 2–1 XPS analysis of CMK char.

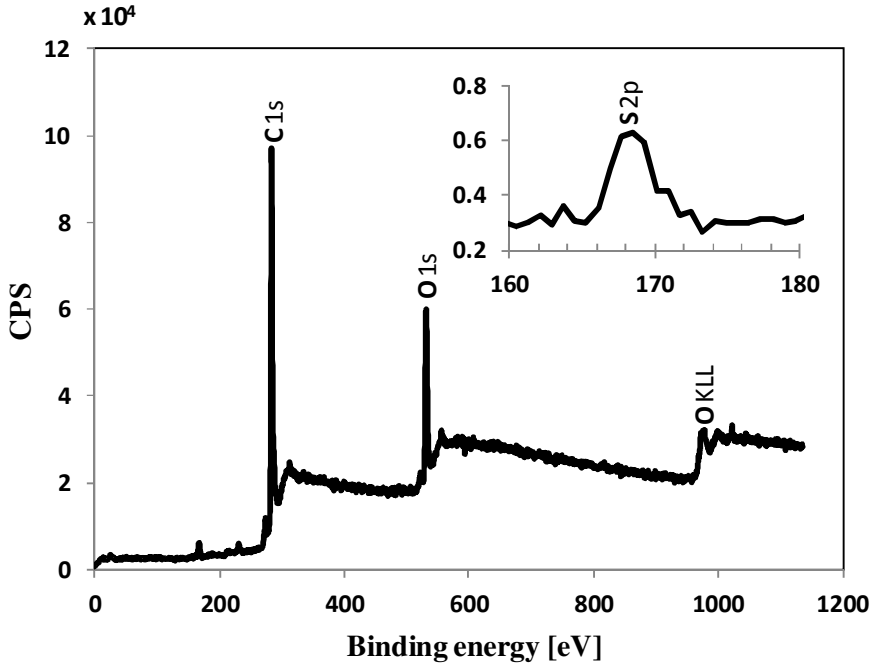

Figure 2–2 XPS analysis of CMK-w-SO_3H.

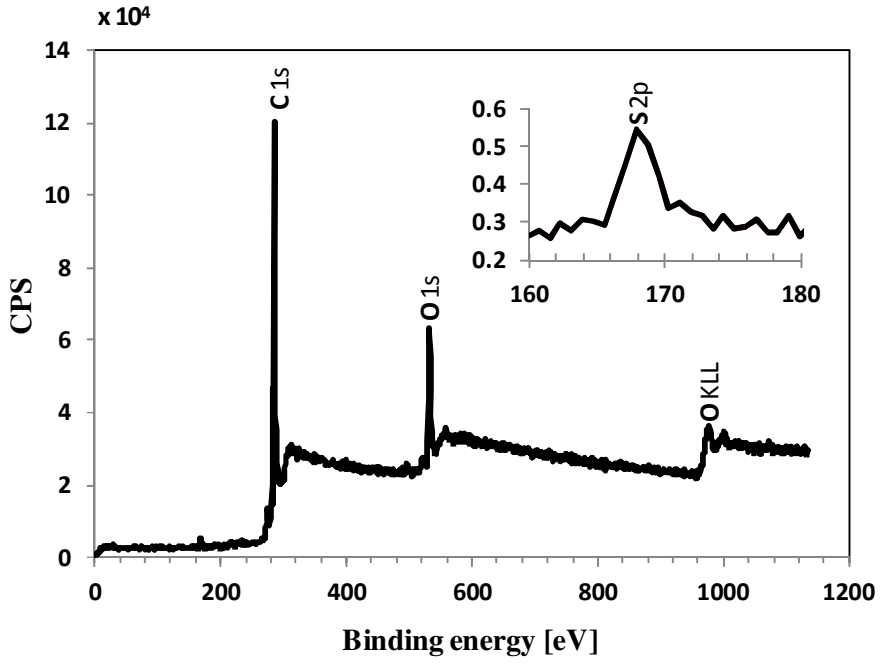

Figure 2–3 XPS analysis of CMK-SO_3H-w.

2.3.2 Characterization of the carbon-based catalysts

The particle characterization using N_2 isotherm at -196°C is a useful tool to obtain information on specific surface area, pore diameter, pore volume, and pore volume distribution. This information is essential to understand the property and the activity of the catalyst, as well as to provide guidance for catalyst design in terms of controlled surface area and pore size distribution. Specific surface area can be calculated using various equations such as single point surface area at p/p^o of 0.2, BET, Langmuir, t-Plot micropore, and t-Plot external surface area. In this thesis, the specific surface area was taken from the BET value which takes into account the multilayer adsorption as opposed to a single layer adsorption used by the Langmuir equation, and is considered to be more accurate (Brunauer et al. 1938). Pore volume was taken from the Barrett-Joyner-Halenda (BJH) desorption cumulative volume of pores between 17 and 3000 Å, while pore size was taken from the adsorption average pore width (4V/A by BET). Pore size distribution was taken from BJH desorption data. As shown in Figure 2-4, the nitrogen sorption isotherm was used to characterize the carbon-based catalysts and the silica template-removed char (CMK-w). CMK-w and CMK-SO_3H-w showed a typical type IV isotherm with significant hysteresis. CMK-w showed the highest amount of nitrogen adsorbed, reduced slightly for CMK-SO_3H-w, and a very low adsorption for CMK-w-SO_3H and sugar catalyst. The large amount of nitrogen adsorbed by CMK-w can be attributed to its high surface area as a result of the confined activation process. The sequence of sulfonation and washing (removal of the silica template) significantly affected the surface area of the char.

Sulfonation after removing the silica template as occurred in CMK-w-SO_3H caused a total destruction of the internal pores (Table 2-1), whereas the sulfonation before removing the silica

template retained 67% of the initial surface area of the char. This indicated that the sulfonation caused the internal pores to collapse; however, as a comparison, the collapse of the internal pores was minimal with silica template intact in the sample during sulfonation. This suggests that the silica template served as a barrier for the sulfuric acid from reaching the internal surface, in agreement with Xing et al. (2007b) and Peng et al. (2010). In contrast, sugar catalyst and CMK-w-SO_3H showed a very low nitrogen adsorption reflective of a non-porous material.

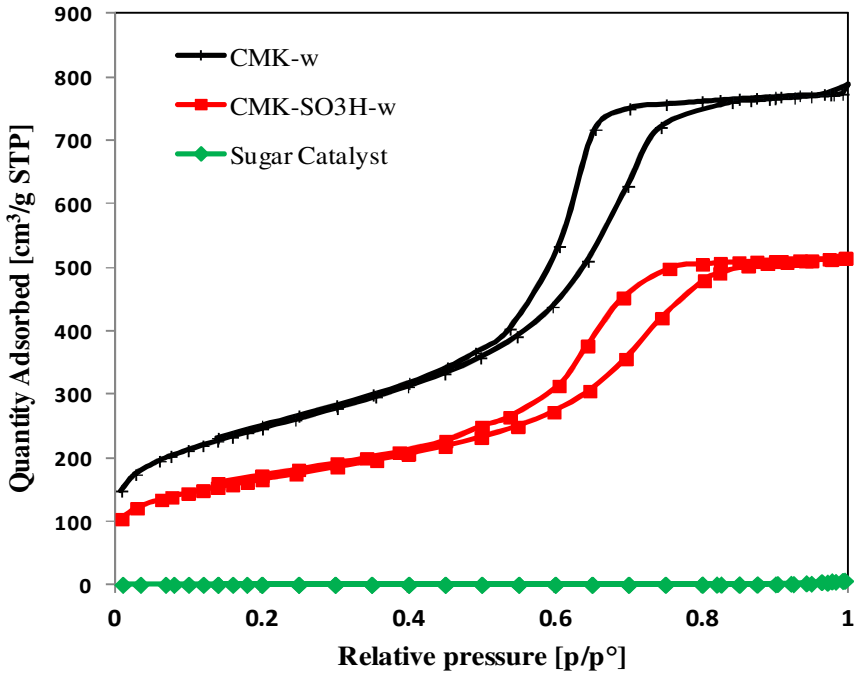

Figure 2–4 N_2 adsorption isotherms of CMK-w, CMK-SO_3H-w, and the sugar catalyst measured at -196°C. Sorption isotherm of CMK-w-SO_3H is not shown as it overlaps with the sorption isotherm of the sugar catalyst.

The porosity of the char and the carbon-based catalysts were analyzed using the Barrett-Joyner-Halenda (BJH) method, as shown in Figure 2-5. CMK-w and CMK-SO_3H-w showed mesoporous characteristics with the average pore size ranging from 4 to 7 nm (Figure 2-5). CMK-SO_3H-w indicated a bi-modal distribution of pore size. The pore volume of CMK-SO_3H-w decreased by 33% compared with the CMK-w. The reduction of pore volume and the low surface area of the CMK-w-SO_3H indicate that the internal walls of the porous char collapsed during sulfonation.

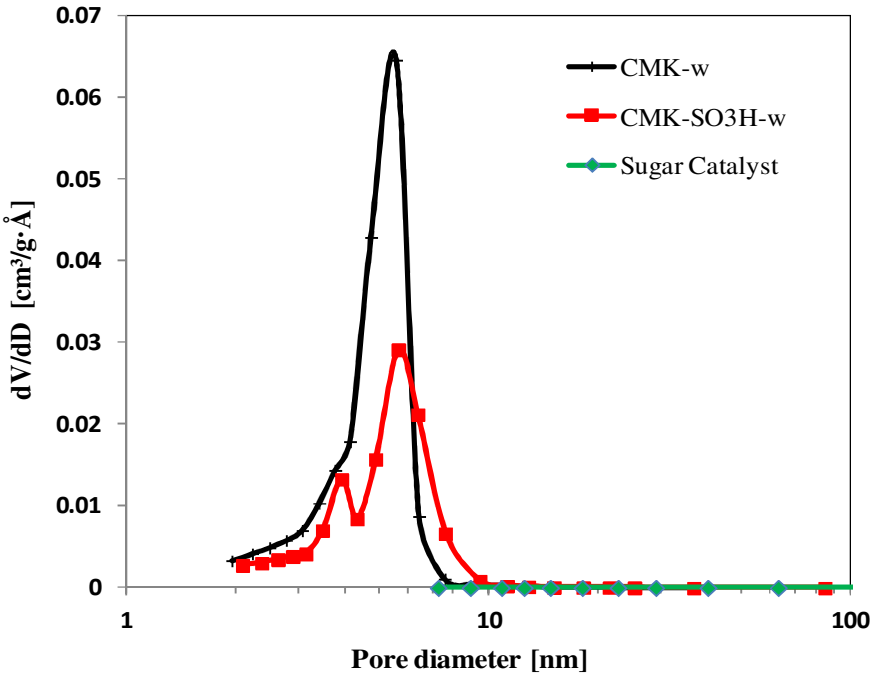

Figure 2–5 BJH (desorption) pore size distribution plots of CMK-w and the carbon-based catalysts. Porosity of CMK-w-SO_3H was undetectable.

Table 2-1 Characteristics and catalytic activity of the samples.

Catalyst	N_2 adsorption[a]			Total acidity[b]	Initial formation rate[c] based on			[MO][d],
	S.A	P.D.	P.V.	mmolg^{-1}	Weight	S.A	Acidity	mmolL^{-1}
CMK–w	880	4.8	1.24	-	-	-	-	-
CMK-w-SO_3H	<1	-	-	4.04	9.1±1.1	4.5	1.1	1550±252
CMK-SO_3H-w	588	5.3	0.83	2.52	3.4±1.2	2.9×10^{-3}	0.7	633±130
Sugar Catalyst	<1	-	-	3.89	8.1±1.4	4.0	1.0	1561±554
H_2SO_4	-	-	-	20.4[e]	11.2±1.4	-	0.3	1477±365

[a] BET surface area (S.A.) in m^2/g; pore diameter (P.D.) in nm; pore volume (P.V.) in cm^3/g.
[b] By acid-base back-titration.
[c] Calculated for the first 4 h. Unit: Weight (mM/min.gcat); Surface area (mM/min.m^2); Acidity (mM/min.mmol H^+)
[d] Average of 4-6 measurements with standard deviation.
[e] From the data of Toda et al. (2005)

The information on functional groups and the chemical structure of the sample was studied using a Fourier transform- Infrared (FT-IR) technique. FT-IR is a technique which is used to obtain an infrared spectrum of adsorption of a solid, liquid, or gas. In infrared spectroscopy, IR radiation is passed through a sample. Some of the infrared radiation is absorbed by the sample and some of it is passed through (transmitted). The resulting spectrum represents the molecular absorption and transmission, creating a molecular fingerprint of the sample. Like a fingerprint, no two unique molecular structures produce the same infrared spectrum. The measured interferogram signal can not

be interpreted directly. A means of "decoding" the individual frequencies is required. This can be accomplished via a well-known mathematical technique called the Fourier transformation. This transformation is performed by the computer which then presents the user with the desired spectral information for analysis (Thermo Nicolet Corporation 2001). The spectrum can be related to the spectra library or from the published literature to identify the functional group or structure of the sample being analyzed. As shown in Figure 2-6, the FT-IR analysis of CMK-w-SO_3H, sugar catalyst and CMK-SO_3H-w showed peaks at 1742 cm^{-1} and 1032 cm^{-1}, which can be assigned to the SO_3H groups (Takagaki et al. 2006; Nakajima et al. 2007). These peaks were also detected in CMK-SO_3H-w but weaker on 1032 cm^{-1}. All samples showed a strong band at around ~1600 cm^{-1} due to C=C stretching (Xing et al. 2007a; b). Furthermore, the broad band at 1260 cm^{-1} and the overlapping band at 1700 cm^{-1} for the carbon-based catalysts can be assigned to the aryl-hydroxyl (Ar-OH) (Kellner et al. 2004; Xing et al. 2007b; Andreas Stein et al. 2009), and carboxylic acids (Boehm 2002) stretching, respectively. The overall FT-IR analysis suggests that the carbon-based catalysts consist of polycyclic aromatic carbon sheets containing SO_3H, COOH, and OH moieties, in agreement with the published literature for acid-functionalized incomplete carbonized sugars (Toda et al. 2005; Wang et al. 2007; Peng et al. 2010).

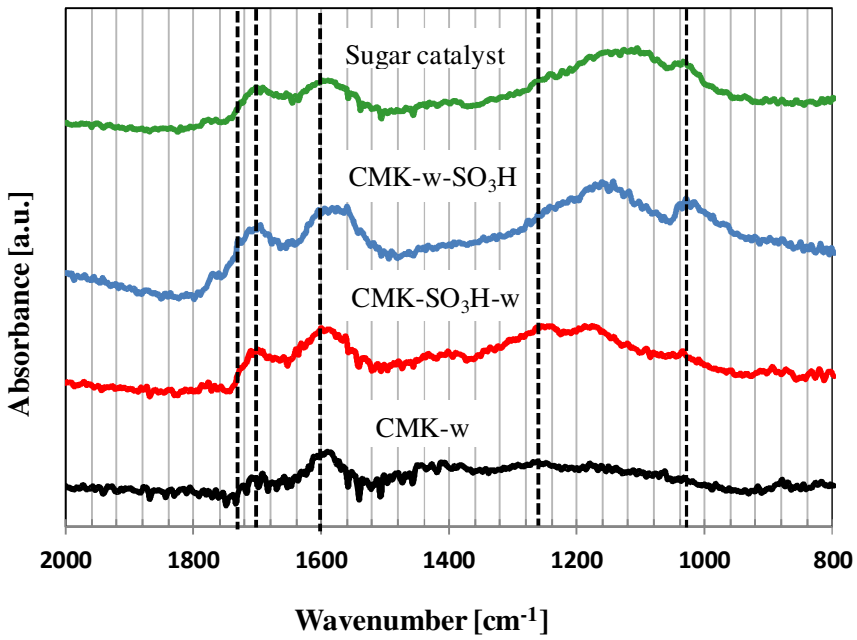

Figure 2–6 FT-IR spectra of char and the carbon-based catalysts.

The chemical composition of the carbon-based catalyst was analysed using elemental analysis technique. In contrast to the XPS technique where the elemental composition is analyzed only on the surface of the material, a chemical elemental analysis provides the elemental composition of the bulk of the material. Tables 2-2 and 2-3 show the elemental analysis and XPS studies (up to about 10 nm surface depth) of the carbon based catalysts, respectively. According to Table 2-2, the amount of C,

O, and S in CMK-w-SO_3H and sugar catalyst are relatively close. On the other hand, the ratio of O to S against C is much less in CMK-SO_3H-w. This is in agreement with the XPS analysis for CMK-w-SO_3H. These analyses, coupled with the FT-IR study, suggest that CMK-w-SO_3H and sugar catalyst consist of polycyclic aromatic carbon sheets that are higher in SO_3H, COOH, and OH functional groups, compared to CMK-SO_3H-w.

Table 2-2 Elemental analysis of the carbon-based catalysts.

Catalyst	Elemental composition (wt.%)				Ratio to C		
	C	H	O	S	H:C	O:C	S:C
CMK-w-SO_3H	57.55	1.90	33.12	4.13	0.03	0.58	0.07
CMK-SO_3H-w	70.32	2.36	19.58	1.71	0.03	0.28	0.02
Sugar catalyst	56.18	2.39	30.65	4.17	0.04	0.55	0.07

Table 2-3 XPS analysis of the CMK-w-SO_3H and CMK-SO_3H-w.

Sample	Elemental composition (wt.%)			Ratio to C	
	C	O	S	O:C	S:C
CMK-w-SO_3H	73.60	24.38	1.55	0.33	0.02
CMK-SO_3H-w	84.39	14.68	0.47	0.17	0.01

The thermal stability of the sample was investigated using a thermo-gravimetric analysis (TGA) technique. In a TGA technique, a sample is heated at the desired temperature program under a constant flow of gas. Heating under inert gas such as nitrogen enable the collection of information on the decomposition of the sample due to thermal alone; whereas, heating under air provides the decomposition due to thermal and combustion reactions. The weight loss of the carbon-based catalysts sample can be associated with the decomposition of the functional groups as well as the carbon structure. Figures 2-7 and 2-8 show the thermo-gravimetric (TGA) and the differential thermal analyses (DTA) of carbon-based catalysts under nitrogen, respectively. Weight loss at 100-115^oC is associated with the evaporation of moisture. CMK-w-SO_3H and sugar catalyst showed similar trends of decomposing at around 236 and 247^oC, respectively. This is contrary to CMK-SO_3H-w where it is thermally more stable than the CMK-w-SO_3H and sugar catalyst. This can be explained from the elemental compositions that CMK-SO_3H-w is predominant in C. CMK-SO_3H-w had a relatively higher amount of C compared with CMK-w-SO_3H possibly because during the sulfonation process, the silica template blocked the sulfuric acid from reaching to the carbon surfaces, leaving significant carbon surface unreacted with the sulfuric acid. This most likely explains why CMK-SO_3H-w had higher amount of C, but lower total acidity compared with CMK-w-SO_3H.

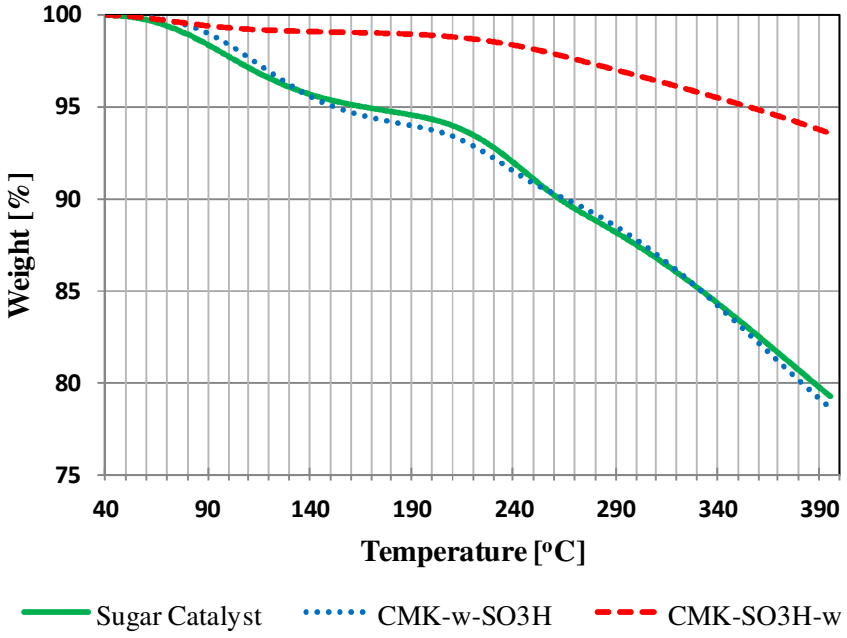

Figure 2–7 Thermo-gravimetric analysis (TGA) of the sugar catalyst, CMK-w-SO_3H, and CMK-SO_3H-w under nitrogen.

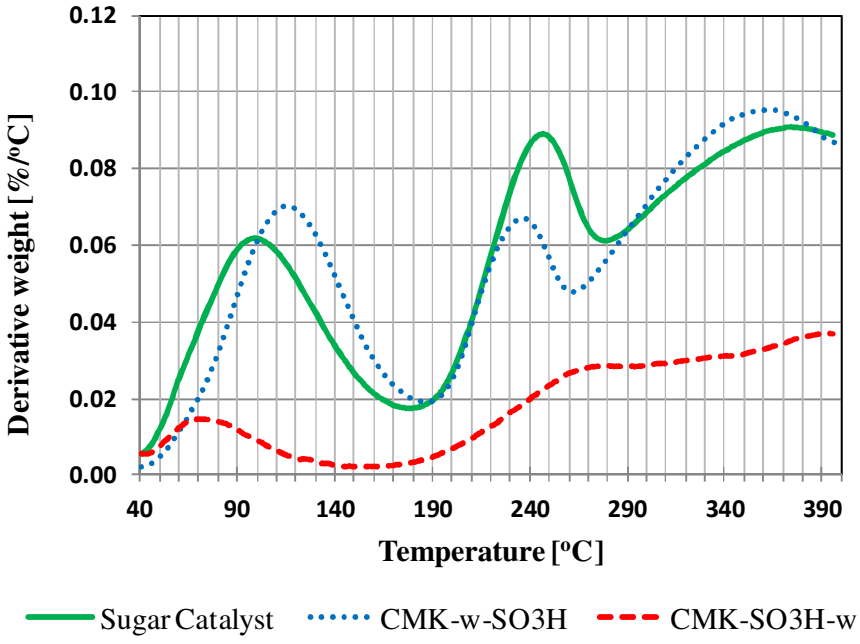

Figure 2–8 Derivative thermal analysis (DTA) of the sugar catalyst, CMK-w-SO_3H, and CMK-SO_3H-w under nitrogen.

The SEM and TEM images of the carbon-based catalysts are shown in Figures 2-9 and 2-10, respectively. The SEM images show the physical change in CMK-w-SO_3H compared with the CMK-w. As a result of the harsh sulfonation process, the porosity in the CMK-w was destroyed and the

collapsed-walls appeared as flakes in Figure 2-9 (b). The TEM images (Figure 2-10) appear to be similar to the TEM images reported by Hu et al. (2006) for a carbon material prepared by the confined activation process. The random pattern of black and white spots in the images may suggest that they are disordered amorphous materials, in agreement with the conclusion drawn by Hu et al. (2006). The route of the production of the carbon-based catalysts showing the hard silica template process and the effect of different sulfonation sequence on the porosity can be described as in Figure 2-11.

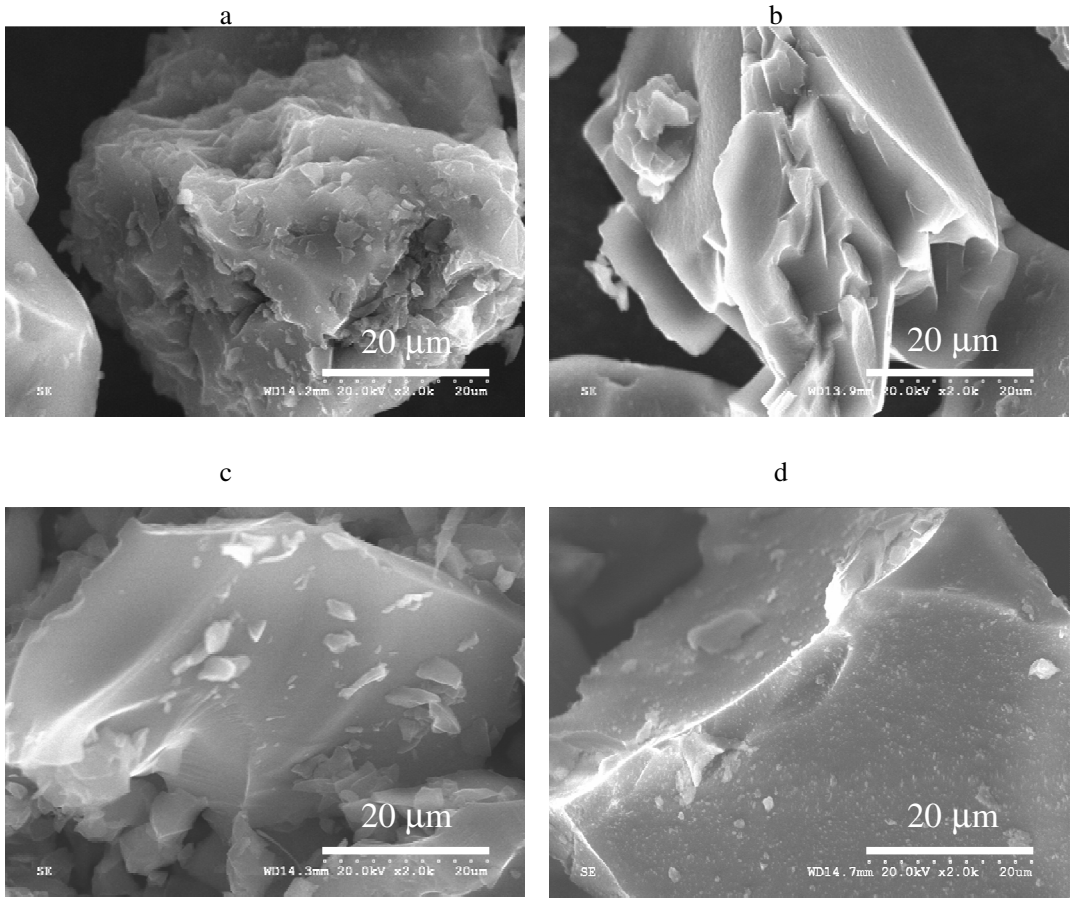

Figure 2–9 SEM images of: (a) CMK-w; (b) CMK-w-SO_3H; (c) CMK-SO_3H-w; and (d) Sugar catalyst.

2.3.3 Role of silica template on the characteristics of the carbon-based catalysts

Data on pore size and pore volume (Table 2-1) provide insight on the effect of sulfonation on the internal porosity of the catalysts with and without the presence of silica template. The total acidity (Table 2-1) and sulfur content (Tables 2-2 and 2-3) of CMK-w-SO_3H were higher than CMK-SO_3H-w despite the higher surface area of CMK-SO_3H-w. In addition, sugar catalyst showed a high total acidity and sulfur content in spite of its low surface area. The surface area and total acidity of sugar catalyst in this study were comparable to those reported by Mo et al. (2008a) and Peng et al. (2010) Data obtained for total acidity of CMK-SO_3H-w was comparable to CMK-3-873-SO_3H catalyst

reported by Peng et al. (2010). Note that CMK-3-873-SO_3H was prepared at 600°C, whereas CMK-SO_3H-w at 400°C. In comparison, though CMK-w-SO_3H lost its internal porosity, it yielded a high total acidity and sulfur content which may suggest that functionalization by the SO_3H groups occurred on the outer surface of the char. This was further confirmed by a large total acidity and sulfur content of the sugar catalyst even though it was a non-porous material. In order to understand the significance of the catalysts characteristics on its activity, the carbon-based catalysts and sulfuric acid were used to catalyze the esterification of oleic acid with methanol.

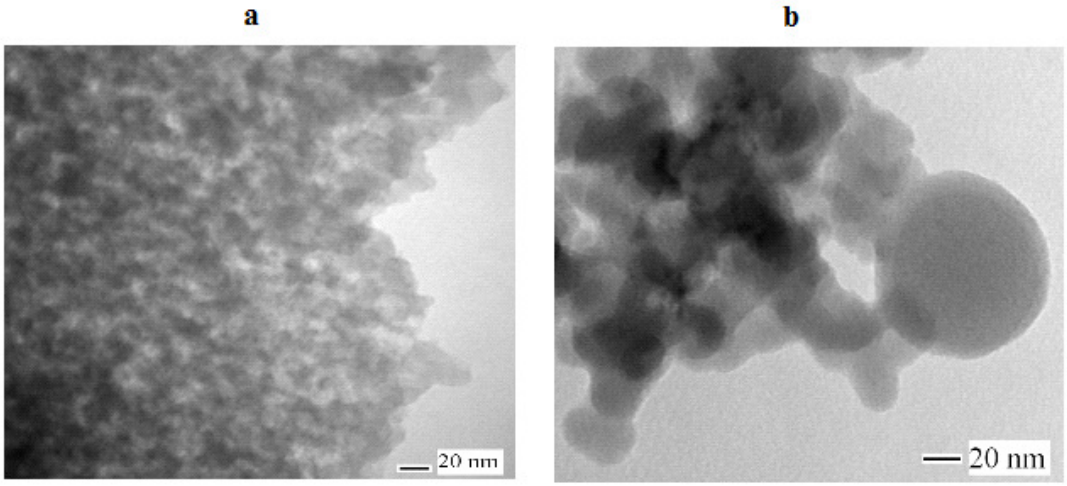

Figure 2–10 TEM images of: (a) CMK-SO_3H-w; and (b) CMK-w-SO_3H showing disordered amorphous materials.

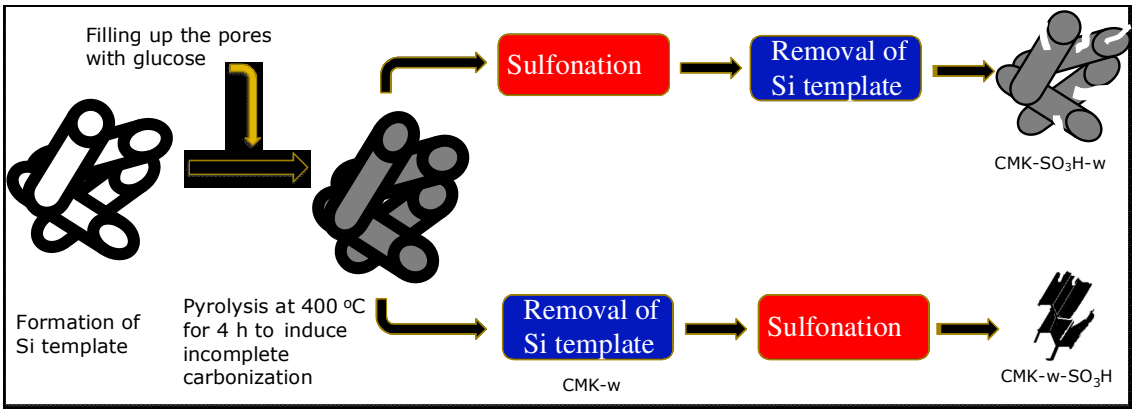

Figure 2–11 Schematic illustration of the preparation of CMK-w-SO_3H and CMK-SO_3H-w.

2.3.4 Reaction activities

Figure 2-12 shows the activity of the carbon-based catalysts and sulfuric acid on the esterification of oleic acid with methanol. Sulfuric acid showed the highest initial formation rate compared with the rest of the carbon-based catalysts (Table 2-1); however, sulfuric acid is not favoured as it is an unrecoverable homogeneous catalyst, and requires neutralization causing additional cost, and requiring expensive chemical resistant equipment. The methyl oleate produced by the sugar catalyst, CMK-w-SO_3H, and H_2SO_4 were comparable in the first 10 h of reaction as shown by their overlapping error bars (Figure 2-12). The large standard deviation of the experiments was due to difficulties in getting homogeneous sample during the sampling as the mixture consisted of two immiscible liquids. CMK-SO_3H-w showed the lowest initial formation rate and the concentration of methyl oleate produced in spite of having the largest surface area.

The results are explained from the total acidity and sulfur content of CMK-SO_3H-w. The total acidity of CMK-w-SO_3H and sugar catalyst mainly comes from the SO_3H groups as indicated by higher S content (Tables 2-2 and 2-3) in addition to COOH and OH moieties. Whereas, CMK-SO_3H-w had a lower total acidity due to lower S and O content resulting in lower activity. In addition, the OH and COOH functional groups do not catalyze esterification reaction (Takagaki et al. 2006; Nakajima et al. 2007). As shown in Table 2-1, the initial formation rate of sugar catalyst is higher than the CMK-SO_3H-w. This result contradicts the data reported by Peng et al. (2010) where the initial formation rate (in μmol min^{-1} $g.cat^{-1}$) of sugar catalyst and CMK-3-873-SO_3H were comparable; although, the sugar catalyst had higher total acidity than the CMK-3-873-SO_3H. Peng et al. (2010) concluded that the large pore size of the CMK-3-873-SO_3H contributed to its higher activity over sugar catalyst, which indirectly suggested that pore size played a more significant role than the density of SO_3H in catalyst activity. Our results suggest that catalytic activity for the esterification of oleic acid is independent of the specific surface area, and dependent on the total acidity. This conclusion is also supported by Kitano et al. (2009) for the esterification of acetic acid by sulfonated porous carbon catalyst.

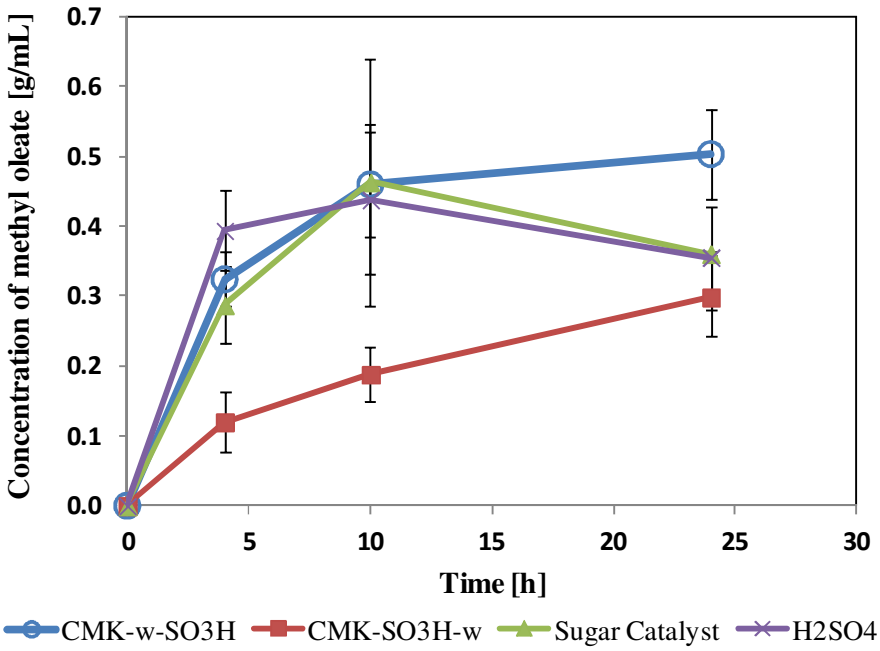

Figure 2–12 Activity of the carbon-based catalysts and sulfuric acid for comparison on the esterification of oleic acid. Reaction conditions: molar ratio of methanol to oleic acid at 10 to 1, 7 wt.% catalyst based on oleic acid, reaction temperature at 80°C, and stirrer speed at 800 rpm. Error bars indicate the standard deviation of 4-6 runs.

In a broader perspective, the findings showed that the development of higher surface area and mesoporous carbon-based catalysts might not be helpful in increasing the activity without having the high total acidity, in particular the SO_3H functional groups. Nevertheless, it is anticipated that mesoporous and high surface area carbon-based materials with high acidity could become effective catalysts with wider application. In addition, the possible recovery of the silica as opposed to disposal together with the hydrofluoric acid needs to be explored for making the preparation process more economical. Other sulfonation techniques such as non-covalent functionalization via π-π bonding may be worth investigating.

2.4 Conclusions

The role of silica template on the preparation of sulfonated mesoporous carbon catalysts has been investigated based on the surface area, pore size, pore volume, total acidity, sulfur content, and esterification of oleic acid. The silica template method via the confined activation process technique produced disordered mesoporous sugar char at low pyrolysis temperature (400°C). Sulfonation before removing the silica template retained 67% of the surface area, while decreasing the pore volume by 33% relative to the sugar char (CMK-w). On the other hand, sulfonation after removing the silica template totally collapsed the internal pores. Silica template provided support to the internal pores of the char, but prevented sulfuric acid from effectively reaching the internal surface during the

sulfonation process. The esterification of oleic acid was dependent on the total acidity, but independent of the surface area. In general, the development of mesoporosity and high surface area carbon-based catalysts are not useful without having the high acidity.

Chapter 3 Controlled functionalization of amorphous carbon using multiple vapour phase sulfonation

3.1 Introduction

Solid catalysts are widely preferred over liquid catalysts in industry due to their controllable physical and chemical properties (Sheldon and van Bekkum 2001). In the design of a solid catalyst, high surface area, mesoporous, and high total acidity are often the important characteristics. Nevertheless, the synthesis of a solid catalyst with these attributes coupled with a high catalytic activity has always been a challenge. For instance, the effective control over surface area and porosity may not necessarily promote the control of the acidity or basicity of the catalyst. Furthermore, the catalytic activity of a solid catalyst can be influenced by its chemical and physical characteristics, as well as the nature of the reaction such as molecular size of the reactants and products. In addition, factors such as catalyst deactivation and accessibility of active sites also affect the activity of a catalyst. In spite of this complexity, the design of a solid catalyst is still crucial. Solid catalysts are also advantageous based on the ease of grafting the desired functional groups to the surface, e.g. sulfonation of incomplete-carbonized sugar produce sulfonic acid, carboxylic acid, and hydroxyl functional groups on the char (Takagaki et al. 2006). The type of catalyst material affects the overall properties such as thermal stability, hydrophobic properties, electrical conductivity, and cost. In contrast, liquid catalysts do not have the flexibility of solid catalysts; though they are still used in industrial processes due to their favourable activity (Bartholomew and Farrauto 2006). Other advantages of solid catalysts over liquid catalysts are their ease of separation, recovery, and regeneration, which are crucial in industrial practice (Di Serio et al. 2007; Janaun and Ellis 2010).

Carbon-based catalysts are a relatively new and important class of solid catalysts. The discovery of the sugar catalyst (Toda et al. 2005) has attracted considerable interest because it can be prepared from renewable sources such as sugars and cellulose, using low energy in the pyrolysis step (carbonization temperature ~400^{o}C), and ease of functionalization of the carbon surface by heating in sulfuric acid to produce acid catalysts. Furthermore, the activity of the sugar catalyst is comparable with sulfuric acid for the esterification reaction (Takagaki et al. 2006; Zong et al. 2007). The improvements in preparation, properties, and applications of carbon-based catalysts have been reported, as summarized in Table 3-1. In general, for the synthesis of carbon-based catalysts, investigations have mainly focused on the preparation, using new carbon precursors, different sulfonating agents, and pre-treatment conditions to increase the carbon surface area and porosity. However, research on improved and effective functionalization techniques is often overlooked. For example, Table 3-1 shows only one study on the vapour phase sulfonation technique; whereas, all other investigations have used liquid phase sulfonation. Liquid phase and vapour phase sulfonation

occur by soaking the char in the sulfonating agent in the former case; whereas, in the latter the char is suspended in the vapour of the sulfonating agent at the desired temperature. A recent review by Stein et al. (2009) gives a detailed evaluation of the functionalization of porous carbons. However, to the best of the author's knowledge, the effect of repeated vapour phase sulfonation on amorphous carbon has never been reported. This lack of information, in addition to wanting to explore a more effective sulfonation process, motivated this aspect of research. In this chapter, a new multi-step functionalization technique to synthesize high surface area and mesoporous carbon-based catalysts called multiple vapour phase sulfonation is reported. As shown, this technique results in a higher loading of functional groups onto the char.

Table 3-1 Summary of investigation in the field of carbon-based catalysts.

Carbon precursor	Sulfonating agent	Sulfonation technique	Surface area, m^2g^{-1}	Total acidity, $mmolg^{-1}$	Ref.
Glucose	Fuming sulfuric acid	Liquid phase	<1	2.5	(Toda et al. 2005)
Starch	Sulfuric acid	Liquid phase			(Budarin et al. 2007)
Mesoporous polymer	Fuming sulfuric acid	Vapour phase	447 - 539	-NA	(Xing et al. 2007a)
Furfuryl alcohol	4-benzene-diazonium sulfonate	Liquid phase	610 - 813	1.17 – 1.95	(Liu et al. 2008)
Wood powder	Fuming sulfuric acid	Liquid phase	3 – 1560	2.40 – 9.98	(Kitano et al. 2009)
Glucose	Sulfuric acid	Liquid phase	660 - 1020	-NA	(Nakajima et al. 2009)
Glucose	Fuming sulfuric acid	Liquid phase	1 – 588	2.52 - 4.04	(Janaun and Ellis 2011)
Biochar	Fuming sulfuric acid	Liquid phase	1 - 14	0.036 – 3.2	(Dehkhoda et al. 2010)
Glucose	Sulfuric acid	Liquid phase	2.2	7.2	(Macia-Agullo et al. 2010)
Cellulose	Fuming sulfuric acid	Liquid phase	2-3	7.3	(Suganuma et al. 2010)
Cellulose	Fuming sulfuric acid	Liquid phase	< 5	-NA	(Fukuhara et al. 2011)
Sucrose	4-benzene-diazoniumsulfonate	Liquid phase	39 - 805	-NA	(Geng et al. 2011)
Resorcinol-formaldehyde resin	Fuming sulfuric acid	Liquid phase	1 - 433		(Suganuma et al. 2011)
Soluble phenolic resin	Sulfuric acid	Liquid phase	44 - 514	-NA	(Tian et al. 2011)

3.2 Experimental

3.2.1 Multiple vapour phase sulfonation of mesoporous char

The study of multiple vapour phase sulfonation on CMK-w was performed in an experimental setup as shown in Figure 3-1. The setup consisted of a 1000 mL round bottom flask (Fisher Scientific) containing 100 mL fuming sulfuric acid (20 wt.% free SO_3) (Sigma-Aldrich), placed on a temperature-controlled heating mantle (Thermolyne). 6 g of CMK-w sample was placed in a condenser (6 mm inner tube diameter and 30 cm height) and both ends of the tube were plugged with quartz wool to prevent the sample from escaping. The glass condenser was connected to the round bottom flask and its other end was connected with a silicon tube, which was dipped into a 1M NaOH. This was to neutralize the fuming sulfuric acid vapour before it was released in the fume hood. The temperature of the sample bed was controlled by connecting the condenser to a heat exchanger (Julabo F12) as shown in Figure 3-1. The type of fluid used in the heat exchanger was R134a refrigerant.

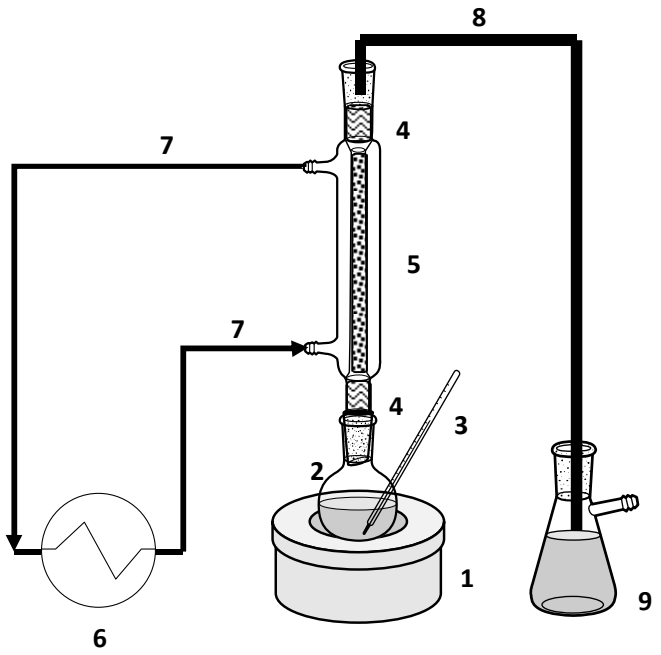

Figure 3–1 A schematic diagram of the multiple vapour phase sulfonation experimental setup: 1 – A temperature controlled heating mantle; 2 – A 1000 mL volumetric flask with a thermometer port; 3 – A thermometer; 4 – Quartz wool; 5 – A jacketed condenser, the dotted inner column indicates the char sample location; 6 – A heat exchanger; 7 – A silicon tube; 8 – A silicon tube; 9 – An Erlenmeyer flask containing NaOH solution.

The temperature of the heat exchanger was set to 60°C. The temperature of the sample bed was not directly measured. Fuming sulfuric acid was then heated to 210°C for 4 h. Upon heating, fuming sulfuric acid vapourized, and the vapour was forced to escape through the char bed and passed

through the NaOH solution. The contacting between the vapour and char caused the sulfonation reaction. It was shown through calculation that the vapour would likely to condense in the pores of the char sample (See Appendix B.1), meaning that, the vapour saturated the char before being able to pass through the char bed. After sulfonation, the sulfonated char was carefully withdrawn and washed repeatedly with hot distilled water until the pH of the wash water became neutral and no sulphate ion was detected (procedure given in Appendix **A.1**). The sample was dried in an oven at 110^{o}C overnight. This sample was denoted as VPS1 indicating that the sample char (CMK-w) underwent functionalization via the vapour phase sulfonation one time. The effect of multiple vapour phase sulfonation was studied via repeating the sulfonation and washing steps. The sample produced from sulfonation of VPS1 was denoted as VPS2; while, the sample produced from sulfonation of VPS2 was denoted as VPS3. The effects of char bed temperature and the time for sulfonation on the characteristics of the sample were studied by the sulfonation of CMK-w at various sample bed temperatures (22 – 80^{o}C) and sulfonation times (1 – 8 h). All samples were kept in a desiccator at room temperature until it was further used. VPS1, VPS2, VPS3, and sugar catalysts are termed as the carbon-based catalysts.

3.2.2 Non-covalent sulfonation of mesoporous char

Non-covalent sulfonation of mesoporous char was done with 1-pyrenesulfonic acid (PSA) in three types of solvent; ethanol, heptane, and acetone. In a typical experiment, 0.25 g of PSA and 0.5 g of mesoporous char (CMK-w) were mixed with a 50 mL ethanol, heptane, or acetone in a 125 mL Erlenmeyer flask separately. The mixtures were sonicated for 30 min at room temperature. The CMK-w samples were then filtered and dried in a fume hood at room temperature. After that, the samples were washed with hot distilled water repeatedly until the pH of the water became neutral and no sulfate ions were detected. The samples were dried in an oven at 110^{o}C overnight, and were analyzed for total acidity content.

3.2.3 Characterization

The particle size distribution of the samples was measured on a Mastersizer 2000 (Malvern Instruments), using an approximate sample size of 0.1 g, and the particle refraction index used was 2.420A, a refractive index of carbon (diamond) (Source: Knovel database). The procedures for porosimetry, total acidity, FT-IR, elemental analysis, XPS, and TGA under nitrogen are similar as described in Section 2.2.2. TGA under air was also performed. In a typical analysis, a sample (~20 mg) was purged with extra dry air for 30 min at 30^{o}C before the temperature was ramped at 10^{o}C/min to 700^{o}C under 100 mL/min extra dry air flow rate.

3.3 Results and discussion

3.3.1 Characterization

3.3.1.1 Samples prepared through the multiple vapour phase sulfonation

Investigation on effective functionalization of amorphous carbon, a mesoporous sugar char (CMK-w) prepared via confined activation process, was done by repeating the vapour phase sulfonation with washing. VPS1, VPS2, and VPS3 were the catalysts obtained after first, second, and third sulfonation step, respectively.

Figure 3-2 shows the particle size distribution of the carbon-based catalysts. The particle size mean based on volume weighted mean for VPS1, VPS2, VPS3, and the sugar catalyst were 74, 61, 54, and 65 µm, respectively.

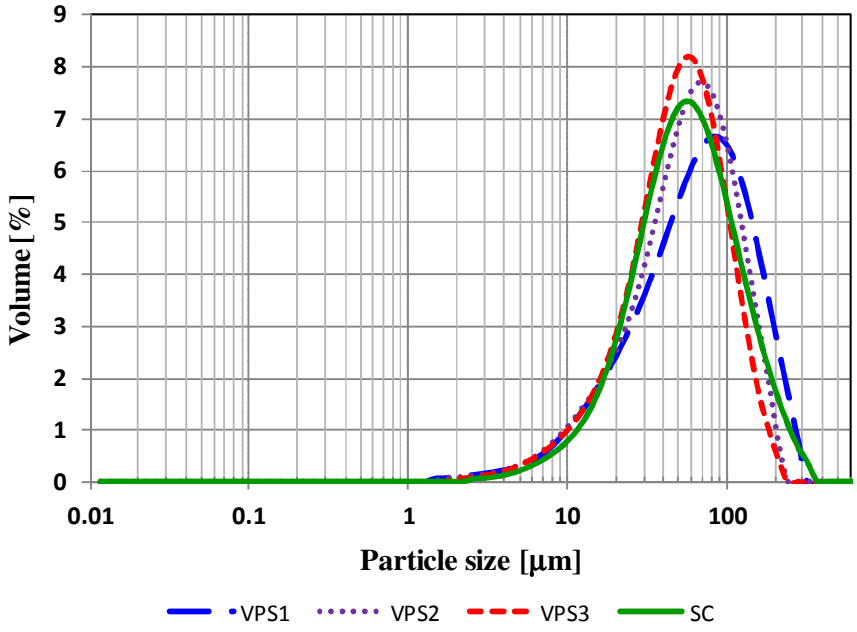

Figure 3–2 Particle size distribution of VPS1, VPS2, VPS3, and sugar catalyst measured using Mastersizer 2000.

Figures 3-3 and 3-4 show the adsorption-desorption isotherms and pore size distributions of CMK-w, VPS1, VPS2, and VPS3. The plots of VPS2 and VPS3 in Figure 3-3 are not readable because they are smaller in surface area than VPS1 and CMK-w. Figures 3-5 through 3-8 show the individual plots of VPS2 and VPS3 for their adsorption-desorption isotherms and pore size distributions. The y-axis (dV/dD) represents the derivation of specific pore volume against pore diameter. CMK-w and VPS1 had a clear hysteresis with the adsorption-desorption isotherms identified as Type IV according to the IUPAC classification (Sing 1982). This indicates that CMK-w and VPS1 were mesoporous materials. VPS2 and VPS3 had a similar adsorption-desorption isotherm trend, with a clear hysteresis, but differ from the typical Type IV isotherm. The desorption lines of VPS2 and VPS3 did not close with the adsorption lines. This might be due to irregular shapes of the pores where the void is larger than its pore mouth, like an 'ink-bottle' shape. It may be plausible that the condensate produced in the void as a result of capillary condensation could not completely escape

during desorption due to a narrow pore mouth resulting in the disconnected hysteresis adsorption – desorption isotherm (Sample calculation of the capillary condensation is given in Appendix **B.1**).

CMK-w, VPS1, VPS2, and VPS3 showed bimodal pore size distributions with CMK-w and VPS1 having similar average pore diameters of 4 - 5 nm. The pore volumes of VPS1, VPS2, and VPS3 decreased as much as 61, 93, and 98%, respectively, compared with the pore volume of CMK-w. Consequently, VPS1, VPS2 and VPS3 lost its specific surface area as much as 51, 87, and 95%, respectively. This indicated that the more sulfonation steps the more pore destruction would occur. In addition, the trend of pore size distribution of VPS1, VPS2, and VPS3 (Figures 3-4, 3-6, and 3-8, respectively) show shrinking and shifting of the peaks, suggesting that the structure of the pores may have eroded and collapsed. The mechanism of vapour phase sulfonation is discussed further in Section 3.3.2.

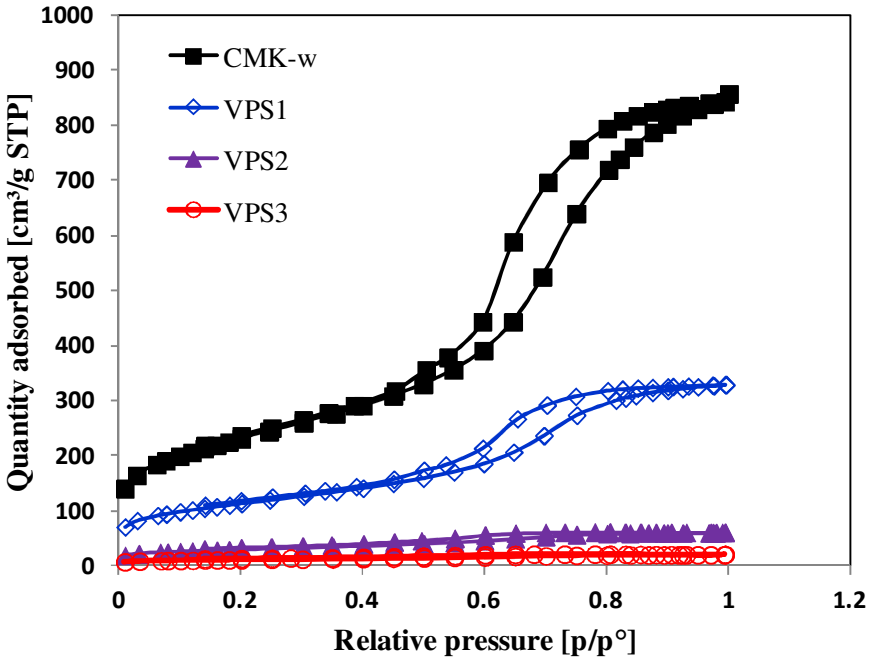

Figure 3–3 Nitrogen adsorption and desorption isotherms of VPS1, VPS2, VPS3, and CMK-w measured at -196°C.

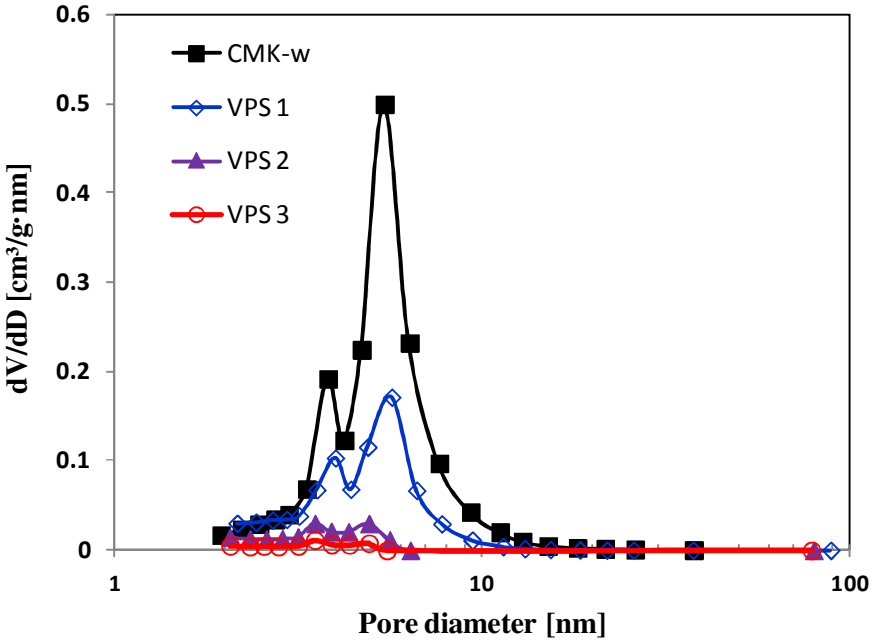

Figure 3–4 BJH desorption pore size distribution of VPS1, VPS2, VPS3, and CMK-w.

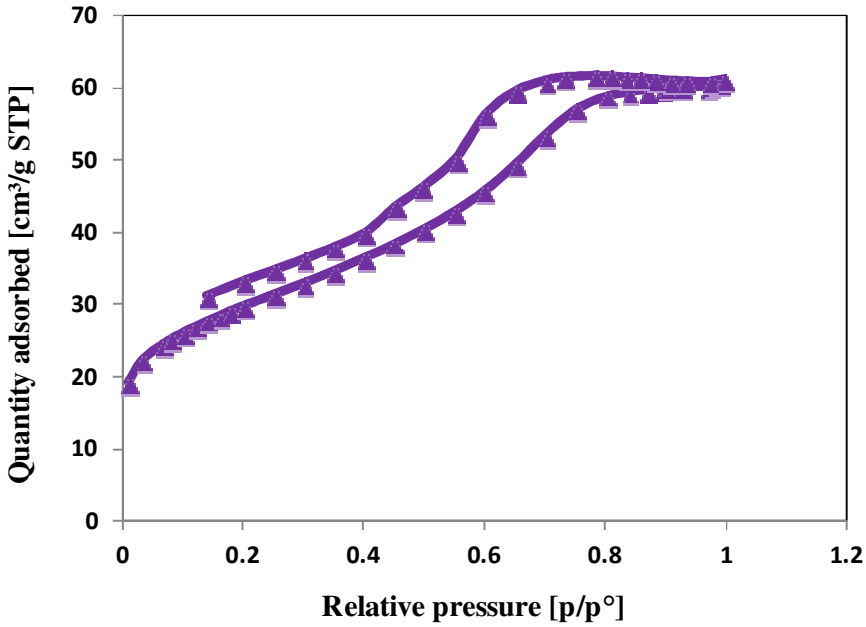

Figure 3–5 Nitrogen adsorption – desorption isotherms of VPS2 measured at -196°C.

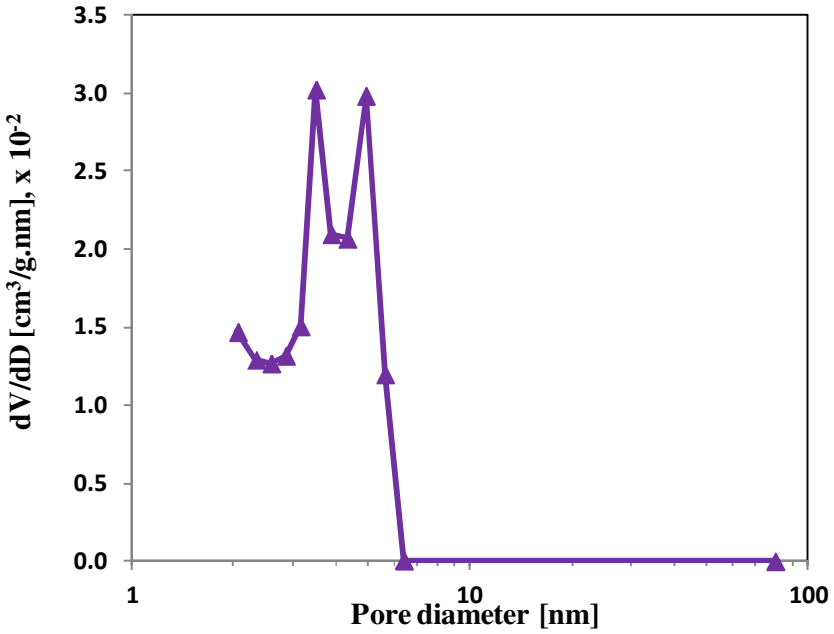

Figure 3–6 BJH desorption pore size distributions of VPS2. The y-axis is the derivative of specific pore volume against pore diameter.

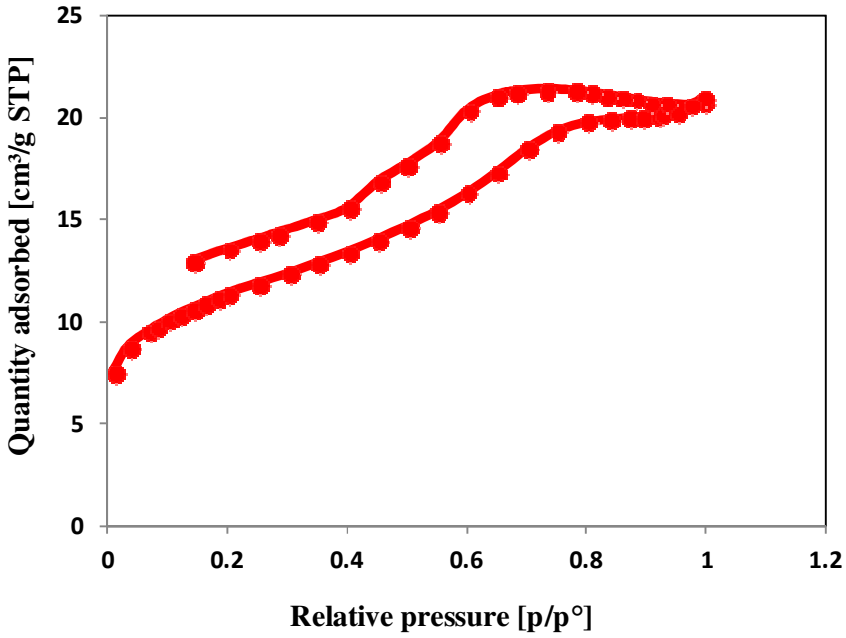

Figure 3–7 Nitrogen adsorption – desorption isotherms of VPS3 measured at -196°C.

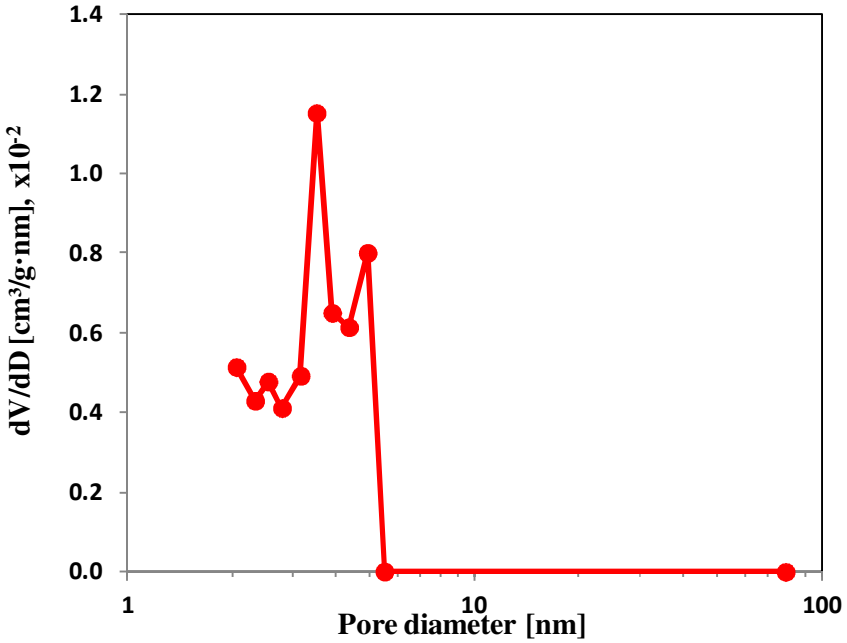

Figure 3–8 BJH desorption pore size distributions of VPS3.

Figures 3-9 through 3-12 show the XPS of CMK-w, VPS1, VPS2, and VPS3. The XPS analyses indicated that the main elements in all samples were C and O. The major difference among the samples was the absence of S in sample CMK-w, which was expected since CMK-w had not been sulfonated. The detection of peak at 168 eV in VPS1, VPS2, and VPS3 was attributed to the energy of electron ejected from S 2p orbital, which corresponds to the oxidation state of -SO_3H (Takagaki et al. 2006). Since there is only a single peak associated to S, this suggests that all S atoms are contained in SO_3H. This is consistent with the literature on the sulfonation of amorphous carbon (Okamura et al. 2006; Macia-Agullo et al. 2010; Fukuhara et al. 2011).

As shown in Figure 3-13, the FT-IR analysis of the carbon-based catalysts showed peaks at 1742 and 1032 cm^{-1}, which were assigned to the SO_3H group (Takagaki et al. 2006; Nakajima et al. 2007). All samples showed a strong band at ~1600 cm^{-1} due to C=C stretching (Xing et al. 2007a; b). Furthermore, the broad band at 1260 cm^{-1} and the overlapping band at 1700 cm^{-1} for the carbon-based catalysts can be assigned to aryl-hydroxyl (Ar-OH) (Kellner et al. 2004; Xing et al. 2007b; Andreas Stein et al. 2009), and carboxylic acid stretching (Boehm 2002), respectively. The overall FT-IR analysis suggests that the carbon-based catalysts consist of polycyclic aromatic carbon sheets containing -SO_3H, -COOH, and -OH moieties, in agreement with the published literature on sulfonated amorphous carbons (Toda et al. 2005; Okamura et al. 2006; Suganuma et al. 2008; Suganuma et al. 2010; Fukuhara et al. 2011).

Figures 3-14 and 3-15 show the thermal stability of the carbon-based catalysts under N_2. The weight loss at ~90°C is attributed to the loss of moisture. There were two significant weight loss peaks that occurred at ~240 and ~360°C, which can be associated with the decomposition of the functional groups. The TGA data indicated that the carbon-based catalysts were thermally stable up to 240°C.

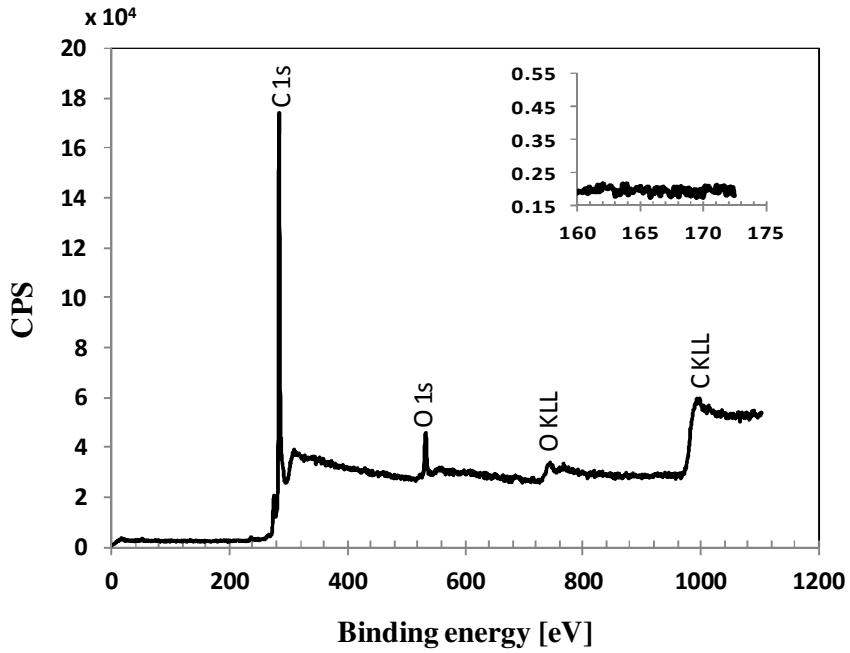

Figure 3–9 XPS of CMK-w. Inset is the enlarged binding energy at 160 – 180 eV.

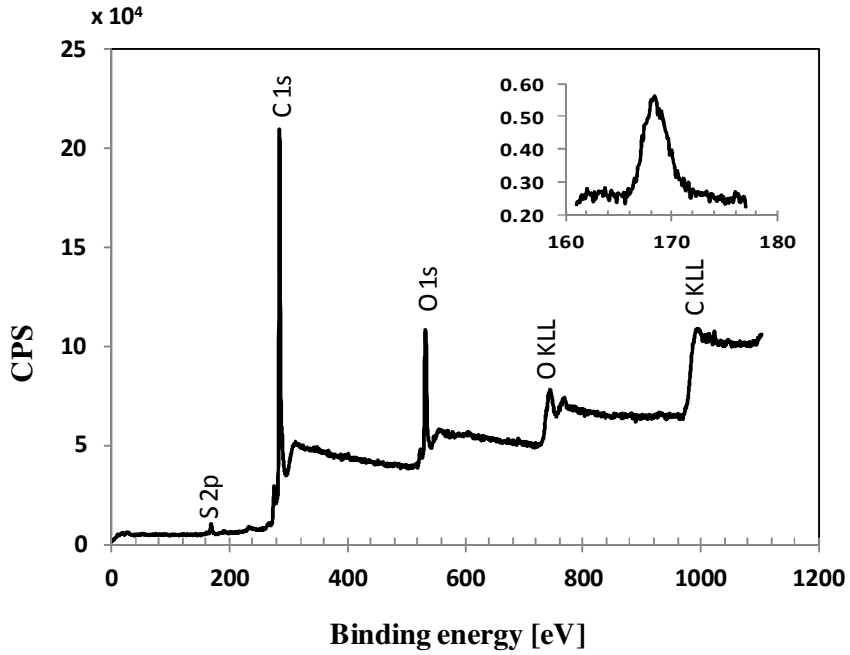

Figure 3–10 XPS of VPS1. Inset is the enlarged binding energy at 160 – 180 eV.

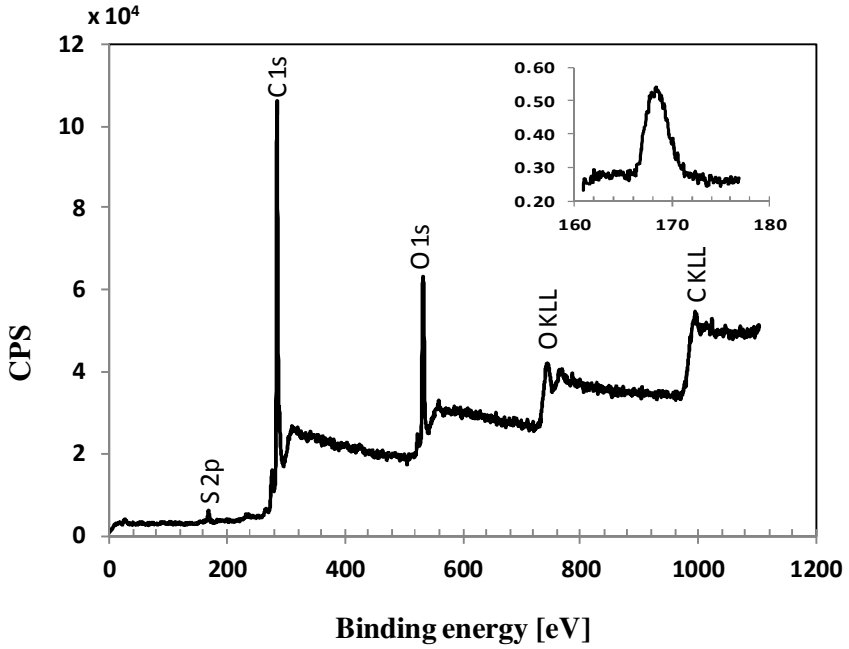

Figure 3–11 XPS of VPS2. Inset is the enlarged binding energy at 160 – 180 eV.

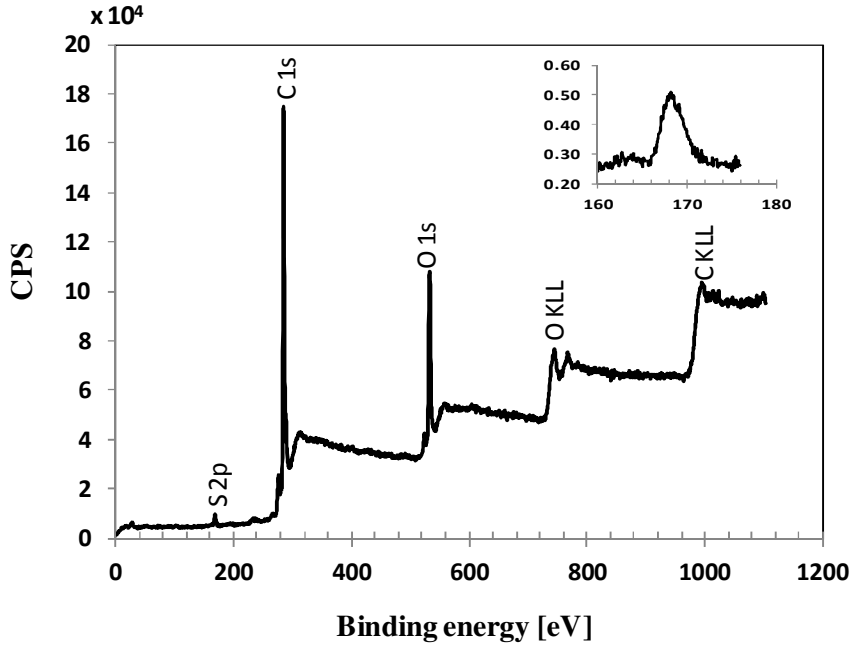

Figure 3–12 XPS of VPS3. Inset is the enlarged binding energy at 160 – 180 eV.

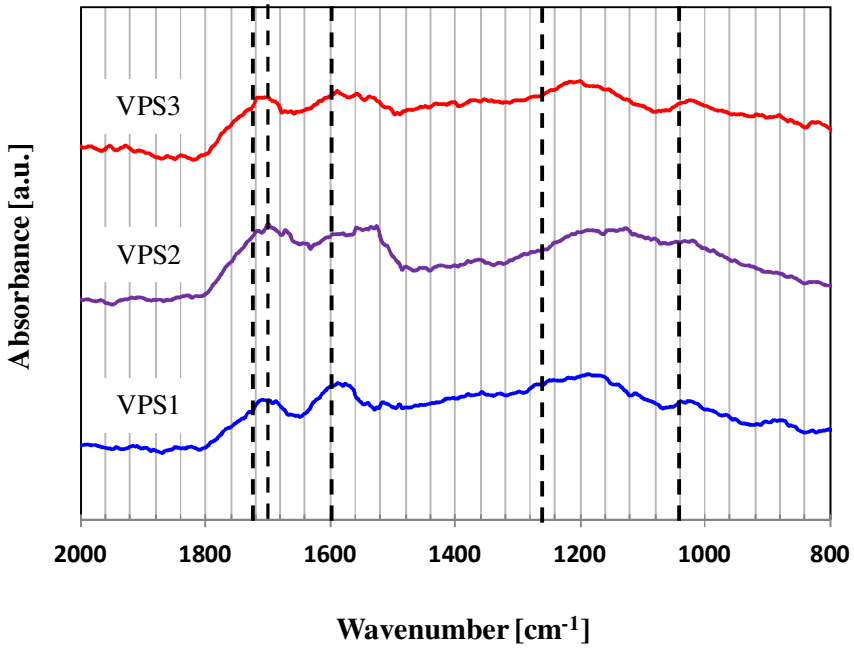

Figure 3–13 FT-IR spectra of VPS1, VPS2, and VPS3.

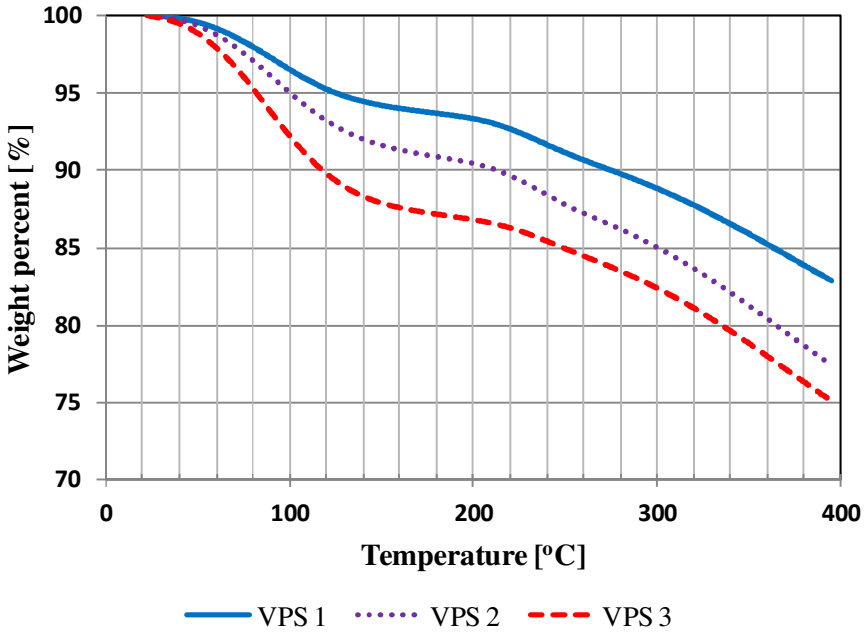

Figure 3–14 Thermo-gravimetric analysis of VPS1, VPS2, VPS3 and sugar catalyst under nitrogen.

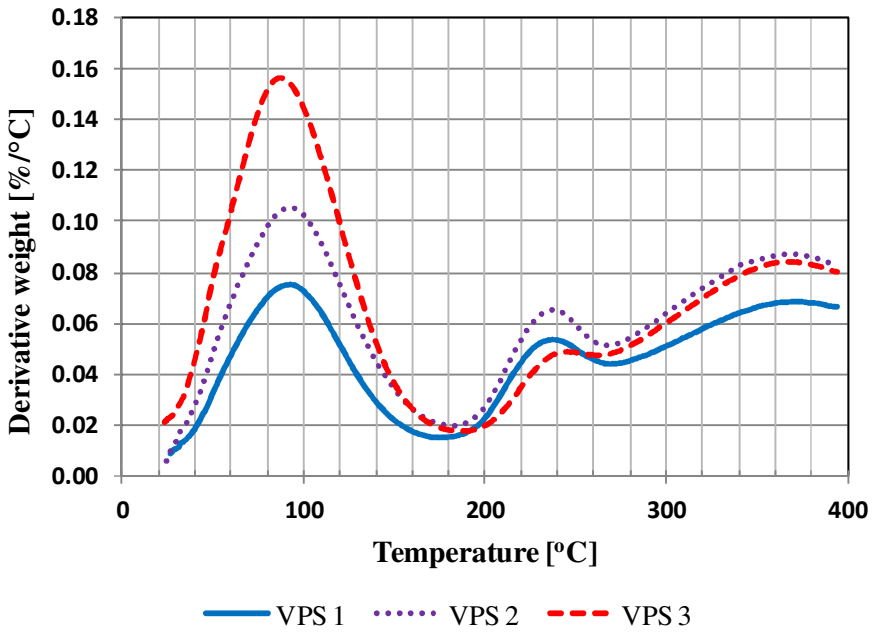

Figure 3–15 Derivative thermal analysis of VPS1, VPS2, VPS3 and sugar catalyst under nitrogen

Figures 3-16 and 3-17 show the TGA and DTA of the carbon-based catalysts and CMK-w under air, respectively. The carbon-based catalysts showed similar thermal stability. The DTA peaks at ~100 and ~240°C can be associated with decomposition of water and the functional groups, respectively. This result is consistent with the TGA under nitrogen.

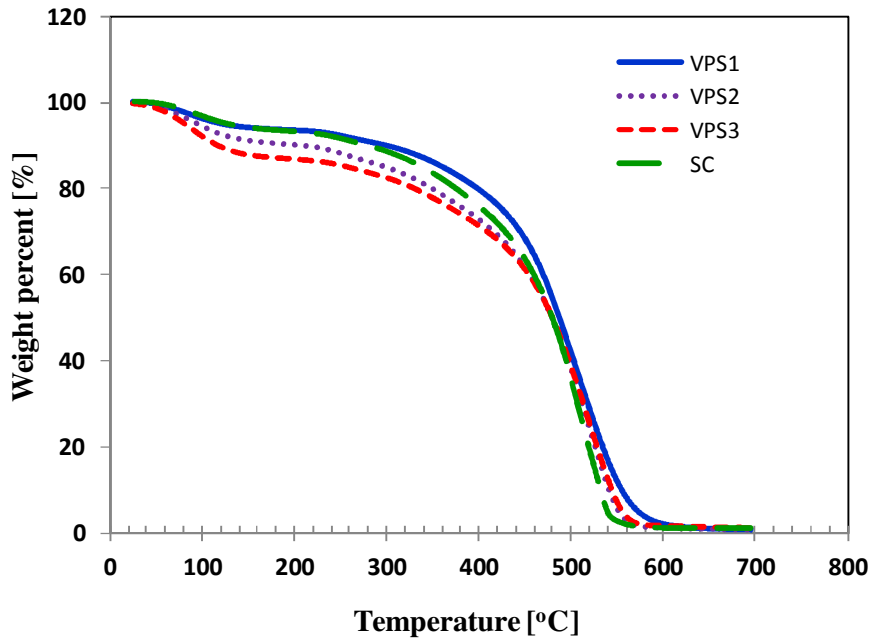

Figure 3–16 Thermo-gravimetric analysis of the carbon-based catalysts under air.

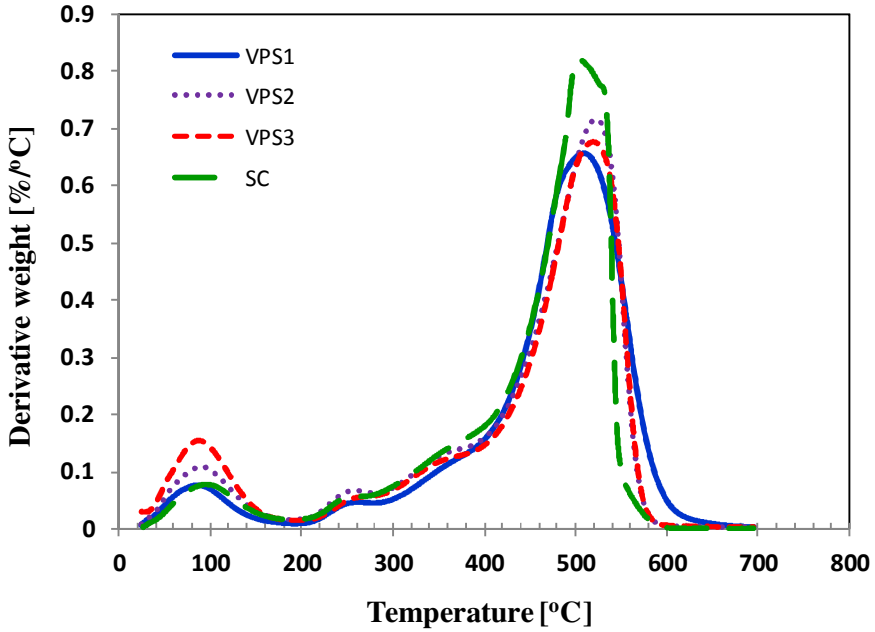

Figure 3–17 DTA of the carbon-based catalysts under air.

The composition of the carbon-based catalysts determined by elemental and XPS analyses are reported in Tables 3-2 and 3-3, respectively. Table 3-2 shows that the H, O, and S concentration increased as the number of sulfonation steps increased. This suggests that more functional groups were packed on the char through each sulfonation step. In contrast, Table 3-3 shows that the O and S concentration increased from the first to the second sulfonation. Second and third sulfonation had comparable amount of O and S (Note that H is undetectable in XPS analysis technique). Furthermore, the mole ratio of S:C in chemical elemental analysis (Table 3-2) were 3 – 4 times higher than the mole ratio of S:C in XPS elemental analysis (Table 3-3). This suggested that the majority of the functional groups were located away from the surface for VPS1, VPS2, and VPS3, and were undetectable by the XPS analysis technique.

Table 3-2 Elemental analysis of the carbon-based catalysts.

Catalyst	Elemental analysis (wt.%)				Weight ratio to carbon			Empirical formula
	C	H	O	S	H:C	O:C	S:C	
VPS1	63.81	2.20	26.43	2.81	0.034	0.414	0.044	$CH_{0.411}O_{0.311}S_{0.016}$
VPS2	58.37	2.12	32.92	3.49	0.036	0.564	0.060	$CH_{0.433}O_{0.423}S_{0.022}$
VPS3	56.10	2.20	34.25	3.37	0.039	0.611	0.060	$CH_{0.467}O_{0.458}S_{0.023}$
SC	60.18	2.08	33.18	3.28	0.035	0.551	0.055	$CH_{0.412}O_{0.414}S_{0.020}$

Table 3-3 Elemental analysis by XPS technique of the CMK-w and the carbon-based catalysts.

Catalyst	Elemental analysis by XPS (wt.%)			Mole ratio to carbon	
	C	O	S	O:C	S:C
CMK-w	92.55	7.30	0	0.059	0
VPS1	80.82	17.62	1.02	0.164	0.00473
VPS2	77.93	20.07	1.13	0.193	0.00543
VPS3	78.27	19.75	1.13	0.189	0.00541

Figures 3-18 and 3-19 show the effect of heat exchanger temperature and sulfonation time on total acidity and surface area, respectively. The result showed that an increase in heat exchanger set temperature from 40 to 60°C resulted a 9.8% increase in the total acidity and a 8.6% decrease of the surface area. However, further temperature increase to 80°C showed that total acidity had increased only 0.8%, with surface area had decreased to 13.8%. This implied that the increase in temperature beyond 80°C was not effective in increasing the total acidity, but rather caused internal pores to collapse. The result showed that 4 h sulfonation time was sufficient to achieve saturation of the char. Once the char is saturated with sulfuric acid vapour, additional sulfonation time does not significantly increase the total acidity, this might be attributed to the formation of 'film' by the vapour and prevent the access to the available surfaces.

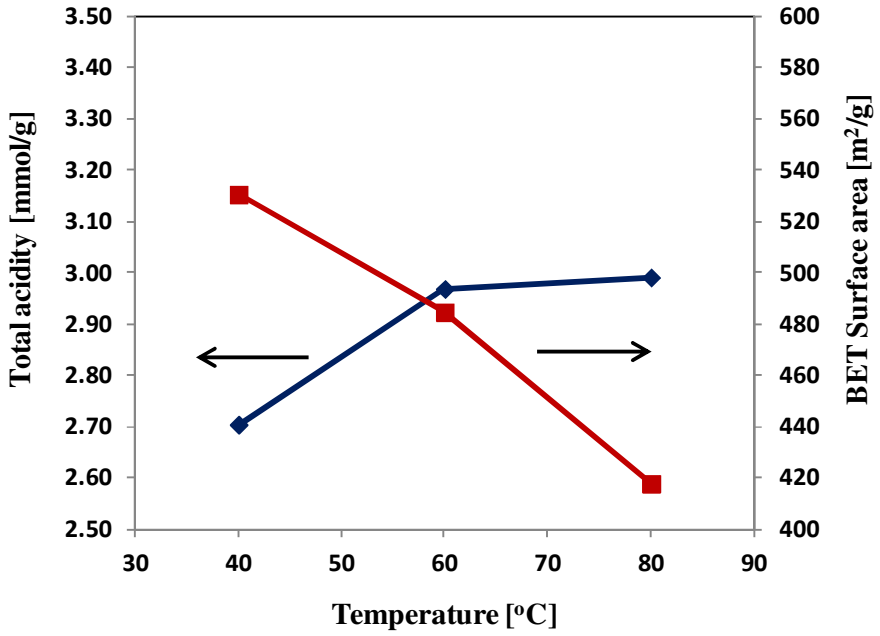

Figure 3–18 Effect of bed heating temperature on total acidity and surface area. Sulfonation time was 1 h.

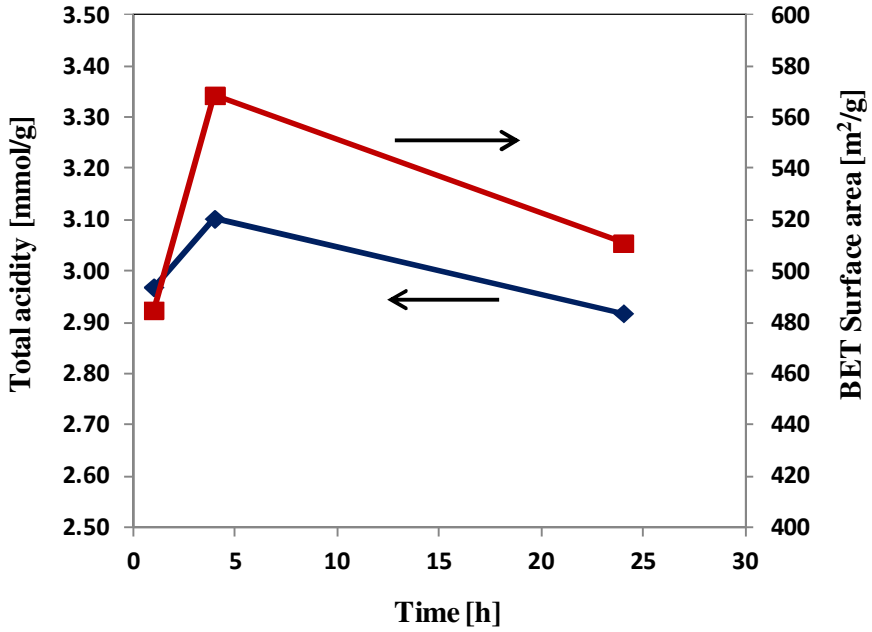

Figure 3–19 Effect of vapour phase sulfonation time on total acidity and surface area. Reaction temperature was arbitrarily chosen at 60°C.

Figure 3-20 shows the results of vapour phase sulfonation of CMK-w at various char bed temperatures and sulfonation times. VPS1, VPS2, and VPS3 are labeled on the plot for clarity. The results showed that the total acidity and the pore volume were correlated to the surface area with particular trends as shown by the solid lines. The trends implied that the chemical and physical characteristics of the carbon-based catalysts, prepared via vapour phase sulfonation, were predictable. Consequently, for the same type of carbon precursor (CMK-w), a change in the sulfonation condition (i.e., bed temperature, time, and number of sulfonation steps) will likely produce a catalyst that fit the trends.

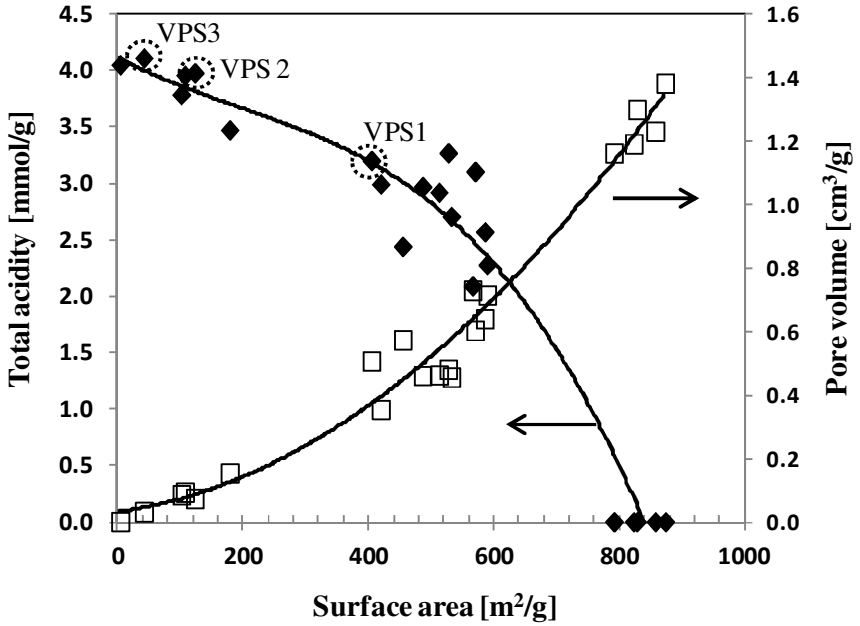

Figure 3–20 The relationship of surface area, total acidity, and pore volume of amorphous carbon functionalized via multiple vapour phase sulfonation.

3.3.1.2 Samples prepared through the non-covalent sulfonation

The results of total acidity analysis showed that all samples contained no acidity. This suggested that the non-covalent sulfonation, for the condition used, was not able to graft the 1-pyrenesulfonic acid (PSA) to the carbon surface through π-π bonding.

3.3.2 Vapour versus liquid phase sulfonation

This section discusses the difference and similarity between vapour and liquid phase sulfonation. The proposed mechanism of multiple vapour phase sulfonation is described in Figure 3-21 (A general mechanism of aromatic carbon sulfonation is given in Appendix **B.2**). In the vapour phase sulfonation process, heating of the fuming sulfuric acid produced sulfuric acid vapour continuously. This caused a vapour pressure build up in the round bottom flask that forced the vapour to penetrate through the char bed. This provided efficient contacting between the vapour and the char particles. For instance, the time taken to achieve sulfonation saturation in this study was only 4 h. In contrast, Xing et al. (2007a) used 24 h for a vapour phase sulfonation in an enclosed container (in this setup, the sample was suspended in the vapour phase of heated fuming sulfuric acid in an autoclave reactor). Furthermore, the highest total acidity achieved by their technique was only 2.5 mmol/g, which was 22% lower than the total acidity of VPS1. The forced flow through the bed had an advantage compared with theirs because the contacting in their setup depended mainly on the diffusion driven by the concentration gradient of the vapour between the outer and the inner surfaces of the bed, requiring a longer time to reach saturation.

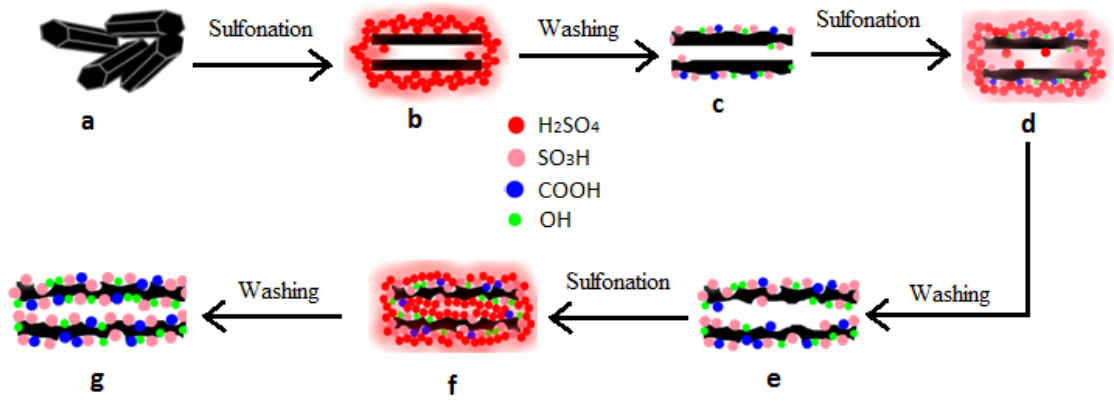

Figure 3–21 Schematic illustration of the multiple vapour phase sulfonation of the mesoporous char: (a) CMK-w, a disordered mesoporous char, prepared using hard silica templating method; (b) the char 'rods' showing the coating of H_2SO_4 film; (c) the washing step removes loosely attached H_2SO_4 leaving the char with the functional groups and available surface, this is VPS1; (d) the second sulfonation allows adsorption on the available surface; (e) as a result more functional groups attach to the char surface, this is VPS2; (f) the third sulfonation causes a complete adsorption of the H_2SO_4 on the external and internal surfaces of the char; (g) the char is grafted with a maximum amount of functional groups, i.e., VPS3.

The major difference between liquid versus vapour phase sulfonation is the impact on the physical and chemical properties of the catalyst. Liquid phase sulfonation of CMK-w caused a total collapse of its pores; whereas, vapour phase sulfonation caused a 51% loss of surface area and a reduction of pore volume from 1.3 to 0.5 m^3/g as indicated by VPS1 (Table 3-4). This difference can be attributed to the sulfonation mechanism. In a liquid phase, the capillary effect had caused complete filling of the internal pores. In addition, the concentration of sulfuric acid in the liquid and vapour phases were ca. 18.35 and 0.0083 mol/L (at 60°C), respectively (Sample calculation given in Appendix **B.3**). Higher sulfuric acid concentration in the liquid phase caused a harsh reaction that likely destroyed the pore walls. In contrast, a lower sulfuric acid concentration in the vapour phase caused a milder reaction and more likely preserved the pore walls.

In vapour phase sulfonation, diffusion of vapour promoted the adsorption of the sulfuric acid vapour, first onto the external surfaces and then into the internal pores of the char particles. It is speculated that the diffusion and adsorption occurred rapidly causing the formation of a sulfuric acid "film" around the char particles. In addition, the sulfuric acid vapour condenses in the pores due to capillary effect. Excess sulfuric acid vapour formed multiple layers on top of the film and rapidly saturated the char bed, leaving some surface available for adsorption, but unreachable due to blockage by the film. Removal of the film and free sulfuric acid by washing makes the available surfaces accessible by the subsequent sulfonation. As a result, the overall concentration of acid sites increases as the sulfonation and washing steps are repeated. Nevertheless, the increase in total acidity is at the expense of the particle surface area.

Table 3-4 Characteristics of the carbon-based catalyst and CMK-w.

Sample	N_2 adsorption[a]			Acidity, mmol/g	
	S.A.	P.D.	P.V.	Total[b]	SO_3H[c]
CMK-w	827	6.28	1.30	-	-
VPS1	403	5.02	0.51	3.20 ± 0.10	0.88
VPS2	106	3.54	0.09	3.96 ± 0.07	1.09
VPS3	40	3.18	0.03	4.11 ± 0.10	1.05
SC	< 1	-	-	4.15 ± 0.05	1.02

[a] BET surface area (S.A.) in m^2/g; pore diameter (P.D.) in nm; pore volume (P.V.) in cm^3/g.
[b] By acid-base back-titration.
[c] By elemental analysis.

The washing step after each sulfonation removed loosely bound sulfuric acid and functional groups, leaving only covalently bonded SO_3H, COOH, and OH groups. This provided the possibility for further sulfonation on the available surface. In the second sulfonation, sulfuric acid vapour was adsorbed on the available external surfaces and reacted with available carbon. In the third sulfonation, most of the available external and internal surfaces were fully reacted by the sulfuric acid vapour. Every sulfonation step eroded the pore wall, as shown by the BET results (Figures 3-3 and 3-4), in which it eventually collapsed the internal pore walls almost fully after the third sulfonation. It is worth mentioning that the presence of functional groups on the surface likely altered the char wetting property (Kakade and Pillai 2008; Pavese et al. 2008), which aided the sulfonation coverage on the surface in the subsequent sulfonation. This explains why the total acidity of the samples was a function of the number of sulfonation steps. However, the specific surface area and pore volume were inversely proportional to the number of sulfonation steps. This indicated that the collapse of the pore walls caused the material to deteriorate and lose its porosity, resulting in the decrease of pore volume and surface area. For the experimental conditions used, the amount of functional groups (mol of SO_3H/g cat) grafted on the char increased at the expense of its surface area and porosity. It is anticipated that the degree of surface area and porosity reduction in the multiple vapour phase sulfonation will depend on the carbonization temperature and the structure of char such as its wall thickness. In general, sulfonation of char prepared at carbonization temperature <450°C results in a 40% reduction in surface area; whereas, at a carbonization temperature >550°C, the surface area does not decrease. However, the lower carbonization temperature (<550°C) produces an active catalyst, while the higher carbonization temperature (>550°C) produces an inactive catalyst due to the ordering of carbon sheets (Kitano et al. 2009; Suganuma et al. 2011). Since functionalization occurs at the edges of the carbon sheets, a randomly packed carbon sheets has an advantage in flexibility such as the ability to swell during the reaction. In contrast, the ordered carbon sheets do not have this flexibility, making them an inactive catalyst (Nakajima et al. 2007; Mo et al. 2008a).

3.4 Conclusions

Multiple vapour phase sulfonation was effective in loading controlled concentration of total acidity (SO_3H, COOH, and OH) on the carbon-based catalysts. Vapour phase sulfonation via forcing the fuming sulfuric acid vapour to pass through the char bed achieved rapid saturation (4 h) due to an excellent vapour and char contacting. The increase in total acidity with repeated sulfonation was, however, at the expense of the surface area and pore volume of the catalyst. First, second, and third sulfonation steps produced carbon-based catalysts with 3.2, 3.96, 4.11 $mmolg^{-1}$ total acidity, respectively. The pore volumes of first (VPS1), second (VPS2), and third (VPS3) sulfonation decreased as much as 61, 93, and 98%, respectively, compared with the pore volume of char (CMK-w). Consequently, VPS1, VPS2 and VPS3 lost its specific surface area as much as 51, 87, and 95%, respectively. However, vapour phase sulfonation was less destructive on the pore of the char compared with liquid phase sulfonation due to a lower sulfuric acid concentration in the vapour phase. The carbon-based catalysts had a high thermal stability (up to 260^oC) making them suitable catalysts for many reactions such as transesterification. In a broader perspective, the technique of multiple vapour phase sulfonation can be used to design a specific concentration of functional groups, and controlled size of surface area and pore volume in carbon base materials.

Chapter 4 Activity of carbon-based catalysts on esterification of oleic acid with methanol

4.1 Introduction

Production of biodiesel from low grade feedstock such as waste oils and fats attracts global interest because they potentially reduce the use of edible oils as well as prevent environmental pollution caused through disposal of these materials. However, it is a challenging task because, besides containing useful triglycerides, waste oils and fats usually contain impurities including high amounts of free fatty acids and water. Generally, the strategy to deal with this shortcoming is to perform an esterification of the free fatty acids catalyzed by an acid catalyst (commonly H_2SO_4), followed by a transesterification of the triglycerides, usually catalyzed by strong alkaline base such as NaOH. Although base catalysts are generally more active than acid catalysts in transesterification reaction, the former requires stringent feedstock quality such as low water and FFA content (i.e., less than 0.5 wt.%) beyond which the downstream washing and product separation are more complicated due to the formation of soap as a byproduct, as well as reducing the catalyst activity (Di Serio et al. 2006; Zafiropoulos et al. 2007; Di Serio et al. 2008; Zabeti et al. 2009). This limitation can be overcome by the use of solid acid catalysts because their tolerance to water is high, in addition to having an easy catalyst separation from the final products. Furthermore, the operation with heterogeneous catalysis is reported to be safer than homogeneous system since it does not require a neutralization step (Salzano et al. 2010).

Information on the synthesis of solid acid catalysts for esterification reaction is well established in the literature (Chouhan and Sarma 2011; Leung et al. 2010; Shahid and Jamal 2011; Sharma et al. 2011). In addition, several solid acid catalysts have been tested for simultaneous esterification and transesterification reactions (Kulkarni et al. 2006; Celikten et al. 2010; Lien et al. 2010; Luque and Clark 2011). As discussed in Section 1.1.1.1, sugar catalyst had a high activity on esterification and transesterification reactions, comparable to that of sulfuric acid (Toda et al. 2005; Okamura et al. 2006; Zong et al. 2007). This chapter reports the activity of VPS1, VPS2, VPS3, sugar catalyst (classified as carbon-based catalysts) and sulfuric acid on esterification of oleic acid, a typical model compound for free fatty acids, with methanol. Figure 4-1 shows the stoichiometric reaction of oleic acid esterification with methanol; whereas, information about the molecular structure of oleic acid is presented in Appendix **C.1**. A mathematical model derived from reaction kinetics and catalyst decay is also described in this chapter.

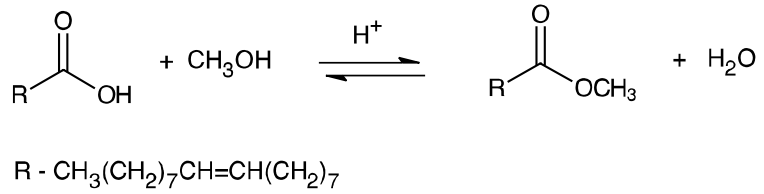

Figure 4–1 Esterification of oleic acid with methanol.

4.2 Experimental

4.2.1 Catalyst activity

The activity of the carbon-based catalysts and sulfuric acid on esterification of oleic acid with methanol was studied in a batch reactor (STEM-OMNI Reacto Station 6100), at 80±2°C under reflux, stirred at 800 rpm. The molar ratio of methanol to oleic acid was 10 to 1, and the amount of catalyst was 3 wt.% with respect to oleic acid. The amount of reactants used were 250 mmol of methanol and 25 mmol of oleic acid. Catalyst activity was studied at several reaction times, namely 1, 2, 4, 8, and 12 h. Once the reaction was completed, products were filtered to remove the catalyst. The filtrate, which consisted of two immiscible layers (water and methyl oleate), was separated using a separatory funnel. The weight of each layer was measured, and its density was determined using a 2 mL specific gravity bottle. Once the volume of each layer was determined, a total of 100 µL sample comprised of both layers was taken based on the fraction of the layers and mixed. This sample was further diluted with heptane and homogeneously mixed using a vortex before being analyzed on GC/MS (Varian) using a fused silica 60 m x 0.25 mm x 0.25 µm with CPWax52CB coating column. The temperature program was ramped at 20°C/min from 150 to 240°C, using helium as the carrier gas with a column flow of 2 mL/min. The quantitative analysis was done using methyl oleate as the external standard. The details of the preparation of the methyl oleate calibration curve are given in Appendix **C.2**. Sample calculation for the initial formation rate is given in Appendix **C.3**.

4.2.2 Catalyst leaching

The catalyst leaching was investigated by analyzing the presence of functional groups in the esterification products (at 2 and 8h reaction times): by analyzing the elemental composition of the spent catalyst (only for VPS2); by measuring the total acidity of the spent catalysts; and by analyzing the weight loss of the spent catalysts on a TGA under N_2. The spent catalysts were washed with acetone and methanol and filtered repeatedly (at least 5 times), and then dried in an oven at 110°C overnight before they were analyzed. The presence of functional groups in the esterification products were investigated by measuring the pH and detecting the sulfate ions according to the procedures described in Appendix A.1.

Catalyst deactivation was studied by developing a mathematical model from the reaction kinetic and catalyst deactivation equations to determine the reaction constant and deactivation constant of the catalytic systems.

4.3 Results and discussion

4.3.1 Catalytic activity of the carbon-based catalysts and H_2SO_4

Figure 4-2 shows the comparison of the activity of the carbon-based catalysts and H_2SO_4 on the esterification of oleic acid with methanol at 80°C in terms of the concentration of methyl oleate produced. The broken lines are the best curve fit using a 'ligand binding, one site saturation + nonspecific' model available in SigmaPlot 10.0 software. H_2SO_4 had the highest activity, which can be attributed to its greater total acidity (Table 2-1). VPS1, VPS2, and sugar catalyst had comparable activities for the first 240 min, beyond which sugar catalyst showed slightly higher activity followed by VPS2 and VPS1. Furthermore, VPS3 had the lowest activity in spite of a larger surface area and comparable total acidity with sugar catalyst. The difference in catalytic activity among the carbon-based catalysts and H_2SO_4 can be attributed to catalyst deactivation and the accessibility of active sites, which is discussed in greater detail in the following section.

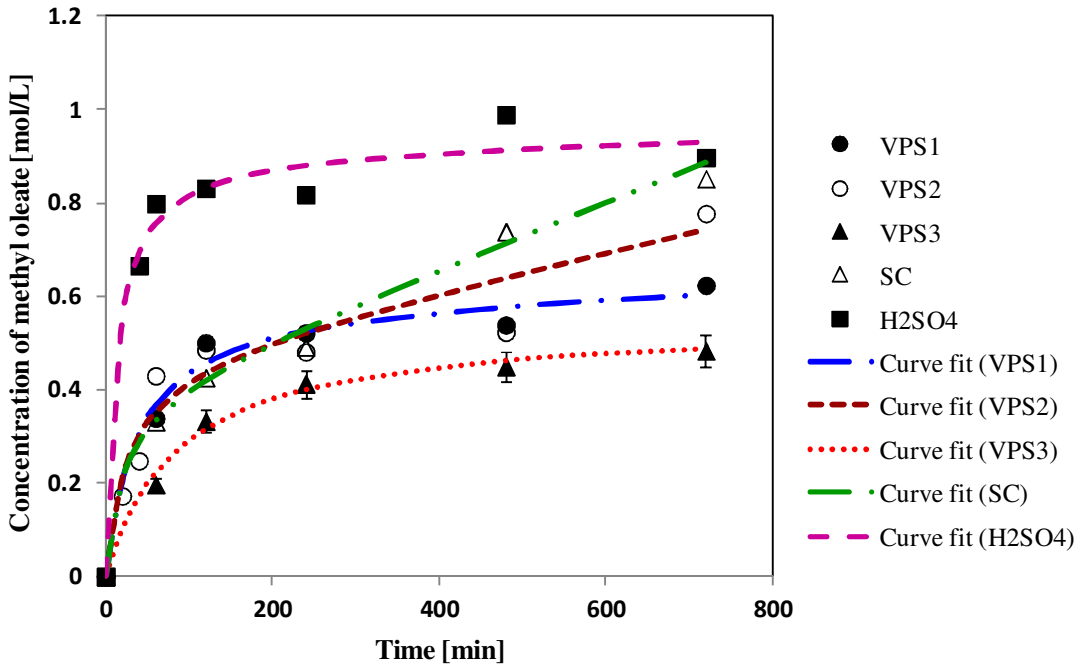

Figure 4–2 Experimental data with the best curve fit (broken lines) for the concentration of methyl oleate for all catalytic systems. Reaction conditions: molar ratio of methanol to oleic acid of 10 to 1, 3 wt.% catalyst based on oleic acid, reaction temperature at 80°C, and stirrer speed at 800 rpm. (Error bars represent the experimental standard deviation of two repeats)

As discussed in Chapter 3, the functional groups of the carbon-based catalysts consist of SO_3H, COOH, and OH; however, COOH and OH functional groups are inactive for esterification reaction (Takagaki et al. 2006; Nakajima et al. 2007). The reactivity of the carbon-based catalysts comes from Brønsted type active sites (SO_3H). It is generally known that strong liquid mineral acids such as H_2SO_4 and HCl are effective for the esterification of carboxylic acids, which also consist of

Brønsted type active sites (Liu et al. 2006). The reaction mechanism first involves protonation of the carboxylic acid, which activates the carboxylic acid for reaction with nonprotonated methanol to yield a tetrahedral intermediate which, by decomposition, produces the products of reaction, i.e., ester and water (Liu et al. 2006). The controlling step of the reaction is the nucleophilic attack of the alcohol on the protonated carbonyl group of the carboxylic acid (Lotero et al. 2005). One might expect a similar mechanism on solid acid catalysts with mainly Brønsted type active sites as shown in Figure 4-3 (Lerkkasemsan et al. 2010).

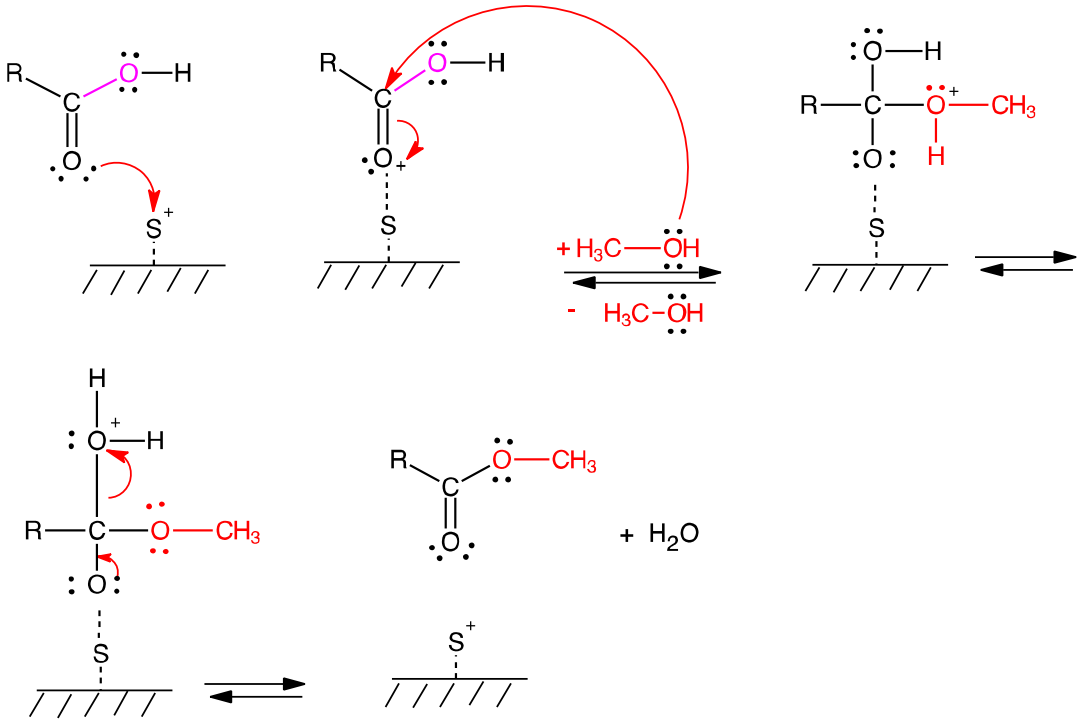

Figure 4–3 Mechanism of oleic acid esterification over carbon-based catalysts. Adapted from Lerkkasemsan et al. (2010).

Theoretically, a conversion of a reactant depends on the thermodynamics of the reaction such as temperature and molarity of the reactants; moreover, equilibrium conversion would be similar regardless of the type of catalyst. The difference among the catalysts is the rate of reaction, which is affected by their activity. H_2SO_4, VPS1, and VPS3 achieved maximum production of methyl oleate within 240 min into the reaction; whereas, SC and VPS2 showed an increasing production over time (Figure 4-2). This may be attributed to the difference in the magnitude of the catalyst deactivation. The equilibrium conversion (X_e) for the esterification of oleic acid with methanol at 80°C for an equal molar feed, calculated using the change in the Gibbs free energy (Fogler 2006), was 75% (Sample calculation is given in Appendix **C.4**). However, a higher methanol to oleic acid molar ratio (10:1) should drive the reaction forward for a complete conversion of oleic acid. The results showed that the conversion of oleic acid failed to achieve a complete conversion in all catalytic systems despite a high methanol to oleic acid molar ratio (Figure 4-2). Furthermore, this indicated that all catalysts underwent deactivation during the reaction.

4.3.2 Catalyst leaching

Generally, there are five causes of catalyst deactivation namely poisoning, fouling, thermal degradation (sintering, evapouration) often initiated by high temperature, mechanical damage and corrosion/leaching by the reaction mixture (Moulijn et al. 2001). Toda et al. (2005) reported that sugar catalyst does not dissolve in any solvent including hexane, methanol and acetone; however, Mo et al. (2008a) showed that the functional groups of the sulfonated carbon catalyst leach out when washed with methanol. Hence, study of catalyst leaching is necessary for the carbon-based catalysts.

The leaching of functional groups was studied by analysing the esterification product (the top layer) for pH and sulfate ions. The TGA, total acidity and chemical elemental analysis were analyzed for spent carbon-based catalysts. Figure 4-4 shows the comparison of the total acidity of fresh and spent carbon-based catalysts. The carbon-based catalyst lost as much as 11.6 – 21.4% acidity.

The determination of pH and the detection of sulfate ions of the esterification products at 2 and 8 h reaction times showed that the pH of all samples were very acidic (~pH 1) and traces of sulfate ions were detected in all samples. Since the functional groups of the carbon-based catalysts consisted of SO_3H, COOH, and OH, this implied the leaching of SO_3H and possibly COOH and OH groups into the reaction medium. Furthermore, Table 4-1 shows the elemental analysis of spent VPS2. In comparison with fresh VPS2, the mole amount of C and H had increased by 7 and 28%, respectively; whereas O and S had decreased by 10 and 33%, respectively. The amount of SO_3H of the spent VPS2 had decreased as much as 33% compared with the fresh VPS2.This further supports the potential leaching during the reaction. Nonetheless, the leaching of COOH and OH functional groups needs further investigation to ascertain this speculation.

Table 4-1 Elemental analysis of spent VPS2.

Sample	Elemental composition (wt.%)				Amount of SO_3H mmol/g	Mole ratio to carbon		
	C	H	O	S		H:C	O:C	S:C
Fresh VPS2	58.37	2.12	32.92	3.49	1.09	0.433	0.423	0.022
Spent VPS2	62.45	2.72	29.59	2.34	0.73	0.519	0.356	0.014

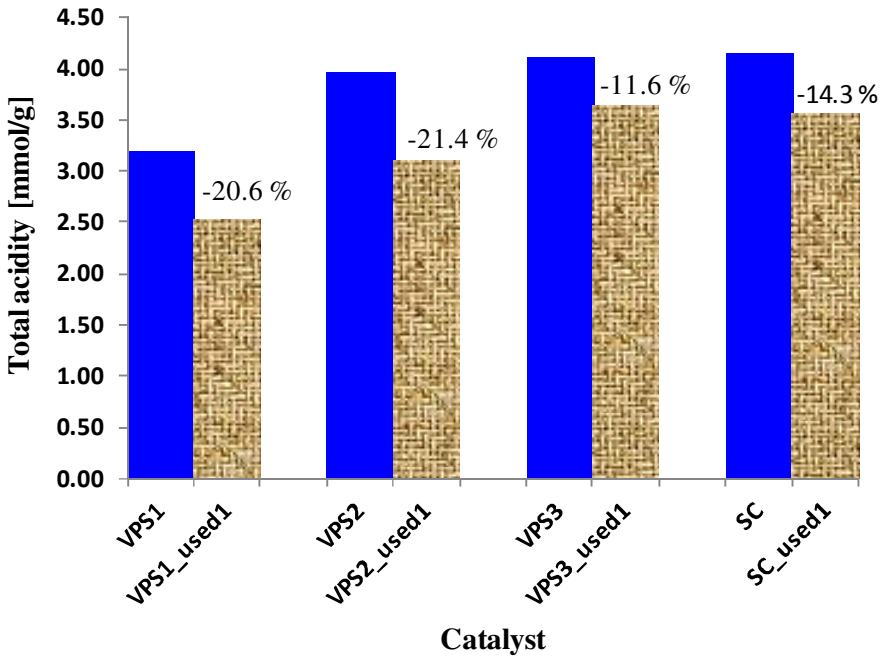

Figure 4–4 A comparison of total acidity between fresh and spent carbon-based catalysts. The percentages on the used catalyst bars are total acidity decrease among the catalysts.

The results of the thermo-gravimetric analysis of the VPS1 spent catalyst is shown in Figure 4-5, and for clarity, the result of the respective fresh catalyst is also included in the plot (The results of VPS2, VPS3, and sugar catalyst are shown in Appendix **C.5**). The DTA plots of the spent catalysts have a common similarity in comparison with the fresh catalysts (Figure 4-6). The spent catalysts do not have a peak at ~240^{o}C, instead, a smaller peak in terms of peak area is recorded at ~210^{o}C. This suggests that the spent catalysts did not have the same amount of functional groups as those of the fresh catalysts. In addition, the spent catalysts were less stable as the functional group decomposed at lower temperature (~210^{o}C). All but spent sugar catalyst had weight loss peak at lower temperatures compared to the fresh catalyst. This suggested that sugar catalyst was more thermally stable than the other carbon-based catalysts. The differences in weight loss among the fresh and spent catalysts at their respective functional groups decomposition temperatures were 1.9, 2.0, 2.4, and 1.0 % for VPS1, VPS2, VPS3, and sugar catalyst, respectively. This indicated that some of the functional groups had leached out during the reaction.

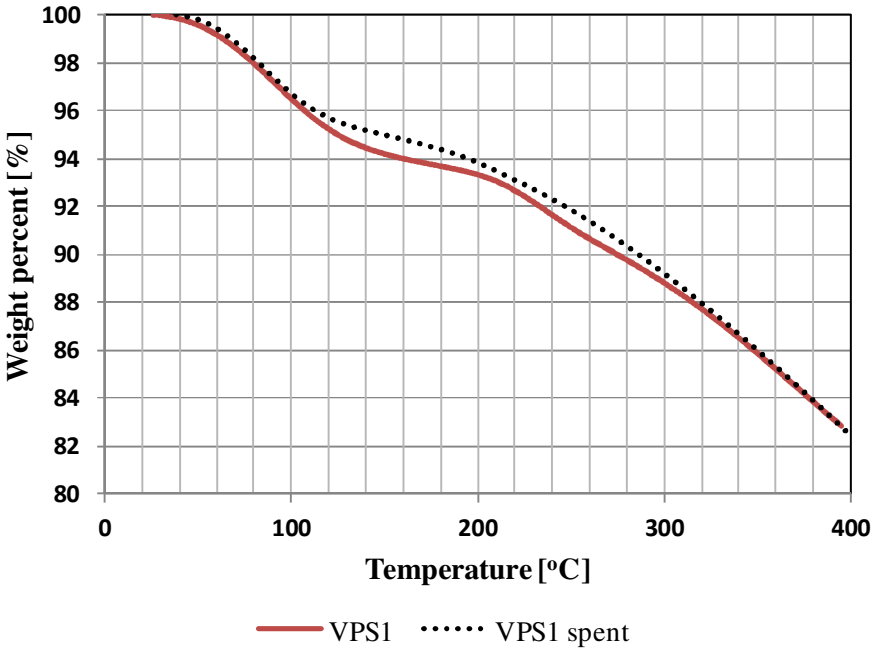

Figure 4–5 TGA of fresh and spent VPS1 under N_2.

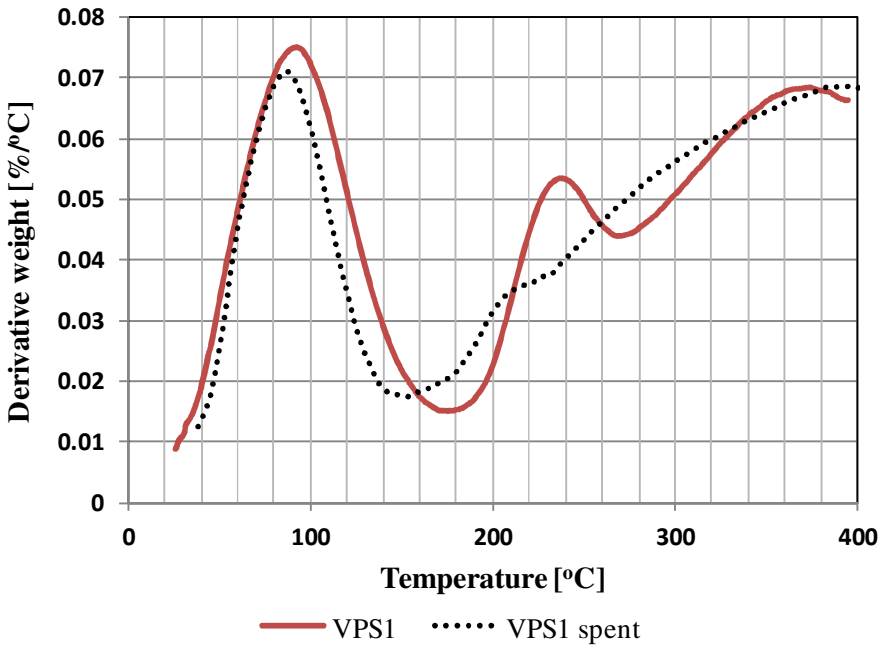

Figure 4–6 DTA of fresh and spent VPS1 under N_2.

As a summary, all analyses were in agreement that the functional groups of the carbon-based catalysts had leached out during the reaction. The leaching of functional groups as a result of the catalyst washing with acetone and methanol was, however, not ascertained. Further investigation on this possibility is useful to understand the property of the carbon-based catalysts. In addition, surface area, porosity and inductively coupled plasma (ICP) analyses could also be performed to understand the

physical changes in the spent catalysts. However, regardless of the cause of the leaching, understanding on the catalyst deactivation during the reaction is essential. In order to evaluate the magnitude of the catalyst deactivation, a mathematical model incorporating the kinetic of reaction and the kinetic of deactivation was developed.

4.3.3 Modelling of the catalyst deactivation

In general, the kinetic analysis of the reaction shows that the simple first and second order reaction models with respect to oleic acid concentration fit the data poorly for all catalytic systems (See kinetic analysis in Appendix **C.6**). This suggests that a different type of model is needed which incorporates a catalyst deactivation term. Several mathematical models reported in the literature describe the profile of the data for esterification of free fatty acids catalyzed by solid acid catalysts. These models are developed based on a single site (Eley-Rideal) theory (Liu et al. 2006; Lerkkasemsan et al. 2010). Even though the models fit the data very well, and the effect of water as the agent for catalyst deactivation is included, they are lacking explicit information on the magnitude of the catalyst deactivation. Hence, this study examines a kinetic model based on reaction kinetics and catalyst decay. As discussed in the previous section, one of the possible types of the catalyst deactivation is by pore blockage or inaccessibility of the internal active sites. This type of catalyst deactivation mimics the sintering problem encountered in general catalysis, which can be represented by second order catalyst deactivation kinetics (Fogler 2006).

Esterification of oleic acid with methanol is a reversible process producing methyl oleate and water, as shown in the stoichiometric equation in Figure 4-1 or, in a simplified form

$$A + M \leftrightarrows B + W$$

where: A – Oleic acid; M – Methanol; B – Methyl oleate (Biodiesel); W – Water.

The catalyst deactivation kinetic model was developed based on the following assumptions:

1. Reversible reaction is neglected since a large M:A ratio (10:1) was used in the experiments.
2. The order of reaction is a second order with respect to A. This is based on the kinetic analysis shown in Appendix **C.6**. A second order reaction fits the data better than first order reaction especially for the sugar catalyst system.
3. There was no methyl oleate and water at t = 0.
4. The rate of noncatalyzed reactions could be neglected compared to catalyzed ones.

In addition, the estimation of diffusion- and reaction-limited regimes using Weisz-Prater Criterion for internal diffusion showed that the esterification of oleic acid with methanol catalyzed by VPS1, VPS2, VPS3 is free from diffusion limitation (See Appendix **C.7**). Thus, the reaction is mainly controlled by the kinetics. Furthermore, internal diffusion is not an issue for sugar catalyst because it is a non-porous material.

An equation for conversion as a function of time can be obtained as follows:

Design equation:

$$N_{AO}\frac{dX}{dt} = -r_A{}'W$$

Equation 4-1

Reaction rate law:

$$-r_A{}' = k'a(t)C_A{}^2$$

Equation 4-2

Where a(t) is the catalyst deactivation activity.

Deactivation law: For second order deactivation

$$r_d = k_d a^2 = -\frac{da}{dt}$$

Integrating, with a =1 at time t = 0, yields

$$-\int_1^a \frac{1}{a^2}\,da = k_d\int_0^t dt$$

$$-\left[-\frac{1}{a}\right]_1^a = k_d t$$

$$\frac{1-a}{a} = k_d t$$

$$a(t) = \frac{1}{1+k_d t}$$

Equation 4-3

Stoichiometry:

$$C_A = C_{AO}(1-X) = \frac{N_{AO}}{V}(1-X)$$

Equation 4-4

Combining gives

$$\frac{dX}{dt} = \frac{W}{N_{AO}}k'a(t)\left(\frac{N_{AO}}{V}(1-X)\right)^2$$

$$\frac{dX}{dt} = \frac{WN_{AO}}{V^2}k'\left(\frac{1}{1+k_d t}\right)(1-X)^2$$

Equation 4-5

Let

$$k = \frac{WN_{AO}}{V^2}k'$$

Then, separating variables, we have

$$\frac{dX}{(1-X)^2} = ka(t)dt$$

Substituting for a and integrating yields

$$\int_0^X \frac{dX}{(1 - X)^2} = k \int_0^t \frac{1}{1 + k_d t} dt$$

$$\frac{1}{1 - X} - 1 = \frac{k}{k_d} \ln(1 + k_d t)$$

Solving for the conversion X at any time t, we find an equation involving the deactivation constant (k_d)

$$X = 1 - \frac{1}{\left(1 + \frac{k}{k_d} \ln(1 + k_d t)\right)}$$

Equation 4-6

The conversion of oleic acid is defined as

$$X_A = \left(1 - \frac{C_A}{C_{AO}}\right) \times 100\ \%$$

Equation 4-7

where C_{AO} is the initial concentration of oleic acid (mol/L), and C_A is the concentration of oleic acid at any time (mol/L).

The values of k and k_d were solved simultaneously using the nonlinear regression program in POLYMATH software (6.10 Educational release version), using the initial guess value of 1 for both model parameters (k and k_d). As shown in Figure 4-7, the catalyst deactivation model fits the data fairly well. The magnitude of the catalyst deactivation and its relationship with the chemical and physical properties of the carbon-based catalyst are discussed in the following section.

4.3.2.1 Effect of chemical and physical properties on the catalyst deactivation

Figure 4-7 shows that the conversion has more or less reached a plateau after 120 min of reaction. The maximum conversion of all the catalytic systems are varied and lower then the theoretical equilibrium conversion (0.75). These are consistent with the attributes of catalyst deactivation. As shown in Table 4-2, the values of k_d for all catalysts including H_2SO_4, indicated that all catalysts underwent deactivation during the esterification reaction. The deactivation constant is larger than the reaction constant for all catalytic systems indicating that the reaction was fast and the magnitude of the deactivation was significant. The values of reaction constant, deactivation constant, and conversion of oleic acid were gradually decreasing from VPS1, VPS2, to VPS3. Whereas, the sugar catalyst and sulfuric acid had the lowest and the highest k and k_d, respectively. Interestingly, the sugar catalyst and sulfuric acid had a comparable oleic acid conversion.

Table 4-2 Catalytic activity and kinetic model parameters.

Catalyst	Initial formation rate based on the catalyst			k, min^{-1}	k_d, min^{-1}	X, %
	Weight[a]	Surface area[b]	Acidity[c]			
VPS1	21.4	0.011	1.41	0.0204	0.1154	40
VPS2	33.3	0.066	1.77	0.0110	0.0403	38
VPS3	13.8	0.073	0.71	0.0062	0.0367	32
SC	26.2	5.500	1.33	0.0046	0.0050	61
H_2SO_4	68.1	-	0.70	0.1305	0.3404	65

[a] unit: mM/min.gcat; [b] unit: mM/min.m^2; [c] unit: mM/min.mmol H^+

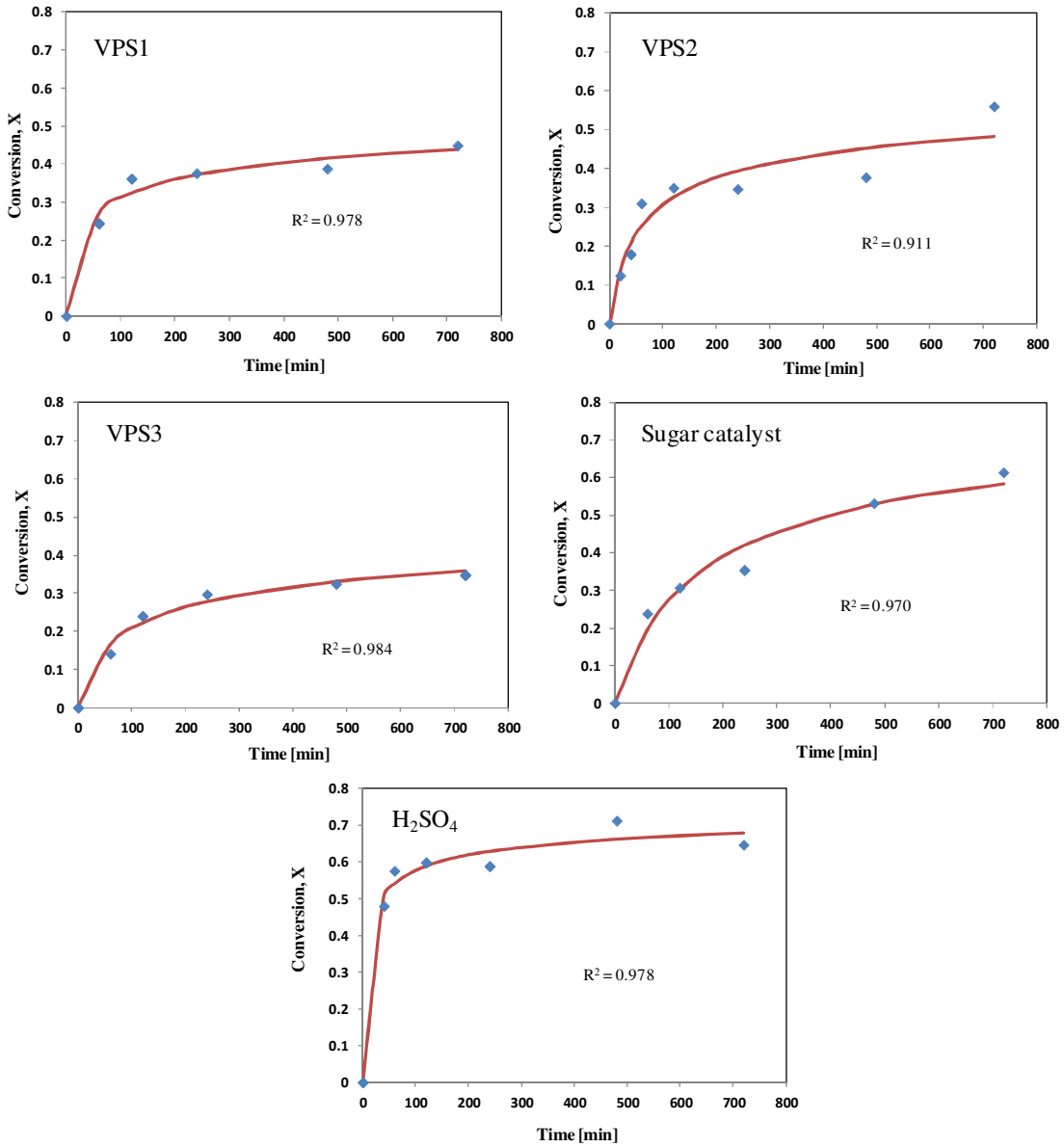

Figure 4–7 Comparison of experimental data with values predicted by the deactivation model (solid line) of VPS1, VPS2, VPS3, sugar catalyst, and H_2SO_4.

Since sulfuric acid is a homogeneous catalyst, leaching does not occur; instead, the deactivation is most likely due to the decrease of acid strength as a result of water solvation. It is well known that water deactivates homogeneous and heterogeneous catalysts in esterification of free fatty acid (Liu et al. 2006; Park et al. 2010a;b). Furthermore, water deactivates a catalyst by decreasing its acid strength due to the preference for water solvation of the protons over methanol solvation (Lotero et al. 2005). The driving force behind this behaviour was probably water's ability to form hydrogen-bonding networks that can delocalize 'free' protons in solutions (Liu et al. 2006). The activity of a catalyst is related to the population of the active sites on the surface; therefore, the catalyst deactivation can be considered as the decrease in the number of active sites on the surface (Forzatti and Lietti 1999). This implies that similar effect could also occur with the carbon-based catalysts.

Among the carbon-based catalysts, the sugar catalyst had the lowest deactivation constant (k_d). Being a non-porous material, the deactivation by pore blockage is unlikely to occur with the sugar catalyst. Hence, the deactivation is likely attributed to the catalyst leaching, on top of the decrease of acid strength due to water solvation effect. It is most likely that water causes the leaching of SO_3H group during the reaction, as the aromatic carbon sulfonation is a reversible reaction, and the presence of water could promote the formation of sulfuric acid (see Appendix **B.2**). Favourable reaction conditions such as high temperature and acidic medium make the reversible sulfonation reaction possible to occur. The decrease of SO_3H concentration in spent catalyst and the detection of sulfate ions in reaction product also supports SO_3H leaching. In addition, water also can cause the leaching of OH group through hydration of OH (Shu et al. 2010). The decrease of total acidity in all spent carbon-based catalyst might be attributed to the loss of OH group as well, in addition to the loss of SO_3H group.

Nevertheless, since the deactivation constant of VPS1, VPS2, and VPS3 are larger than the deactivation constant of the sugar catalyst, this suggests that there are other factors that influence the magnitude of the deactivation constant in VPS1, VPS2, and VPS3. Assuming the hydrophobicity of the carbon-based catalysts are comparable, since they are made from the same material, the accessibility of the active sites influence the deactivation constant in VPS1, VPS2, and VPS3. Since, the deactivation constants are decreasing from VPS1, VPS2, and VPS3, and the pore diameter and pore volume (Table 3-4) are also decreasing from VPS1, VPS2, and VPS3. This is counter-intuitive in a sense that the accessibility in larger pores is better than the smaller pores; however, suggests that the deactivation in the carbon-based catalysts is a combination of decrease of acid strength, leaching of functional groups, and accessibility of the active sites.

It is worthwhile to mention that a large surface area and mesoporous carbon-based catalyst as shown by VPS1 did not give any advantage on the catalyst activity. The activity of the catalyst depends on the accessibility and concentration of the active sites. The results also showed that the catalyst deactivation constant is independent of the surface area and the total acidity.

4.4 Conclusions

The activity of the carbon-based catalysts and H_2SO_4 on esterification of oleic acid with methanol was studied. VPS1, VPS2, VPS3, sugar catalyst, and H_2SO_4 had oleic acid conversion of 40, 38, 32, 61, and 65%, respectively. The difference in the catalytic activity among the catalysts tested was attributed to the density of acid sites per gram catalyst, catalyst deactivation, and accessibility of the active sites. For instance, H_2SO_4 showed the highest activity which is attributable to its high density of acid sites per gram. Even though VPS3 had the highest total acidity compared with VPS1 and VPS2, it had the lowest activity which is attributable to inaccessibility of the active sites. Furthermore, catalyst deactivation due to a decrease of acid strength and leaching of functional groups also affected the catalytic activity of the catalysts. The carbon-based catalysts lost 11.6 – 21.4% total acidity after first use in esterification of oleic acid. This loss was attributed to the leaching of functional groups as a result of reaction with water. H_2SO_4 underwent deactivation which is attributable to a decrease in acid strength because of solvation effect caused by water. The sugar catalyst had the lowest deactivation constant among the carbon-based catalysts which implied that it had the least catalyst deactivation. This might be attributable to its surface hydrophobicity and strategic location of the active site on the external surface. The catalyst deactivation analysis, as indicated by reaction and deactivation constants, implied that the order of catalyst activity, from the highest to the lowest, was H_2SO_4, sugar catalyst, VPS1, VPS2, and VPS3.

Chapter 5 Activity of carbon-based catalysts on etherification of glycerol

5.1 Introduction

As discussed in Chapter 1, Section 1.1.3, increased biodiesel production results in producing a large quantity of glycerol since 10 wt.% of the transesterification of triglycerides products is glycerol. This causes a large surplus of glycerol on the market globally. This issue has resulted in extensive research on converting glycerol into useful products (Pagliaro et al. 2007; Behr et al. 2008; Rahmat et al. 2010). One of the highly potential solutions is the conversion of glycerol to fuel oxygenates as the demand in the transportation industry is huge (Noureddini 2000; Behr and Obendorf 2001; Melero et al. 2010). Glycerol can be etherified using isobutylene or *tert*-butanol to produce mono, di- and tri-*tert*-butylglycerol ethers (Klepacova et al. 2005;2006a). In the fuel industry, di- and tri- *tert*-butylglycerol ethers (DTBGs and TTBG) are more useful products than mono- *tert*-butylglycerol ethers (MTBGs) because they can be blended with biodiesel to improve its properties such as reducing the cold flow properties (Noureddini 2000), and the emission toxicity (Jaecker-Voirol et al. 2008). DTBGs and TTBG can also be used as fuel oxygenates in diesel to enhance its Cetane Number (Bradin 1996; Bianchi and Battistel 2008). Since the use of methyl-*tert*-butyl ether (MTBE) as fuel oxygenate has been banned in the US due to its toxicity to the underground water, a substitute that is available in large quantity is needed (Borak et al. 1998; Ahmed 2001; Nadim et al. 2001). Hence, DTBGs and TTBG, which may become readily available in large quantity is highly potential as a substitute for MTBE.

Meanwhile, MTBGs cannot be used as biodiesel or diesel blends because they are not miscible. Higher polarity of MTBGs is associated to this low solubility (Klepacova et al. 2007). Nonetheless, there are limitations and benefits of using isobutylene and *tert*-butanol as etherifying agents. For instance, glycerol etherification with *tert*-butanol can be performed in ambient pressure; however, the selectivity to DTBGs and TTBG is low (Frusteri et al. 2009). The use of isobutylene produces a high yield of DTBGs and TTBG (Lee et al. 2010); however, the reaction condition is more complicated, such as the use of high pressure reaction (2 MPa) to overcome the thermodynamic limitation (to keep isobutylene in liquid phase), or the use of hazardous solvents such as dioxane, dimethyl sulfoxide and sulfolane (Klepacova et al. 2007).

Etherification of glycerol can be catalyzed by acid catalysts. There are numerous efforts in investigating the activity of commercial catalysts, as well as synthesizing new solid acid catalysts for etherification of glycerol (Barrault and Jerome 2008; Jerome et al. 2008). Klepáčová and co-workers (Klepacova et al. 2003;2005;2006a;2006b;2007) tried several commercial solid acid catalysts such as Amberlysts (15, 31, 35 and 119), ion-exchange resins (A-31 and A-119), and large-pore zeolites (H-Y and H-Beta) to catalyze glycerol etherification with isobutylene or *tert*-butanol. They found that etherification with *tert*-butanol leads to a lower conversion and selectivity owing to the presence of

water formed by dehydration of *tert*-butanol, which deactivates the catalysts. Nevertheless, Xiao et al. (2011) reported that the performance of H-Y Zeolites was enhanced after regeneration by washing with acid. Several new catalysts have been shown to be highly active, such as sulfonic-acid-functionalized mesostructured silicas (Melero et al. 2008), silicotungstic acid, cesium salt of silicotungstic acid, and ionic liquid containing sulfonic acid groups (Lee et al. 2010), and sulfonated peanut shell catalyst (Zhao et al. 2010).

It is known that acidity and pore structure of a catalyst are key factors for the etherification of glycerol by isobutylene and *tert*-butanol (Klepacova et al. 2006; Melero et al. 2008; Lee et al. 2011). In addition, the performance of a catalyst is also governed by the polarity of its surface. Materials with strong hydrophobic character are not active as they do not allow the adsorption of the glycerol. On the other hand, a strong adsorption of glycerol on the polar surfaces leads to low activity (Pariente et al. 2009). Based on the reaction nature of glycerol etherification, carbon-based catalysts are suitable because of their known high acidity and acid strength, their tunable pore structures and surface area, and the hydrophobic and hydrophilic characteristics on their surfaces (Liu et al. 2008; Hara 2010). In this chapter, the activity of the carbon-based catalysts on etherification of glycerol with isobutylene and the activity of the sugar catalyst on etherification of glycerol with *tert*-butanol (TBA) are reported.

5.2 Experimental

5.2.1 Etherification of glycerol with *tert*-butanol catalyzed by the sugar catalyst.

The etherification reaction was performed under batch conditions in a OMNI-Reactor Model 6100 at 80^{o}C, stirred at 800 rpm. A catalyst loading of 7 wt.% with respect to glycerol, with glycerol to *tert*-butanol molar ratio of 9:1 was used for the reaction. A 50 μL of sample was taken after 8 h of reaction and centrifuged at 10,000 rpm for 10 min to remove the catalyst. The clear supernatant was further diluted with methanol before being analyzed on a GC-MS (Varian), the mass spectrophotometer (Varian MS4000) was equipped with EI source, and the column was CPWax52CB (60 m x 0.25 mm x 0.25 μm). The heating program involved: initial column temperature at 40^{o}C held for 10 min; then heating ramped at 4^{o}C/min to 115^{o}C; and then at 15^{o}C/min to 240^{o}C. Total run time was ~50 min. Injection and detection chamber temperatures were set at 250^{o}C, with helium flow rate at 1.4 mL/min. The sample was not derivatized prior to analysis.

5.2.2 Etherification of glycerol with isobutylene catalyzed by the carbon-based catalysts.

The experiments were conducted in a 50 mL autoclave (Parr) equipped with: a sampling cylinder to inject a required amount of isobutylene; a sampling port to withdraw sample during the reaction; a vent line for purging the system with nitrogen as well as for venting; and a mechanic impeller, as shown in Figure 5-1.

The reaction conditions of the etherification study were: isobutylene to glycerol molar ratio at 2:1 (350 mmol of isobutylene and 175 mmol of glycerol); catalyst of 2 wt.% with respect to glycerol;

reaction temperature at 80°C; stirrer speed at 1200 rpm; and reaction pressure of 2 MPa. In a typical experiment, 175 mmol of glycerol was charged into the autoclave reactor, and then the system was purged with nitrogen three times. Isobutylene was charged into a 100 mL sampling cylinder (the isobutylene tank was padded with helium gas in order to deliver the required amount of isobutylene into the sampling cylinder). The sampling cylinder was quickly disconnected from the line and weighed to ensure the required amount of isobutylene in the sampling cylinder, which was then reconnected to the line. Isobutylene was then injected into the autoclave reactor by opening the outlet valve of the sampling cylinder and the inlet valve of the reactor. The stirrer was turned on and the reactor was pressurized to 2 MPa using nitrogen, followed by turning on the heater. The reaction was timed once the required temperature was reached which typically took 50 min. Reaction samples were taken at 3, 5, 8, 12 and 22 hr of reaction times. Further details of the experiment are given in Appendix **D**.

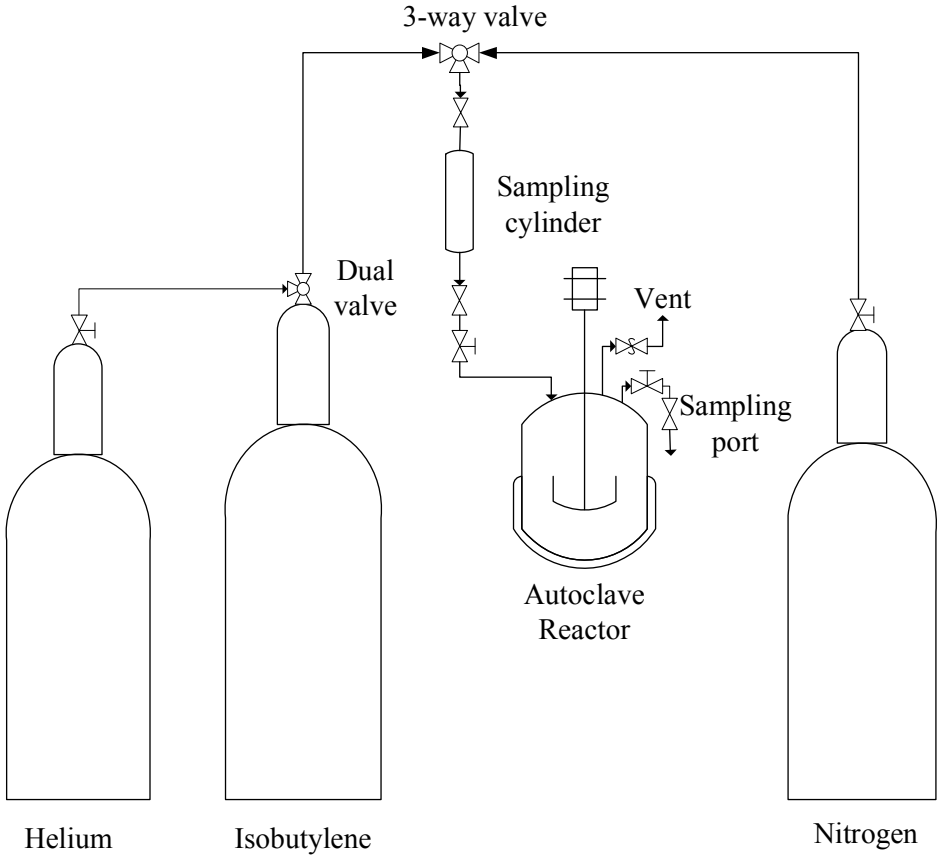

Figure 5–1 Schematic diagram of the experimental setup for the etherification of glycerol with isobutylene experiments.

5.2.2.1 Sample analysis

In principle, glycerol, MTBG, DTBG, and TTBG can be analyzed on highly inert columns coated with apolar stationary phases without derivatization. However, the inertness of the column, required to obtain good peak shapes, cannot be easily maintained in routine analysis. Derivatization by trimethylsilylation of the free hydroxyl groups of glycerol, MTBGs, DTBGs, and TTBG, ensures excellent peak shapes, good recoveries and low detection limits, and enormously improves the ruggedness of the procedure (Plank and Lorbeer 1995; Lee et al. 2010). Further structural information of glycerol molecule is given in Appendix **D.1**. Samples were thus derivatized by trimethylsilylation before being analyzed with a GC-MS. For complete silylation of glycerol and the glyceryl ethers, the condition of the derivatization was controlled carefully. In a typical derivatization, 10 µL of fresh sample was diluted 500 fold with dioxane. 50 µL of the diluted sample was mixed with 10 µL of internal standard and N-methy-N-(trimethylsilyl) trifluoroacetamide (MSTFA). The internal standard was prepared by dissolving 0.37 mmol 1,3-propanediol in 972 µL pyridine. The mixture was left for 30 min in a fume hood at ambient condition for the derivatization reaction to complete. The samples were further diluted with heptane before being analyzed with a GC-MS using a fused silica 60 m x 0.25 mm x 0.25 µm with CPWax52CB coating column. The temperature program was ramped at 10°C/min from 40 to 220°C and held for 2 min, using helium as the carrier gas with a column flow of 2 mL/min.

The glycerol conversion is defined as

$$X_G = \left(1 - \frac{C_G}{C_{GO}}\right) \times 100\ \%$$

Equation 5-1

where C_{GO} is the initial concentration of glycerol (mol/L), and C_G is the concentration of glycerol at any time (mol/L).

Whereas, the selectivity to glycerol ethers is defined as

$$S_y = \left(\frac{C_y}{C_{GO} - C_G}\right) \times 100\ \%$$

Equation 5-2

where C_y is the product concentration in which the subscript y refers to MTBGs, DTBGs, or TTBG.

5.3 Results and discussion

5.3.1 Etherification of glycerol with *tert*-butanol by using the sugar catalyst.

The objective of this experiment is to evaluate the activity of the sugar catalyst in terms of selectivity to fuel oxygenates (DTBGs and TTBG). The scheme of etherification of glycerol (G) with *tert*-butanol (TBA) main reactions is shown in Figure 5-2, water is produced as a co-product. Figure 5-3 shows the chromatogram and EI mass spectrum of the sample taken at 8 h of reaction. Using standard solution of MTBG (3-*tert*-butoxy-1,2-propanediol), peaks 1A and 2A were identified to be the isomers of MTBG.

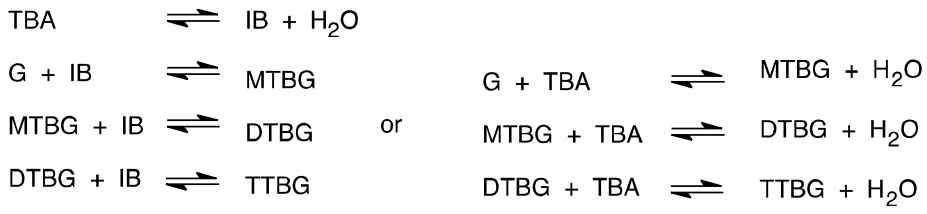

Figure 5–2 The scheme of etherification of glycerol with *tert*-butanol main reactions. Adapted from Klepacova et al. (2006a).

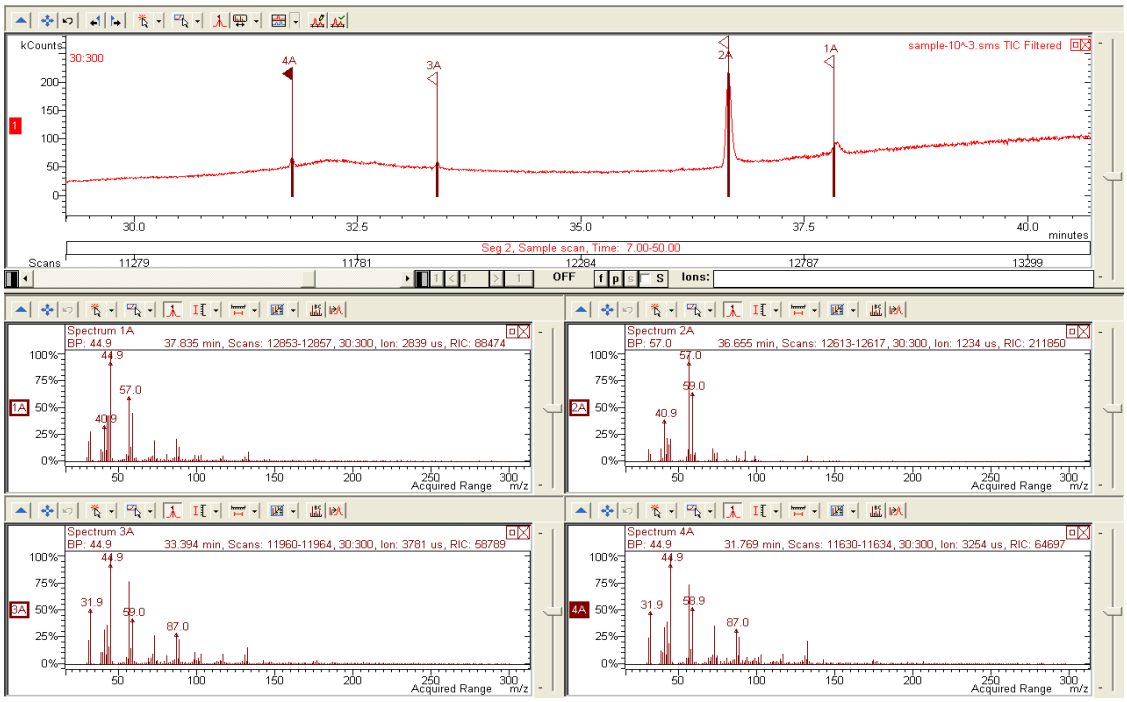

Figure 5–3 The chromatograms and EI mass spectrum of the etherification sample. Spectra (1A) and (2A) are isomers of mono-tert-butoxy-propane-1,2-diol, M = 148; spectra (3A) and (4A) are isomers of di-tert-butoxy-propane-2-ol, M = 204.

Direct comparison to the standard solutions of DTBGs and TTBG was not possible because at the time the experiment was done, they were not available on the market. Hence, the EI spectra were used to probe the presence of DTBGs and TTBG. Almost all EI spectra of the peaks were very similar to each other. The base peak at m/z = 45 corresponding to fragment ion $[C_3H_9]^+$, was detected in all spectra. Peak at m/z = 57 corresponds to fragment ion $[C_4H_9]^+$. These spectra are slightly different from the one report by Jamróz et al.(2007) where a peak at m/z = 57 was dominant. $[C_3H_9]$ is coming from – $(CH_3)_3$, forming *tert*-butoxy group in the glyceryl ethers. The spectra of peaks 3A and 4A suggest they are the isomers of DTBGs. The total peak area of 1A and 2A is greater than the total peak area of 3A and 4A, implying that for the reaction conditions used, the etherification selectivity is greater towards the formation of MTBGs.

Higher selectivity to MTBGs is most likely attributed to the formation of water as the co-product of the glycerol etherification with *tert*-butanol. The presence of water may cause deactivation of sugar catalyst, and shift the equilibrium reaction. The etherification of glycerol with *tert*-butanol can be catalyzed by the sugar catalyst, which is beneficial as the reaction does not require extreme conditions such as operating at high pressure, but the higher selectivity to MTBGs is not favourable. Hence, further investigation was necessary to find out a better glycerol etherification that gives a higher selectivity to DTBGs and TTBG. The results of the investigation of glycerol etherification with isobutylene, which has no water as co-product, catalyzed by the sugar catalyst, VPS1, VPS2, and VPS3 are presented in the following section.

5.3.2 Etherification of glycerol with isobutylene catalyzed by the carbon-based catalysts

The main objective is to evaluate the activity of the carbon-based catalysts (VPS1, VPS2, VPS3, and sugar catalyst) on etherification of glycerol with isobutylene. These catalysts have a varied range of total acidity as well as specific surface area as shown in Table 3-4. The spectrum of products from the etherification of glycerol with isobutylene is given in Figure 5-4. The main products are the glycerol ethers: two isomers of mono-*tert*-butylglycerols (MTBGs); di-*tert*-butylglycerols (DTBGs); and a tri-*tert*-butylglycerol (TTBG). There are two side products, i.e., *tert*-butanol and the dimers of isobutylene. In general, the etherification of glycerol is preferred on primary hydroxyl groups, i.e., formation of 1-*tert*-butylglycerols and 1,3-di-*tert*-butylglycerol (instead of 1,2- di-*tert*-butylglycerol) due to steric hindrance (Klepacova et al. 2007).

Glycerol and isobutylene in pure forms were immiscible. MTBGs functioned as a solvent that promoted the formation of a mixture. In this experiment, it was observed that the system became completely mixed only after 180 min into the reaction. Sampling was done only at the homogeneous mixture of the reaction. The glycerol conversion and the selectivity to MTBGs, DTBGs, and TTBG are shown in Figures 5-5 through 5-8. VPS1, VPS2, and SC showed comparable activity in glycerol conversion, and selectivity to MTBGs and DTBGs. Di-isobutylene was detected in all samples at 1320 min of reaction time.

Main reactions

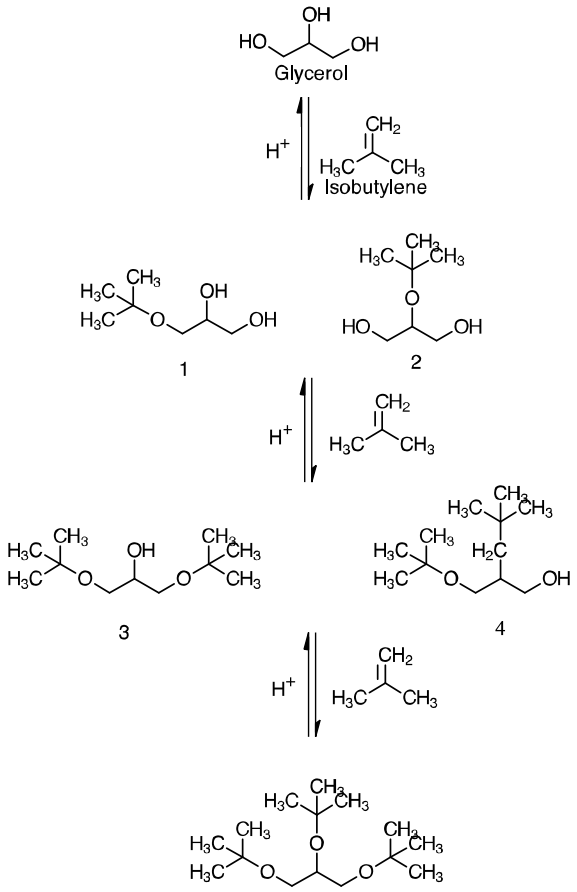

Side reactions

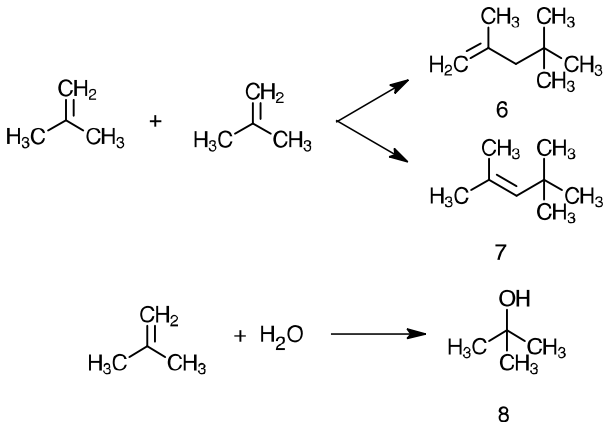

Figure 5–4 Product spectrum of glycerol etherification by isobutylene, showing the main and side reactions. (1) 3-*tert*-Butoxypropan-1,2-diol; (2) 2-*tert*-Butoxypropan-1,3-diol; (3) 1,3-Di-*tert*-butoxypropan- 2-ol; (4) 2,3-Di-*tert*-butoxypropan-1-ol; (5) 1,2,3-Tri-*tert*-butoxypropan; (6) 2,4,4-Trimethylpenten-1; (7) 2,4,4- Trimethylpenten-; (8) *tert*-Butanol.

Typically, dimerization of isobutylene occurs at relatively higher reaction temperatures (>90^{o}C), high molar ratio of isobutylene to glycerol (>4), and longer reaction time (>120 min) (Lee et al. 2010; Zhao et al. 2010). A 90 - 94% glycerol conversion was achieved after 1320 min of reaction for all carbon-based catalysts. The molar ratio of isobutylene to glycerol (2:1) used in this

experiment was lower than the stoichiometric molar ratio of a complete reaction (3:1) preventing a complete conversion of glycerol. A study using a statistical analysis by Melero et al. (2008) showed that isobutylene/glycerol molar ratio is the most important factor in the glycerol conversion. However, in this experiment, the physical dimension of the autoclave reactor limited the isobutylene/glycerol molar ratio to a maximum of 2:1; in other words, higher molar ratio resulted in lower glycerol liquid level in the reactor than the stirrer causing prolonged initial reaction to take place (Further details are given in Appendix **D.2**).

As shown in Figure 5-5, the catalytic activities of all carbon-based catalysts are comparable. This might be attributed to the relatively high total acidity for all carbon-based catalysts. Furthermore, these results showed that there was no steric hindrance limitation occurring in all catalysts since the activity mainly depends on the total acidity, in particular the amount of SO_3H groups. This is contrary to other types of catalyst such as Amberlyst and Zeolites, in which steric hindrance limits the activity and selectivity of the catalysts (Klepacova et al. 2003;2005;2006a;2006b;2007).

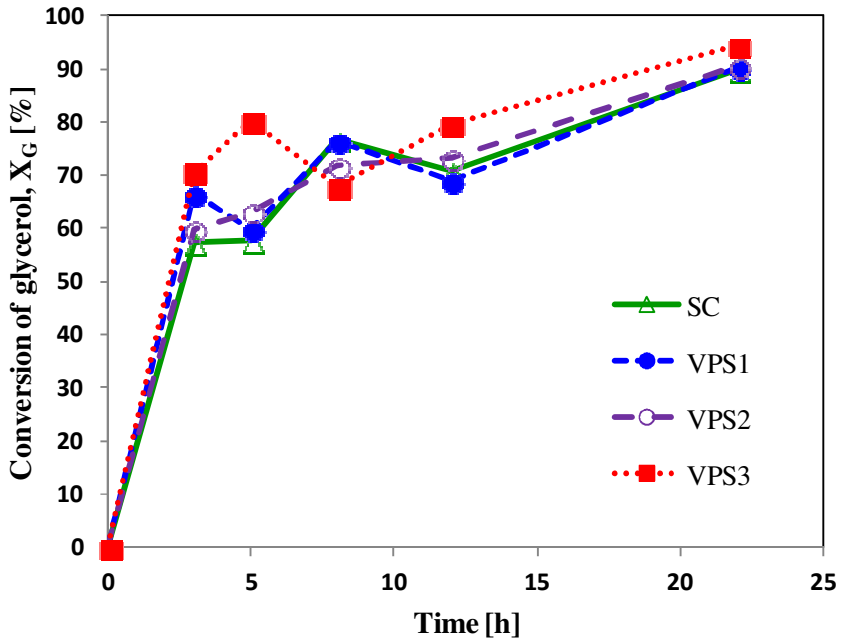

Figure 5–5 Activity of the carbon-based catalysts in terms of glycerol conversion. The reaction conditions: isobutylene to glycerol molar ratio at 2:1; catalyst of 2 wt.% with respect to glycerol; reaction temperature at 80°C; stirrer speed at 1200 rpm; and reaction pressure of 2 MPa.

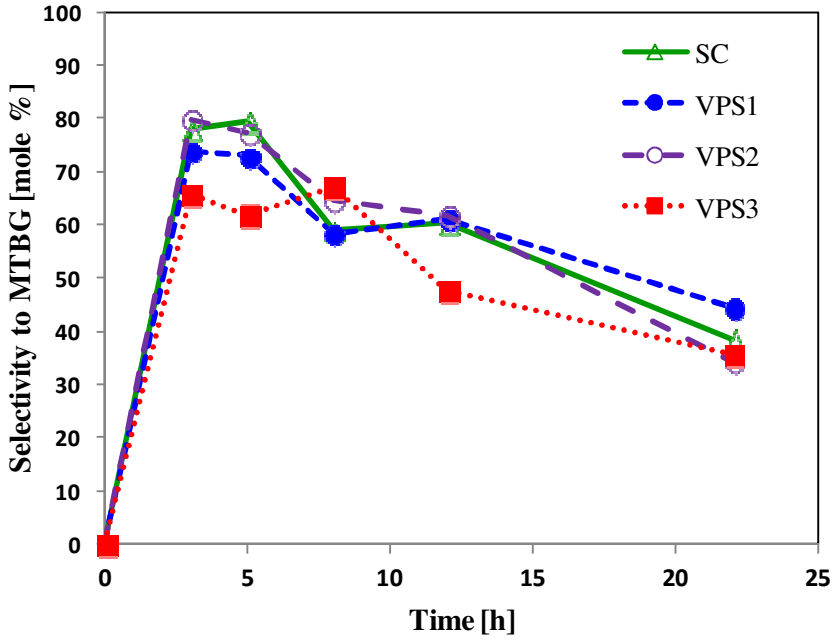

Figure 5–6 Selectivity to MTBG by the carbon-based catalysts in the glycerol etherification with isobutylene. The reaction conditions: isobutylene to glycerol molar ratio at 2:1; catalyst of 2 wt.% with respect to glycerol; reaction temperature at 80°C; stirrer speed at 1200 rpm; and reaction pressure of 2 MPa.

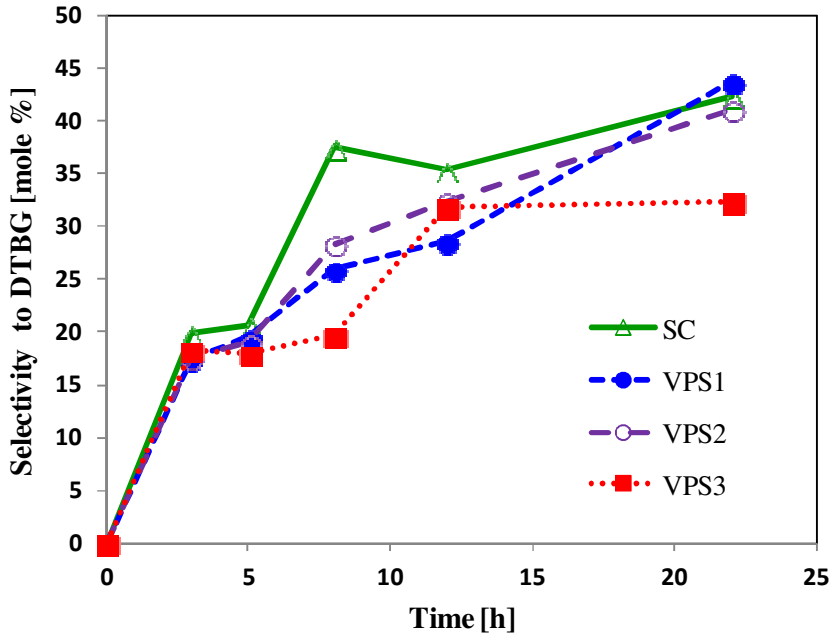

Figure 5–7 Selectivity to DTBG by the carbon-based catalysts in the glycerol etherification with isobutylene. The reaction conditions: isobutylene to glycerol molar ratio at 2:1; catalyst of 2 wt.% with respect to glycerol; reaction temperature at 80°C; stirrer speed at 1200 rpm; and reaction pressure of 2 MPa.

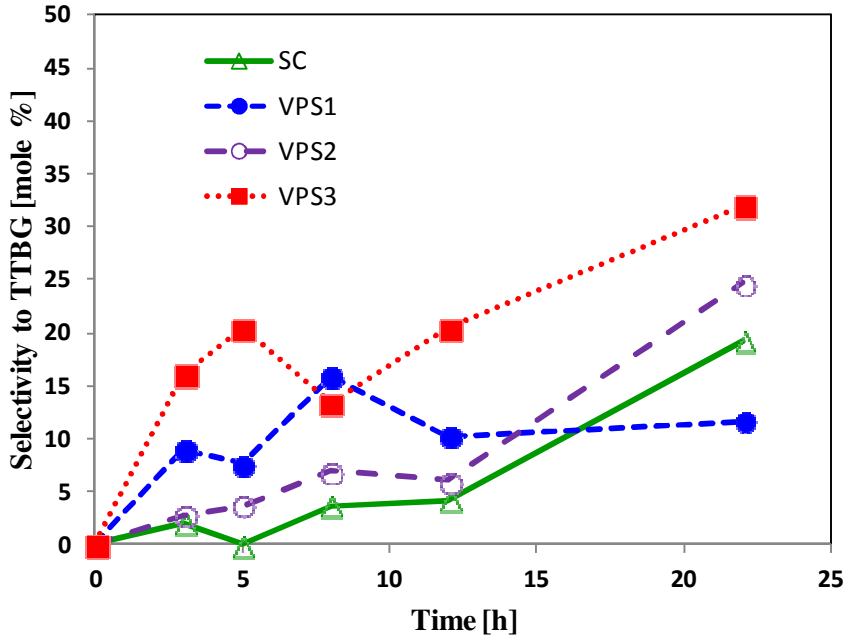

Figure 5–8 Selectivity to TTBG by the carbon-based catalysts in the glycerol etherification with isobutylene. The reaction conditions: isobutylene to glycerol molar ratio at 2:1; catalyst of 2 wt.% with respect to glycerol; reaction temperature at 80°C; stirrer speed at 1200 rpm; and reaction pressure of 2 MPa.

The hydrophobicity of the carbon-based catalysts is also essential. The hydrophobicity of the carbon-based catalysts comes from its carbon structure; whereas, its hydrophilicity comes from the functional groups (SO_3H, COOH, and OH). The hydrophobic and hydrophilic nature of the catalysts favoured the adsorption of the polar glycerol (Pariente et al. 2009). It is speculated that the reaction takes place between the *tert*-butyl cation (tertiary carbocation) and glycerol. Thus, it is likely that initially the electrophilic attack occurs on the primary carbon of glycerol due to steric hindrance and electrostatic effects exerted by OH groups of glycerol (Frusteri et al. 2009).

The selectivity to MTBG has initially increased as glycerol was being converted, but gradually decreased after 180 min of reaction as it was also being converted into DTBG (Figure 5-6). Figure 5-7 shows that the selectivity to DTBG for VPS1, VPS2, and SC are comparable (~42%) at 1320 min of reaction time, but only 32% for VPS3. This was due to a rapid conversion of DTBG into TTBG as shown in Figure 5-8. Longer reaction time favoured higher glycerol conversion and higher yield of higher glyceryl ethers (DTBG and TTBG). However, it had a negative effect as the unwanted side product, di-isobutylene, was also produced.

VPS3 showed the highest selectivity to TTBG at 1320 min of reaction, whereas VPS1 showed the lowest. This could be attributed to the total acidity of the catalysts. VPS1 had the highest surface area but was lowest in total acidity. In contrast, VPS3 had the highest acidity (SO_3H) and low surface area. This implies that the total acidity of the carbon-based catalysts played a key factor in the catalyst activity on the etherification of glycerol with isobutylene.

5.4 Conclusions

The activity of the carbon-based catalysts on etherification of glycerol with isobutylene and the etherification of glycerol with *tert*-butanol catalyzed by the sugar catalyst were studied. The use of *tert*-butanol as the etherifying agent had a high selectivity to MTBG, which was not favourable. In contrast, the use of isobutylene showed high glycerol conversion and selectivity to DTBGs and TTBG for VPS1, VPS2, VPS3 and the sugar catalyst. The results showed that total acidity played the key factor in the catalyst activity. High glycerol conversion (~94%) was achieved at 1320 min of reaction time, but also produced the unwanted di-isobutylene, suggesting that the reaction was best stopped at 720 min into the reaction. All carbon-based catalysts had selectivity to DTBGs and TTBG ranging from 38-52% at 720 min reaction time. In conclusion, the carbon-based catalysts show high potential as catalysts for the integration of esterification, transesterification, and etherification reactions. However, more trials are needed to ensure the reproducibility of the results. In addition, effect of thermal conversion, a reaction without any catalyst, is worth investigating.

Chapter 6 Conclusions and recommendations

6.1 Conclusions

Alternative fuels made from sustainable and renewable sources are essential for energy security, climate change mitigation, and pollution control. Biodiesel has already been produced in large capacity for commercial applications despite some potential setbacks such as escalating food prices and deforestation. In spite of a well-established process, production of biodiesel can be further improved by using low quality feedstock such as waste oils and fats, improving the economics of the process by adding value to the by-product, glycerol, and creating safer manufacturing operation. These improvements may be achieved by having an effective solid acid catalyst that is active on esterification, transesterification, and etherification reactions.

The main objective of this research was to synthesize high surface area, mesoporous, and high acidity carbon-based catalysts that have high activities on esterification and etherification reactions. All synthesized catalysts were physically and chemically characterized using X-ray photoelectron spectroscopy (XPS), porosimeter, Fourier transform-Infrared spectroscopy (FT-IR), scanning electron microscopy (SEM), transmission electron microscopy (TEM), thermo-gravimetric analysis (TGA), Pycnometry, Elemental analysis, and titration. Meanwhile, the activity of the catalysts was tested on the esterification of oleic acid, a typical model compound for free fatty acids, and on the etherification of glycerol, in which all samples were analyzed on a gas chromatrography-mass spectroscopy (GC-MS).

The first major contribution was the synthesis of mesoporous and high surface area carbon-based catalyst using a silica templating method. A silica templating method was prepared using the confined activation process where its pore size could be controlled by adjusting the P/Si molar ratio. Glucose was used as a carbon precursor to fill the pores in the silica template, while pyrolysis at 400^{o}C produced an incomplete carbonized sugar and silica composite. Subsequent removal of the silica template using HF produced a high surface area and mesoporous disordered amorphous sugar char. Sulfonation of the sugar char in a fuming sulfuric acid with or without prior silica template removal produced two different catalysts. Sulfonation before the removal of the silica template produced a catalyst with a high surface area and mesoporous, but low total acidity (CMK-SO_3H-w). In contrast, sulfonation after the silica template removal produced a catalyst with a low surface area and non-porous but high acidity (CMK-w-SO_3H). Sulfonation of the mesoporous char in a liquid fuming sulfuric acid completely destroyed the internal pores. The results showed that the silica template functioned as a support for internal pore walls from collapsing, but prevented effective functionalization on the char during the sulfonation. The comparison of catalyst activity on the esterification of oleic acid with methanol showed that CMK-w-SO_3H was more active than CMK-SO_3H-w. This implied that total acidity played a more important role than the surface area or porosity in the carbon-based catalysts. A better synthesis technique was needed to produce a high surface area,

mesoporous, and high acidity carbon-based catalyst, which led to the second major contribution – the development of a simple and effective functionalization technique called multiple vapour phase sulfonation.

Contrary to the sulfonation by heating in the liquid sulfuric acid (liquid sulfonation), vapour phase sulfonation was a functionalization technique whereby the char was exposed to a stream of sulfuric acid vapour. As a result, high surface area, mesoporous and high acidity carbon-based catalysts were produced. The results showed that repeating sulfonation and washing was able to gradually increase the total acidity but at the expense of its surface area and pore volume. With this technique, a carbon-based catalyst with a predictable surface area and total acidity was easily obtained.

The activities of four carbon-based catalysts (VPS1, VPS2, VPS3, and the sugar catalyst), consisting of a wide range of surface area and total acidity, were investigated on esterification of oleic acid with methanol and on etherification of glycerol with isobutylene. The results for the esterification experiments showed that the activity of the catalysts depended on the concentration of acid sites per gram catalyst, catalyst deactivation, and accessibility of the active sites. Furthermore, the catalyst deactivation was most likely due to the presence of water that caused catalyst leaching and decreased of active site strength. Meanwhile, in the etherification experiments, the results showed that the carbon-based catalysts had a comparable activity with a high selectivity to higher glyceryl ethers (fuel oxygenates). Furthermore, the activity of the carbon-based catalysts was dependent on the total acidity while being independent of surface area and pore diameter.

In conclusion, carbon-based catalysts with high activity on esterification and etherification reactions were successfully synthesized. The carbon-based catalysts are promising catalysts for a more efficient biodiesel production, with potential for the integration of esterification, transesterification and etherification reactions. Nevertheless, investigation on the full life cycle analysis of the carbon-based catalyst preparation ought to be done in order to understand its impact on the environment.

6.2 Recommendations for future works

Further investigations are recommended to understand the behaviour and to explore their commercial application of the carbon-based catalysts, such as:

1. Study of reusability and regeneration of carbon-based catalysts. In addition, study of catalyst leaching due to the washing with solvents is also important.
2. Study of the multiple vapour phase sulfonation of higher surface area, bigger pore size, and thicker pore wall chars.

   The mesoporous sugar char used in this investigation was prepared via the silica templating method using the P/Si molar ratio of 0.31. Had different P/Si molar ratios been used, the physical and chemical properties of the resulting carbon-based

catalysts are speculated to be varied. Mesoporous sugar char can also be prepared from many other techniques such as alumina oxide template, and chemical and physical activation.

3. Study of the sulfonation of char prepared at higher carbonization temperatures (i.e., 450 – 800^{o}C).

   A higher carbonization temperature produces a more graphitic carbon structure and is most likely to exhibit different physical and chemical properties which may be beneficial to the catalyst activity.

4. Determination of the strength of active sites.

   In addition to the total acidity, information on the strength of active sites gives a better understanding of the carbon-based catalysts' characteristics.

5. Study of simultaneous esterification, transesterification, and etherification reactions by the carbon-based catalysts.

   Simultaneous esterification, transesterification, and etherification reactions experiments should be carried out using the carbon-based catalysts. This would give important insight on the development of integrated biodiesel production.

6. Study on the use of a renewable source to replace isobutylene for the etherification process.

   Although the use of isobutylene favour the selectivity to DTBGs and TTBG in the etherification reaction, the use of high pressure to maintain the liquid state requires additional energy. In addition, isobutylene is non-renewable; therefore, a more environmentally-friendly compound should to be sought.

Bibliography

Abdulla, R., Chan, E. S., and Ravindra, P. (2011). "Biodiesel production from Jatropha curcas: a critical review." *Crit. Rev. Biotechnol.,* 31(1), 53-64.

Achten, W. M. J., Maes, W. H., Aerts, R., Verchot, L., Trabucco, A., Mathijs, E., Singh, V. P., and Muys, B. (2010). "Jatropha: From global hype to local opportunity." *J. Arid Environ.,* 74(1), 164-165.

Achten, W. M. J., Verchot, L., Franken, Y. J., Mathijs, E., Singh, V. P., Aerts, R., and Muys, B. (2008). "Jatropha bio-diesel production and use." *Biomass Bioenergy,* 32(12), 1063-1084.

Adhikari, S., Fernando, S. D., and Haryanto, A. (2008). "Hydrogen production from glycerin by steam reforming over nickel catalysts." *Renewable Energy,* 33(5), 1097-1100.

Ahmad, A. L., Yasin, N. H. M., Derek, C. J. C., and Lim, J. K. (2011). "Microalgae as a sustainable energy source for biodiesel production: A review." *Renewable Sustainable Energy Rev.,* 15(1), 584-593.

Ahmed, F. E. (2001). "Toxicology and human health effects following exposure to oxygenated or reformulated gasoline." *Toxicol. Lett.,* 123(2-3), 89-113.

Ali, Y., and Hanna, M. A. (1994). "Alternative diesel fuels from vegetable oils." *Bioresour. Technol.,* 50(2), 153-163.

Altin, R., Cetinkaya, S., and Yucesu, H. S. (2001). "The potential of using vegetable oil fuels as fuel for diesel engines." *Energy Conv. Manag.,* 42(5), 529-538.

American Water Works Association, Water Pollution Control Federation, and American Public Health Association. (1981). *Standard methods for the examination water and wastewater.* American Public Health Association, Washington, D.C.

Anderson, G. (2008). "Adsorbent-catalyst materials for purification of biofuels and biodiesel with supercritical regeneration." *U.S.Pat.Appl.Publ.,* 2008-143706; 2007-945895(2008318763), 14.

Arzamendi, G., Campo, I., Arguiñarena, E., Sánchez, M., Montes, M., and Gandía, L. M. (2007). "Synthesis of biodiesel with heterogeneous NaOH/alumina catalysts: Comparison with homogeneous NaOH." *Chem. Eng. J.,* 134(1-3), 123-130.

Atadashi, I. M., Aroua, M. K., and Aziz, A. A. (2011). "Biodiesel separation and purification: A review." *Renewable Energy,* 36(2), 437-443.

Bakeas, E., Karavalakis, G., and Stournas, S. (2011). "Biodiesel emissions profile in modern diesel vehicles. Part 1: Effect of biodiesel origin on the criteria emissions." *Sci. Total Environ.,* 409(9), 1670-1676.

Balat, M. (2009). "New biofuel production technologies." *Energy Educ. Sci. Technol., Part A,* 22(2), 147-161.

Barrault, J., and Jerome, F. (2008). "Design of new solid catalysts for the selective conversion of glycerol." *Eur. J. Lipid Sci. Technol.,* 110(9), 825-830.

Bartholomew, C. H., and Farrauto, R. J. (2006). *Fundamentals of industrial catalytic processes.* John Wiley & Sons., New Jersey.

Basha, S. A., and Gopal, K. R. (2012). "A review of the effects of catalyst and additive on biodiesel production, performance, combustion and emission characteristics." *Renewable Sustainable Energy Rev.,* 16(1), 711-717.

Basiron, Y. (2007). "Palm oil production through sustainable plantations." *Eur. J. Lipid Sci. Technol.,* 109, 289-295.

Behr, A., Eilting, J., Irawadi, K., Leschinski, J., and Lindner, F. (2008). "Improved utilization of renewable resources: New important derivatives of glycerol." *Green Chem.,* 10(1), 13-30.

Behr, A., and Obendorf, L. (2001). "Process development for acid-catalysed etherification of glycerol with isobutene to form glycerol tertiary butyl ethers." *Chem. Ing. Tech.,* 73(11), 1463-1467.

Bergman, R. G., Ellman, J. A., and Arceo Rebollo, E. (2008). "Conversion of glycerol from biodiesel production to allyl alcohol." *PCT Int.Appl.,* 2008-US52111; 2007-886661(2008092115), 9.

Berrios, M., and Skelton, R. L. (2008). "Comparison of purification methods for biodiesel." *Chem. Eng. J.,* 144(3), 459-465.

Bertram, B., Abrams, C., and Cooke, B. S. (2005). "Magnesium silicate adsorbent for purification of glyceride-based fatty acid Methyl esters (biodiesel)." *U.S.Pat.Appl.Publ.,* 2004-956856; 2003-509959(2005081436), 12.

Bianchi, D., and Battistel, E. (2008). "Glycerol derivatives as fuel components." *Future Feedstocks for Fuels and Chemicals, DGMK Conference September 29 – October 1, 2008, Berlin, Germany*

Bloch, M., Bournay, L., Casanave, D., Chodorge, J. A., Coupard, V., Hillion, G., and Lorne, D. (2008). "Fatty acid esters in Europe: Market trends and technological perspectives." *Oil Gas Sci. Technol.,* 63(4), 405-417.

Boehm, H. P. (2002). "Surface oxides on carbon and their analysis: a critical assessment." *Carbon,* 40(2), 145-149.

Borak, J., Pastides, H., Van Ert, M., Russi, M., and Herzstein, J. (1998). "Exposure to MTBE and acute human health effects: A critical literature review." *Hum. Ecol. Risk Assess.,* 4(1), 177-200.

Brian J., G. (2011). "The economics of producing biodiesel from algae." *Renewable Energy,* 36(1), 158-162.

Brunauer, S., Emmett, P. H., and Teller, E. (1938). "Adsorption of gases in multimolecular layers." *J. Am. Chem. Soc.,* 60, 309-319.

Bruno, T. J., Lovestead, T. M., Riggs, J. R., Jorgenson, E. L., and Huber, M. L. (2011). "Comparison of diesel fuel oxygenate additives to the composition-explicit distillation curve method. Part 1: Linear compounds with one to three oxygens." *Energy Fuels,* 25(6), 2493-2507.

Budarin, V., Clark, J. H., Hardy, J. J. E., Luque, R., Milkowski, K., Tavener, S. J., and Wilson, A. J. (2006). "Starbons: new starch-derived mesoporous carbonaceous materials with tunable properties." *Angew. Chem. Int. Ed.,* 45(23), 3782-3786.

Budarin, V. L., Clark, J. H., Luque, R., Macquarrie, D. J., Koutinas, A., and Webb, C. (2007). "Tunable mesoporous materials optimised for aqueous phase esterifications." *Green Chem.,* 9(9), 992-995.

Canakci, M., and Sanli, H. (2008). "Biodiesel production from various feedstocks and their effects on the fuel properties." *J. Ind. Microbiol. Biotechnol.,* 35(5), 431-441.

Canakci, M., and Van Gerpen, J. H. (2003). "Comparison of engine performance and emissions for petroleum diesel fuel, yellow grease biodiesel, and soybean oil biodiesel." *Trans. ASAE,* 46(4), 937-944.

Carter, C., Finley, W., Fry, J., Jackson, D., and Willis, L. (2007). "Palm oil markets and future supply." *Eur. J. Lipid Sci. Technol.,* 109, 307-314.

Celikten, I., Koca, A., and Arslan, M. A. (2010). "Comparison of performance and emissions of diesel fuel, rapeseed and soybean oil methyl esters injected at different pressures." *Renewable Energy,* 35(4), 814-820.

Cerrate, S., Yan, F., Wang, Z., Coto, C., Sacakli, P., and Waldroup, P. W. (2006). "Evaluation of glycerine from biodiesel production as a feed ingredient for broilers." *Int. J. Poultry Sci.,* 5(11), 1001-1007.

Chen, H., Wang, J., Shuai, S., and Chen, W. (2008). "Study of oxygenated biomass fuel blends on a diesel engine." *Fuel,* 87(15-16), 3462-3468.

Cheng, Y., Lu, Y., Gao, C., and Wu, Q. (2009). "Alga-based biodiesel production and optimization using sugar cane as the feedstock." *Energy Fuels,* 23(8), 4166-4173.

Chew, T. L., and Bhatia, S. (2008). "Catalytic processes towards the production of biofuels in a palm oil and oil palm biomass-based biorefinery." *Bioresour. Technol.,* 99(17), 7911-7922.

Chincholkar, S. P., Srivastava, S., Rehman, A., Dixit, S., and Lanjewar, A. (2005). "Biodiesel as an alternative fuel for pollution control in diesel engine." *Asian J. Exp. Sci.*, 19(2), 13-22.

Chisti, Y. (2008). "Biodiesel from microalgae beats bioethanol." *Trends Biotechnol.,* 26(3), 126-131.

Chouhan, A. P. S., and Sarma, A. K. (2011). "Modern heterogeneous catalysts for biodiesel production: A comprehensive review." *Renewable Sustainable Energy Rev.,* 15(9), 4378-4399.

Chuah, T. G., Wan Azlina, A. G. K., Robiah, Y., and Omar, R. (2006). "Biomass as the renewable energy sources in Malaysia: An overview." *Int. J. Green Energy,* 3(3), 323-346.

Corley, R. H. V. (2009). "How much palm oil do we need?" *Environ. Sci. Policy,* 12(2), 134-139.

Costa, J. A. V., and de Morais, M. G. (2011). "The role of biochemical engineering in the production of biofuels from microalgae." *Bioresour.Technol.,* 102(1), 2-9.

Crabbe, E., Nolasco-Hipolito, C., Kobayashi, G., Sonomoto, K., and Ishizaki, A. (2001). "Biodiesel production from crude palm oil and evaluation of butanol extraction and fuel properties." *Process Biochem.,* 37(1), 65-71.

de Gorter, H., Drabik, D., and Just, D. R. (2011). "The economics of a blender's tax credit versus a tax exemption: the case of U.S.. "splash and dash" biodiesel exports to the European Union." *Appl. Econ. Perspect. Pol., 33(4), 510-527.*

Dehkhoda, A. M., West, A. H., and Ellis, N. (2010). "Biochar based solid acid catalyst for biodiesel production." *Appl. Catal., A,* 382(2), 197-204.

Della Casa, G., Bochicchio, D., Faeti, V., Marchetto, G., Poletti, E., Rossi, A., Garavaldi, A., Panciroli, A., and Brogna, N. (2009). "Use of pure glycerol in fattening heavy pigs." *Meat Sci.,* 81(1), 238-244.

Demirbas, A. (2002). "Biodiesel from vegetable oils via transesterification in supercritical methanol." *Energy Convers. Manage.,* 43(17), 2349-2356.

Demirbas, A. (2006). "Biodiesel production via non-catalytic SCF method and biodiesel fuel characteristics." *Energy Convers. Manage.,* 47(15-16), 2271-2282.

Demirbas, A. (2007). "Comparison of transesterification methods for production of biodiesel from vegetable oils and fats." *Energy Convers. Manage.,* 49(1), 125-130.

Demirbas, M. F. (2009). "World biofuel scenario." *Handbook of plant-based biofuels.* CRC Press, Boca Raton, 13-28.

Di Serio, M., Cozzolino, M., Giordano, M., Tesser, R., Patrono, P., and Santacesaria, E. (2007). "From homogeneous to heterogeneous catalysts in biodiesel production." *Ind. Eng. Chem. Res.,* 46(20), 6379-6384.

Di Serio, M., Ledda, M., Cozzolino, M., Minutillo, G., Tesser, R., and Santacesaria, E. (2006). "Transesterification of soybean oil to biodiesel by using heterogeneous basic catalysts." *Ind. Eng. Chem. Res.,* 45(9), 3009-3014.

Di Serio, M., Tesser, R., Pengmei, L., and Santacesaria, E. (2008). "Heterogeneous catalysts for biodiesel production." *Energy Fuels,* 22(1), 207-217.

Du, W., Li, W., Sun, T., Chen, X., and Liu, D. (2008). "Perspectives for biotechnological production of biodiesel and impacts." *Appl. Microbiol. Biotechnol.,* 79(3), 331-337.

Du, W., Xu, Y., Liu, D., and Zeng, J. (2004a). "Comparative study on lipase-catalyzed transformation of soybean oil for biodiesel production with different acyl acceptors." *J. Mol. Catal. B: Enzym.,* 30(3-4), 125-129.

Du, W., Xu, Y., Zeng, J., and Liu, D. (2004b). "Novozym 435-catalyzed transesterification of crude soya bean oils for biodiesel production in a solvent-free medium." *Biotechnol. Appl. Biochem.,* 40(2), 187-190.

Enweremadu, C. C., and Mbarawa, M. M. (2009). "Technical aspects of production and analysis of biodiesel from used cooking oil—A review." *Renewable Sustainable Energy Rev.,* 13(9), 2205-2224.

Ewing, M., and Msangi, S. (2009). "Biofuels production in developing countries: assessing tradeoffs in welfare and food security." *Environ. Sci. Policy,* 12(4), 520-528.

FAO. (2008). *The State of Food and Agriculture. Biofuels: prospects, risks and opportunities.* Food and Agriculture Organization of the United Nations, Rome. http://www.fao.org/docrep/011/i0100e/i0100e00.htm (11/04, 2011).

Fjerbaek, L., Christensen, K. V., and Norddahl, B. (2009). "A review of the current state of biodiesel production using enzymatic transesterification." *Biotechnol. Bioeng.,* 102(5), 1298-1315.

Flach, B., Lieberz, S., Bendz, K., and Dahlbacka, B. (2011). "EU-27 Annual Biofuels Report." *Rep. No. NL1013,* USDA Foreign Agricultural Service, The Hague.

Fogler, H. S. (2006). *Elements of chemical reaction engineering*. Prentice Hall, Upper Sadle River.

Forzatti, P., and Lietti, L. (1999). "Catalyst deactivation." *Catal. Today,* 52(2-3), 165-181.

Frusteri, F., Arena, F., Bonura, G., Cannilla, C., Spadaro, L., and Di Blasi, O. (2009). "Catalytic etherification of glycerol by *tert*-butyl alcohol to produce oxygenated additives for diesel fuel." *Appl. Catal., A,* 367(1-2), 77-83.

Fukuhara, K., Nakajima, K., Kitano, M., Kato, H., Hayashi, S., and Hara, M. (2011). "Structure and catalysis of cellulose-derived amorphous carbon bearing SO_3H groups." *ChemSusChem,* 4(6), 778-784.

Furuta, S., Matsuhashi, H., and Arata, K. (2004). "Biodiesel fuel production with solid superacid catalysis in fixed bed reactor under atmospheric pressure." *Catal. Commun.,* 5(12), 721-723.

Gaffney, J. S., and Marley, N. A. (2009). "The impacts of combustion emissions on air quality and climate – From coal to biofuels and beyond." *Atmos. Environ.,* 43(1), 23-36.

Gao, Y. (2007). "Novel heterogeneous esterification and transesterification catalysts for producing low-cost biodiesel from high-FFA feedstocks." *Prepr.Symp.- Am.Chem.Soc., Div.Fuel Chem.,* 52(2), 304.

Garcia, E., Laca, M., Perez, E., Garrido, A., and Peinado, J. (2008). "New class of acetal derived from glycerin as a biodiesel fuel component." *Energy Fuels,* 22(6), 4274-4280.

Geng, L., Wang, Y., Yu, G., and Zhu, Y. (2011). "Efficient carbon-based solid acid catalysts for the esterification of oleic acid." *Catal. Commun.,* 13(1), 26-30.

Goetsch, D., Machay, I. S., and White, L. R. (2008). "Production of methanol from the crude glycerol by-product of producing biodiesel." *U.S.,* 2007-825018(7388034), 6.

Goh, C. S., and Lee, K. T. (2010). "A visionary and conceptual macroalgae-based third-generation bioethanol (TGB) biorefinery in Sabah, Malaysia as an underlay for renewable and sustainable development." *Renewable Sustainable Energy Rev.,* 14(2), 842-848.

Greene, A. K., Dawson, P. L., Nixon, D., Atkins, J. R., and Pearl, G. G. (2005). "Safety of animal fats for biodiesel production: a critical review of literature." ATFCAN, Ottawa, Canada.

Gressel, J. (2008). "Transgenics are imperative for biofuel crops." *Plant Sci.,* 174(3), 246-263.

Gu, Y., Azzouzi, A., Pouilloux, Y., Jerome, F., and Barrault, J. (2008). "Heterogeneously catalyzed etherification of glycerol: new pathways for transformation of glycerol to more valuable chemicals." *Green Chem.,* 10(2), 164-167.

Gui, M. M., Lee, K. T., and Bhatia, S. (2008). "Feasibility of edible oil vs. non-edible oil vs. waste edible oil as biodiesel feedstock." *Energy,* 33(11), 1646-1653.

Haldar, S. K., and Nag, A. (2008). "Utilization of three non-edible vegetable oils for the production of biodiesel catalysed by enzyme." *Open Chem. Eng. J.,* 2, 79-83.

Hammond, G. P., Kallu, S., and McManus, M. C. (2008). "Development of biofuels for the UK automotive market." *Appl. Energy,* 85(6), 506-515.

Hanna, M. A., and Isom, L. (2009). "Biodiesel current and future perspectives." *Handbook of plant-based biofuels.* A. Pandey, ed., Boca Raton, 177-181.

Hara, M. (2009). "Environmentally benign production of biodiesel using heterogeneous catalysts." *ChemSusChem,* 2(2), 129-135.

Hara, M. (2010). "Biodiesel production by amorphous carbon bearing SO_3H, COOH and phenolic OH groups, a solid Bronsted acid catalyst." *Top. Catal.,* 53(11-12), 805-810.

Hassan, M. N. A., Jaramillo, P., and Griffin, W. M. (2011). "Life cycle GHG emissions from Malaysian oil palm bioenergy development: The impact on transportation sector's energy security." *Energ. Policy,* 39(5), 2615-2625.

He, H. Y., Sun, S. Y., Wang, T., and Zhu, S. L. (2007). "Transesterification kinetics of soybean oil for production of biodiesel in supercritical methanol." *J. Am. Chem. Soc.,* 84(4), 399-404.

Hoekman, S. K. (2009). "Biofuels in the U.S. – Challenges and opportunities." *Renewable Energy,* 34(1), 14-22.

Holser, R. A. (2008). "Development of new products from biodiesel glycerin." *Biocatalysis and bioenergy,* C. T. Hou, and J. F. Shaw, eds., Wiley-Interscience, New Jersey, 154.

Hu, Q., Pang, J., Wu, Z., and Lu, Y. (2006). "Tuning pore size of mesoporous carbon via confined activation process." *Carbon,* 44(7), 1349-1352.

Huo, H., Wu, Y., and Wang, M. (2009). "Total versus urban: Well-to-wheels assessment of criteria pollutant emissions from various vehicle/fuel systems." *Atmos. Environ.,* 43(10), 1796-1804.

Index Mundi. (2012). "Historical commodity prices." http://www.indexmundi.com/commodities/ (04/16, 2012).

Iriondo, A., Barrio, V. L., Cambra, J. F., Arias, P. L., Guemez, M. B., Navarro, R. M., Sanchez-Sanchez, M. C., and Fierro, J. L. G. (2006). "H_2 production from residual glycerol obtained from biomass transesterification." *Prepr.Symp.- Am.Chem.Soc., Div.Fuel Chem.; Preprints of Symposia - American Chemical Society, Division of Fuel Chemistry,* 51(2), 557-558.

Jaecker-Voirol, A., Durand, I., Hillion, G., Delfort, B., and Montagne, X. (2008). "Glycerin for new biodiesel formulation." *Oil Gas Sci. Technol.,* 63(4), 395-404.

Jamroz, M. E., Jarosz, M., Witowska-Jarosz, J., Bednarek, E., Tecza, W., Jamroz, M. H., Dobrowolski, J. C., and Kijenski, J. (2007). "Mono-, di-, and tri-*tert*-butyl ethers of glycerol - A molecular spectroscopic study." *Spectroc. Acta Pt. A-Molec. Biomolec. Spectr.,* 67(3-4), 980-988.

Janaun, J., and Ellis, N. (2010). "Perspectives on biodiesel as a sustainable fuel." *Renewable Sustainable Energy Rev.,* 14(4), 1312-1320.

Janaun, J., and Ellis, N. (2011). "Role of silica template in the preparation of sulfonated mesoporous carbon catalysts." *Appl. Catal., A,* 394(1-2), 25-31.

Jerome, F., Pouilloux, Y., and Barrault, J. (2008). "Rational design of solid catalysts for the selective use of glycerol as a natural organic building block." *ChemSusChem,* 1(7), 586-613.

Jin, L., Zhang, Y., Dombrowski, J. P., Chen, C., Pravatas, A., Xu, L., Perkins, C., and Suib, S. L. (2011). "$ZnO/La_2O_2CO_3$ layered composite: A new heterogeneous catalyst for the efficient ultra-fast microwave biofuel production." *Appl. Catal., B,* 103(1–2), 200-205.

Johnson, D. T., and Taconi, K. A. (2007). "The glycerin glut: Options for the value-added conversion of crude glycerol resulting from biodiesel production." *Environ. Prog.,* 26(4), 338-348.

Ju, Y., and Rayat, A. C. M. E. (2009). "Biodiesel from rice bran oil." *Handbook of plant-based biofuels.* A. Pandey, ed., Boca Raton., 241-254.

Kahn, J. R., and Franceschi, D. (2006). "Beyond Kyoto: A tax-based system for the global reduction of greenhouse gas emissions." *Ecol. Econ.,* 58(4), 778-787.

Kakade, B. A., and Pillai, V. K. (2008). "Tuning the wetting properties of multiwalled carbon nanotubes by surface functionalization." *J. Phys. Chem. C,* 112(9), 3183-3186.

Kalam, A., Hassan, M. H., Bin Hajar, R., Bin Yusuf, M. S., Bin Umar, M. R., and Mahlia, I. (2009). "Palm oil diesel production and its experimental test on a diesel engine." *Handbook of plant-based biofuels.* A. Pandey, ed., Boca Raton, 225-240.

Kalam, M. A., and Masjuki, H. H. (2002). "Biodiesel from palmoil - An analysis of its properties and potential." *Biomass Bioenergy,* 23(6), 471-479.

Kaltschmitt, M., Reinhardt, A. G., and Stelzer, T. (1997). "Life cycle analysis of biofuels under different environmental aspects." *Biomass Bioenergy,* 12(2), 121-134.

Karavalakis, G., Boutsika, V., Stournas, S., and Bakeas, E. (2011). "Biodiesel emissions profile in modern diesel vehicles. Part 2: Effect of biodiesel origin on carbonyl, PAH, nitro-PAH and oxy-PAH emissions." *Sci. Total Environ.,* 409(4), 738-747.

Karavalakis, G., Stournas, S., and Bakeas, E. (2009). "Effects of diesel/biodiesel blends on regulated and unregulated pollutants from a passenger vehicle operated over the European and the Athens driving cycles." *Atmos. Environ.,* 43(10), 1745-1752.

Kellner, R., Mermet, J.M., Otto, M., Valcárce, M., and Widmer, H.M. (2004). *Analytical chemistry—A modern approach to analytical science.* Weinheim: Wiley-VCH Verlag GmbH,774.

Kinoshita, E., Myo, T., Hamasaki, K., and Nishi, S. (2007). "Diesel combustion characteristics of palm oil ethyl ester." *Nihon Kikai Gakkai Ronbunshu, B Hen/Transactions of the Japan Society of Mechanical Engineers, Part B,* 73(4), 1135-1141.

Kitano, M., Arai, K., Kodama, A., Kousaka, T., Nakajima, K., Hayashi, S., and Hara, M. (2009). "Preparation of a sulfonated porous carbon catalyst with high specific surface area." *Catal. Lett.,* 131 242-249.

Klepacova, K., Mravec, D., and Bajus, M. (2005). "*tert*-Butylation of glycerol catalysed by ion-exchange resins." *Appl. Catal., A,* 294(2), 141-147.

Klepacova, K., Mravec, D., and Bajus, M. (2006a). "Etherification of glycerol with *tert*-butyl alcohol catalysed by ion-exchange resins." *Chem.Pap.-Chem.Zvesti,* 60(3), 224-230.

Klepacova, K., Mravec, D., and Bajus, M. (2006b). "Ion exchange resins - catalysts for glycerol etherification." *Sampling Catal.Res.Pannonian Reg., Proc.Pannonian Int.Catal.Symp., 8th; Sampling Catalysis Research in the Pannonian Region, Proceedings of the Pannonian International Catalysis Symposium, 8th, Szeged, Hungary, July 4-7, 2006,* 137-142.

Klepacova, K., Mravec, D., Hajekova, E., and Bajus, M. (2003). "Etherification of glycerol for diesel fuels." *Pet.Coal,* 45(1-2), 54-57.

Klepacova, K., Mravec, D., Kaszonyi, A., and Bajus, M. (2007). "Etherification of glycerol and ethylene glycol by isobutylene." *Appl. Catal., A,* 328(1), 1-13.

Knudsen, J. G., Hottel, H. C., Sarofim, A. F., Wankat, P. C., and Knaebel, K. S. (1997). "Heat and mass transfer." *Perry's chemical engineers' handbook,* R. H. Perry, D. W. Green, and J. O. Maloney, eds., McGraw-Hill, United States of America, 5-1-5-79.

Koh, M. Y., and Mohd. Ghazi, T. I. (2011). "A review of biodiesel production from Jatropha curcas L. oil." *Renewable Sustainable Energy Rev.,* 15(5), 2240-2251.

Koh, L. P., and Wilcove, D. S. (2007). "Cashing in palm oil for conservation." *Nature,* 448(7157), 993-994.

Kulkarni, M. G., Gopinath, R., Meher, L. C., and Dalai, A. K. (2006). "Solid acid catalyzed biodiesel production by simultaneous esterification and transesterification." *Green Chem.,* 8(12), 1056-1062.

Kumar, S., Chaube, A., and Jain, S. K. (2012). "Sustainability issues for promotion of Jatropha biodiesel in Indian scenario: A review." *Renewable Sustainable Energy Rev.,* 16(2), 1089-1098.

Kumaran, P., Mazlini, N., Hussein, I., Nazrain, M., and Khairul, M. (2011). "Technical feasibility studies for Langkawi WCO (waste cooking oil) derived-biodiesel." *Energy,* 36(3), 1386-1393.

Kusdiana, D., and Saka, S. (2001a). "Kinetics of transesterification in rapeseed oil to biodiesel fuel as treated in supercritical methanol." *Fuel,* 80(5), 693-698.

Kusdiana, D., and Saka, S. (2001b). "Methyl esterification of free fatty acids of rapeseed oil as treated in supercritical methanol." *J. Chem. Eng. Jpn.,* 34(3), 383-387.

Kusdiana, D., and Saka, S. (2004). "Effects of water on biodiesel fuel production by supercritical methanol treatment." *Bioresour. Technol.,* 91(3), 289-295.

Lam, M. K., Tan, K. T., Lee, K. T., and Mohamed, A. R. (2009). "Malaysian palm oil: Surviving the food versus fuel dispute for a sustainable future." *Renewable Sustainable Energy Rev.,* 13(6-7), 1456-1464.

Lapuerta, M., Rodriguez-Fernandez, J., and Agudelo, J. R. (2008). "Diesel particulate emissions from used cooking oil biodiesel." *Bioresour. Technol.,* 99(4), 731-740.

Lee, H., Seung, D., Filimonov, I., and Kim, H. (2011). "Etherification of glycerol by isobutylene. Effects of the density of acidic sites in ion-exchange resin on the distribution of products." *Korean J. Chem. Eng.,* 28(3), 756-762.

Lee, H. J., Seung, D., Jung, K. S., Kim, H., and Filimonov, I. N. (2010). "Etherification of glycerol by isobutylene: Tuning the product composition." *Appl. Catal., A,* 390(1-2), 235-244.

Lee, S., Posarac, D., and Ellis, N. (2011). "Process simulation and economic analysis of biodiesel production processes using fresh and waste vegetable oil and supercritical methanol." *Chem. Eng. Res. Design,* 89(12), 2626-2642.

Lerkkasemsan, N., Abdoulmoumine, N., Achenie, L., and Agblevor, F. (2010). "Mechanistic modeling of palmitic acid esterification via heterogeneous catalysis." *Ind. Eng. Chem. Res.,* 50(3), 1177-1186.

Leung, D. Y. C., Wu, X., and Leung, M. K. H. (2010). "A review on biodiesel production using catalyzed transesterification." *Appl. Energy,* 87(4), 1083-1095.

Li, W., Ma, F., Su, F., Ma, L., Zhang, S., and Guo, Y. (2011). "One-step preparation of efficient and reusable SO4(2-)/ZrO(2)-based hybrid solid catalysts functionalized by alkyl-bridged organosilica moieties for biodiesel production." *ChemSusChem,* 4(6), 744-756.

Li, Y., Horsman, M., Wu, N., Lan, C. Q., and Dubois-Calero, N. (2008). "Biofuels from microalgae." *Biotechnol. Prog.,* 24(4), 815-820.

Liang, Y. C., May, C. Y., Foon, C. S., Ngan, M. A., Hock, C. C., and Basiron, Y. (2006). "The effect of natural and synthetic antioxidants on the oxidative stability of palm diesel." *Fuel,* 85(5-6), 867-870.

Lien, Y., Hsieh, L., and Wu, C. S. J. (2010). "Biodiesel synthesis by simultaneous esterification and transesterification using oleophilic acid catalyst." *Ind. Eng. Chem. Res.,* 49(5), 2118-2121.

Lin, Y., Lee, W., Chao, H., Wang, S., Tsou, T., Chang-Chien, G., and Tsai, P. (2008). "Approach for energy saving and pollution reducing by fueling diesel engines with emulsified biosolution/biodiesel/diesel blends." *Environ. Sci. Technol.,* 42(10), 3849-3855.

Liu, R., Wang, X., Zhao, X., and Feng, P. (2008). "Sulfonated ordered mesoporous carbon for catalytic preparation of biodiesel." *Carbon,* 46(13), 1664-1669.

Liu, Y., Chen, J., Yao, J., Lu, Y., Zhang, L., and Liu, X. (2009). "Preparation and properties of sulfonated carbon–silica composites from sucrose dispersed on MCM-48." *Chem. Eng. J.,* 148(1), 201-206.

Liu, Y., Lotero, E., and Goodwin Jr., J. G. (2006). "A comparison of the esterification of acetic acid with methanol using heterogeneous versus homogeneous acid catalysis." *J. Catal.,* 242(2), 278-286.

Liu, Y., Lin, T., Wang, Y., and Ho, W. (2009). "Carbonyl compounds and toxicity assessments of emissions from a diesel engine running on biodiesels." *J. Air Waste Manage. Assoc.,* 59(2), 163-171.

Lotero, E., Liu, Y., and Goodwin, J. G.,Jr. (2006). "Biodiesel synthesis: assessment of current and potential technologies using heterogeneous catalysis." *Abstracts, 58th Southeast Regional Meeting of the American Chemical Society, Augusta, GA, United States, November 1-4,* SRM06-123.

Lotero, E., Liu, Y., Lopez, D. E., Suwannakarn, K., Bruce, D. A., and Goodwin, J. G.,Jr. (2005). "Synthesis of biodiesel via acid catalysis." *Ind. Eng. Chem. Res.,* 44(14), 5353-5363.

Luque, R., and Clark, J. H. (2011). "Biodiesel-like biofuels from simultaneous transesterification/esterification of waste oils with a biomass-derived solid acid catalyst." *ChemCatChem,* 3(3), 594-597.

Luskin, M. S., and Potts, M. D. (2011). "Microclimate and habitat heterogeneity through the oil palm lifecycle." *Basic Appl. Ecol.,* 12(6), 540-551.

Mabee, W. E. (2007). "Policy options to support biofuel production." *Biofuels,* 108, 329-357.

Macia-Agullo, J. A., Sevilla, M., Diez, M. A., and Fuertes, A. B. (2010). "Synthesis of carbon-based solid acid microspheres and their application to the production of biodiesel." *ChemSusChem,* 3(12), 1352-1354.

MacPherson, I., Roos, J. W., and Quinn, T. G. (2009). "Environmentally-friendly fuel compositions meeting biodegradation, bioaccumulative, and toxicity standards." *Eur.Pat.Appl.,* 2008-161416; 2007-832439(2025737), 38.

Mata, T. M., Cardoso, N., Ornelas, M., Neves, S., and Caetano, N. S. (2011). "Evaluation of two purification methods of biodiesel from beef tallow, pork lard, and chicken fat." *Energy Fuels,* 25(10), 4756-4762.

Mata, T. M., Martins, A. A., and Caetano, N. S. (2010). "Microalgae for biodiesel production and other applications: A review." *Renewable Sustainable Energy Rev.,* 14(1), 217-232.

May, C. Y., Foon, C. S., Liang, Y. C., Nang, H. L. N., Ngan, M. A., and Basiron, Y. (2004). "Palm diesel with low pour point for cold climate countries." *U.S.Pat.Appl.Publ.,* 2003-465847; 2003-440169(2004231236), 7.

May, C. Y., Liang, Y. C., Foon, C. S., Ngan, M. A., Hook, C. C., and Basiron, Y. (2005). "Key fuel properties of palm oil alkyl esters." *Fuel,* 84(12-13), 1717-1720.

McCarthy, J. F., Gillespie, P., and Zen, Z. (2011). "Swimming upstream: local indonesian production networks in "globalized" palm oil production." *World Dev.,* 40(3), 555-569.

Meher, L. C., Naik, S. N., Naik, M. K., and Dalai, A. K. (2009). "Biodiesel production using karanja (*Pongamia pinnata*) and jatropha (*Jatropha curcas*) seed oil." *Handbook of plant-based biofuels.* A. Pandey, ed., Boca Raton, 255-266.

Mehlman, M. A. (2002). "Carcinogenicity of methyl-tertiary butyl ether in gasoline." *Ann. N. Y. Acad. Sci.,* 982, 149-159.

Mehlman, M. A. (1995). "Dangerous and cancer-causing properties of products and chemicals in the oil refining and petrochemical industry .15. health-hazards and health risks from oxygenated automobile fuels (MTBE) - Lessons not heeded." *Int. J. Occup. Med. Tox.,* 4(2), 219-236.

Melero, J. A., Vicente, G., Morales, G., Paniagua, M., Moreno, J. M., Roldan, R., Ezquerro, A., and Perez, C. (2008). "Acid-catalyzed etherification of bio-glycerol and isobutylene over sulfonic mesostructured silicas." *Appl.Catal., A,* 346(1-2), 44-51.

Melero, J. A., Vicente, G., Morales, G., Paniagua, M., and Bustamante, J. (2010). "Oxygenated compounds derived from glycerol for biodiesel formulation: Influence on EN 14214 quality parameters." *Fuel,* 89(8), 2011-2018.

Mittelbach, M. (1996). "Diesel fuel derived from vegetable oils, VI: Specifications and quality control of biodiesel." *Bioresour. Technol.,* 56(1), 7-11.

Mizuno, N., and Misono, M. (1998). "Heterogeneous catalysis." *Chem. Rev.,* 98(1), 199-218.

Mo, X., Lopez, D. E., Suwannakarn, K., Liu, Y., Lotero, E., Goodwin, J. G., and Lu, C. Q. (2008a). "Activation and deactivation characteristics of sulfonated carbon catalysts." *J. Catal.,* 254(2), 332-338.

Mo, X. H., Lotero, E., Lu, C. Q., Liu, Y. J., and Goodwin, J. G. (2008b). "A novel sulfonated carbon composite solid acid catalyst for biodiesel synthesis." *Catal. Lett.,* 123(1-2), 1-6.

Monni, S., and Raes, F. (2008). "Multilevel climate policy: the case of the European Union, Finland and Helsinki." *Environ. Sci. Policy,* 11(8), 743-755.

Mosley, E. E., Powell, G. L., Riley, M. B., and Jenkins, T. C. (2002). "Microbial biohydrogenation of oleic acid to trans isomers in vitro." *J. Lipid Res.,* 43(2), 290-296.

Moulijn, J. A., van Diepen, A. E., and Kapteijn, F. (2001). "Catalyst deactivation: is it predictable?: What to do?" *Appl. Catal., A,* 212(1–2), 3-16.

Muller, T. L. (2007). "Sulfuric acid and sulfur trioxide." *Kirk-Othmer encyclopedia of chemical technology.* Kirk-Othmer, ed., John Wiley & Sons., New Jersey, 1-41.

Murugesan, A., Umarani, C., Subramanian, R., and Nedunchezhian, N. (2009). "Biodiesel as an alternative fuel for diesel engines-A review." *Renewable Sustainable Energy Rev.,* 13(3), 653-662.

Nadim, F., Zack, P., Hoag, G. E., and Liu, S. L. (2001). "United States experience with gasoline additives." *Energ. Policy,* 29(1), 1-5.

Nakajima, K., Hara, M., and Hayashi, S. (2007). "Environmentally benign production of chemicals and energy using a carbon-based strong solid acid." *J. Am. Ceram. Soc.,* 90(12), 3725-3734.

Nakajima, K., Okamura, M., Kondo, J. N., Domen, K., Tatsumi, T., Hayashi, S., and Hara, M. (2009). "Amorphous carbon bearing sulfonic acid groups in mesoporous silica as a selective catalyst." *Chem. Mater.,* 21(1), 186-193.

Nielsen, P. M., and Rancke-Madsen, A. (2011). "Enzymatic large-scale production of biodiesel." *Lipid Technol.,* 23(10), 230-233.

Noureddini, H. (2001). "System and process for producing biodiesel fuel with reduced viscosity and a cloud point below 32 DegF." *U.S.,* 99-271793; 97-961939(6174501), 20.

Noureddini, H. (2000). "Process for producing biodiesel fuel with reduced viscosity and a cloud point below 32 DegF." *U.S.,* 97-961939(6015440), 10.

Ognjanovic, N. D., Saponjic, S. V., Bezbradica, D. I., and Knezevic, Z. D. (2008). "Lipase-catalyzed biodiesel synthesis with differential acyl acceptors." *Acta Period. Technol.,* 39, 161-169.

Okamura, M., Takagaki, A., Toda, M., Kondo, J. N., Domen, K., Tatsumi, T., Hara, M., and Hayashi, S. (2006). "Acid-catalyzed reactions on flexible polycyclic aromatic carbon in amorphous carbon." *Chem. Mat.,* 18(13), 3039-3045.

Pagliaro, M., Ciriminna, R., Kimura, H., Rossi, M., and Della Pina, C. (2007). "From glycerol to value-added products." *Angew. Chem, Int. Ed,* 46(24), 4434-4440.

Pahl, G. (2008). *Biodiesel - Growing a new energy economy.* Chelsea Green Publishing Company, White River Junction, Vermont.

Parawira, W. (2009). "Biotechnological production of biodiesel fuel using biocatalysed transesterification: A review." *Crit. Rev. Biotechnol.,* 29(2), 82-93.

Pariente, S., Tanchoux, N., and Fajula, F. (2009). "Etherification of glycerol with ethanol over solid acid catalysts." *Green Chem.,* 11(8), 1256-1261.

Park, J., Kim, D., and Lee, J. (2010a). "Esterification of free fatty acids using water-tolerable Amberlyst as a heterogeneous catalyst." *Bioresour.Technol.,* 101(Supplement 1), S62-S65.

Park, J., Wang, Z., Kim, D., and Lee, J. (2010b). "Effects of water on the esterification of free fatty acids by acid catalysts." *Renewable Energy,* 35(3), 614-618.

Patz, J. A., Gibbs, H. K., Foley, J. A., Rogers, J. V., and Smith, K. R. (2007). "Climate change and global health: Quantifying a growing ethical crisis." *Ecohealth,* 4(4), 397-405.

Pavese, M., Musso, S., Bianco, S., Giorcelli, M., Pugno, N. (2008). "An analysis of carbon nanotube structure wettability before and after oxidation treatment." *J. Phys: Condens. Matter,* 20(47), 474206.

Peng, L., Philippaerts, A., Ke, X., Van Noyen, J., De Clippel, F., Van Tendeloo, G., Jacobs, P. A., and Sels, B. F. (2010). "Preparation of sulfonated ordered mesoporous carbon and its use for the esterification of fatty acids." *Catal. Today,* 150(1-2), 140-146.

Perdiguero, J., and Jimenez, J. L. (2011). "Sell or not sell biodiesel: Local competition and government measures." *Renewable Sustainable Energy Rev.,* 15(3), 1525-1532.

Pinzi, S., Garcia, I. L., Lopez-Gimenez, F. J., Luque de Castro, M. D., Dorado, G., and Dorado, M. P. (2009). "The ideal vegetable oil-based biodiesel composition: A review of social, economical and technical implications." *Energy Fuels,* 23(5), 2325-2341.

Plank, C., and Lorbeer, E. (1995). "Simultaneous determination of glycerol, and mono-, di- and triglycerides in vegetable oil methyl esters by capillary gas chromatography." *J. Chromatogr. A,* 697(1–2), 461-468.

Prabhavathi Devi, B. L. A., Gangadhar, K. N., Sai Prasad, P. S., Jagannadh, B., and Prasad, R. B. N. (2009). "A glycerol-based carbon catalyst for the preparation of biodiesel." *ChemSusChem,* 2(7), 617-620.

Predojević, Z. J. (2008). "The production of biodiesel from waste frying oils: A comparison of different purification steps." *Fuel,* 87(17-18), 3522-3528.

Rahimi, H., Ghobadian, B., Yusaf, T., Najafi, G., and Khatamifar, M. (2009). "Diesterol: An environment-friendly IC engine fuel." *Renewable Energy,* 34(1), 335-342.

Rahmat, N., Abdullah, A. Z., and Mohamed, A. R. (2010). "Recent progress on innovative and potential technologies for glycerol transformation into fuel additives: A critical review." *Renewable Sustainable Energy Rev.,* 14(3), 987-1000.

Rhew, R. C., Østergaard, L., Saltzman, E. S., and Yanofsky, M. F. (2003). "Genetic control of methyl halide production in arabidopsis." *Curr. Biol.,* 13(20), 1809-1813.

Rhodes, C. J. (2009). "Oil from algae; salvation from peak oil?" *Sci. Prog.,* 92(Pt 1), 39-90.

Saka, S., and Dadan, K. (1999). "Transesterification of rapeseed oils in supercritical methanol to biodiesel fuels." *Proc. Biomass Conf. Am., 4th,* 1 797-801.

Saka, S., and Kusdiana, D. (2001). "Biodiesel fuel from rapeseed oil as prepared in supercritical methanol." *Fuel,* 80(2), 225-231.

Saka, S., Kusdiana, D., and Minami, E. (2006). "Non-catalytic biodiesel fuel production with supercritical methanol technologies." *J. Sci. Ind. Res.,* 65(5), 420-425.

Salzano, E., Di Serio, M., and Santacesaria, E. (2010). "Emerging risks in the biodiesel production by transesterification of virgin and renewable oils." *Energy Fuels,* 24(11), 6103-6109.

Santori, G., Di Nicola, G., Moglie, M., and Polonara, F. (2012). "A review analyzing the industrial biodiesel production practice starting from vegetable oil refining." *Appl. Energy,* 92(0), 109-132.

Santosa, S. J. (2008). "Palm oil boom in Indonesia: From plantation to downstream products and biodiesel." *Clean-Soil Air Water,* 36(5-6), 453-465.

Sarin, A., Arora, R., Singh, N. P., Sarin, R., Malhotra, R. K., and Kundu, K. (2009). "Effect of blends of Palm-Jatropha-Pongamia biodiesels on cloud point and pour point." *Energy,* 34(11), 2016-2021.

Sarin, R., Sharma, M., Sinharay, S., and Malhotra, R. K. (2007). "Jatropha-Palm biodiesel blends: An optimum mix for Asia." *Fuel,* 86(10), 1365-1371.

Sarma, A. K., Sarmah, J. K., Barbora, L., Kalita, P., Chatterjee, S., Mahanta, P., and Goswami, P. (2008). "Recent inventions in biodiesel production and processing - a review." *Recent Pat. Eng.,* 2(1), 47-58.

Sawyer, R. F. (2009). "Science based policy for addressing energy and environmental problems." *Proc. Combust. Inst.,* 32(1), 45-56.

Sern, C. H., May, C. Y., Zakaria, Z., Daik, R., and Foon, C. S. (2007). "The effect of polymers and surfactants on the pour point of palm oil methyl esters." *Eur. J. Lipid Sci. Technol.,* 109(4), 440-444.

Shahid, E. M., and Jamal, Y. (2011). "Production of biodiesel: A technical review." *Renewable Sustainable Energy Rev.,* 15(9), 4732-4745.

Sharma, Y. C., and Singh, B. (2009). "Development of biodiesel: Current scenario." *Renewable Sustainable Energy Rev.,* 13(6-7), 1646-1651.

Sharma, Y. C., Singh, B., and Korstad, J. (2011). "Latest developments on application of heterogenous basic catalysts for an efficient and eco friendly synthesis of biodiesel: A review." *Fuel,* 90(4), 1309-1324.

Sheldon, R. A., and van Bekkum, H. (2001). *Fine chemicals through heterogeneous catalysis*. Weinheim: Wiley-VCH Verlag GmbH.

Shi, X., Yu, Y., He, H., Shuai, S., Wang, J., and Li, R. (2005). "Emission characteristics using methyl soyate-ethanol-diesel fuel blends on a diesel engine." *Fuel,* 84(12-13), 1543-1549.

Shu, Q., Gao, J., Nawaz, Z., Liao, Y., Wang, D., and Wang, J. (2010). "Synthesis of biodiesel from waste vegetable oil with large amounts of free fatty acids using a carbon-based solid acid catalyst." *Appl. Energy,* 87(8), 2589-2596.

Shu, Q., Zhang, Q., Xu, G., Nawaz, Z., Wang, D., and Wang, J. (2009). "Synthesis of biodiesel from cottonseed oil and methanol using a carbon-based solid acid catalyst." *Fuel Process. Technol.,* 90(7-8), 1002-1008.

Shudo, T., Fujibe, A., Kazahaya, M., Aoyagi, Y., Ishii, H., Goto, Y., and Noda, A. (2006). "Effects of ethanol addition to PME on cloud point and exhaust emissions in diesel combustion." *Rev. Automot. Eng.,* 27(2), 215-221.

Shvets, D. I. (2003). "Novel bioactive carbomineral sorbents, including cluster and carbon nanotubes for superselective purification of biodiesel fuel - liquid hydrocarbons and carbohydrate from sulfur containing impurities." Adsorption Science and Technology. *Proceedings of the Third Pacific Basin Conference. Kyongju, Korea, 25 - 29 May 2003,* 318-323.

Siminiceanu, I. (2007). "Methyl tert-butyl ether occurrence and degradation in water." *Environ. Eng. Manage. J.,* 6(2), 143-151.

Sing, K. S. W. (1982). "Reporting physisorption data for gas/solid systems with special reference to the determination of surface area and porosity." *Pure Appl. Chem.,* 54(11), 2201-2218.

Sohling, U., Ruf, F., Ortiz Niembro, J. A., Condemarin, R., and Bello, J. (2008). "Method for purification of biodiesel." *PCT Int.Appl.,* 2007-EP9656; 2006-23142(2008055676), 51.

Solomon, T. W. G., and Fryhle, C. B. (2000). *Organic chemistry.* John Wiley & Sons, Inc., New York.

Soriano Jr., N. U., Migo, V. P., and Matsumura, M. (2006). "Ozonized vegetable oil as pour point depressant for neat biodiesel." *Fuel,* 85(1), 25-31.

Sorrell, S., Speirs, J., Bentley, R., Brandt, A., and Miller, R. (2010). "Global oil depletion: A review of the evidence." *Energ. Policy,* 38(9), 5290-5295.

Stein, A., Wang, Z., and Fierke, M. A. (2009). "Functionalization of porous carbon materials with designed pore architecture." *Adv. Mater.,* 21(3), 265-293.

Stewart, C. N.,Jr. (2007). "Biofuels and biocontainment." *Nat. Biotechnol.,* 25(3), 283-284.

Sticklen, M. (2006). "Plant genetic engineering to improve biomass characteristics for biofuels." *Curr. Opin. Biotechnol.,* 17(3), 315-319.

Sticklen, M. B. (2008). "Plant genetic engineering for biofuel production: towards affordable cellulosic ethanol." *Nat. Rev. Gene.,* 9(6), 433-443.

Suganuma, S., Nakajima, K., Kitano, M., Kato, H., Tamura, A., Kondo, H., Yanagawa, S., Hayashi, S., and Hara, M. (2011). "SO_3H-bearing mesoporous carbon with highly selective catalysis." *Micropor. Mesopor. Mat.,* 143(2-3), 443-450.

Suganuma, S., Nakajima, K., Kitano, M., Yamaguchi, D., Kato, H., Hayashi, S., and , Hara, M. (2008). "Hydrolysis of cellulose by amorphous carbon bearing SO_3H, COOH, and OH Groups." *J. Am. Chem. Soc.,* 130(38), 12787-12793.

Suganuma, S., Nakajima, K., Kitano, M., Yamaguchi, D., Kato, H., Hayashi, S., and Hara, M. (2010). "Synthesis and acid catalysis of cellulose-derived carbon-based solid acid." *Solid State Sci.,* 12(6), 1029-1034.

Sumathi, S., Chai, S. P., and Mohamed, A. R. (2008). "Utilization of oil palm as a source of renewable energy in Malaysia." *Renewable Sustainable Energy Rev.,* 12(9), 2404-2421.

Tabatabaei, M., Tohidfar, M., Jouzani, G. S., Safarnejad, M., and Pazouki, M. (2011). "Biodiesel production from genetically engineered microalgae: Future of bioenergy in Iran." *Renewable Sustainable Energy Rev.,* 15(4), 1918-1927.

Takagaki, A., Toda, M., Okamura, M., Kondo, J. N., Hayashi, S., Domen, K., and Hara, M. (2006). "Esterification of higher fatty acids by a novel strong solid acid." *Catal. Today,* 116(2), 157-161.

O. Takahashi. (2009). "Challenge of climate protection and BDF from used cooking oil in the City of Kyoto, Japan." http://www.iclei.org/documents/Japan/O.Takahashi_Kyoto.pdf (9/15, 2009).

Tan, K. T., Lee, K. T., and Mohamed, A. R. (2009a). "Production of FAME by palm oil transesterification via supercritical methanol technology." *Biomass Bioenergy,* 33(8), 1096-1099.

Tan, K. T., Lee, K. T., Mohamed, A. R., and Bhatia, S. (2009b). "Palm oil: Addressing issues and towards sustainable development." *Renewable Sustainable Energy Rev.,* 13(2), 420-427.

Tan, T., Lu, J., Nie, K., Deng, L., and Wang, F. (2010). "Biodiesel production with immobilized lipase: A review." *Biotechnol. Adv.,* 28(5), 628-634.

Tanaka, S., Nishiyama, N., Egashira, Y., and Ueyama, K. (2005). "Synthesis of ordered mesoporous carbons with channel structure from an organic-organic nanocomposite." *Chem. Commun.,* (16), 2125-2127.

Theinnoi, K., Gill, S. S., Tsolakis, A., York, A. P. E., Megaritis, A., and Harrison, R. M. (2012). "Diesel particulate filter regeneration strategies: Study of hydrogen addition on biodiesel fuelled engines." *Energy Fuels,* 26(2), 1192-1201.

Thermo Nicolet Corporation. (2001). "Introduction to Fourier Tranasform Infrared Spectrometry." http://mmrc.caltech.edu/FTIR/FTIRintro.pdf (03/25, 2012).

Tian, X., Zhang, L. L., Bai, P., and Zhao, X. S. (2011). "Sulfonic-acid-functionalized porous benzene phenol polymer and carbon for catalytic esterification of methanol with acetic acid." *Catal. Today,* 166(1), 53-59.

Toda, M., Takagaki, A., Okamura, M., Kondo, J. N., Hayashi, S., Domen, K., and Hara, M. (2005). "Green chemistry - Biodiesel made with sugar catalyst." *Nature,* 438(7065), 178-178.

United States Department of Agriculture (USDA). (2012). "Economics, Statistics and Market Information System." http://usda.mannlib.cornell.edu/MannUsda/viewStaticPage.do?url=http://usda.mannlib.cornell.edu/usda/ers/89002/2010/index.html (04/16, 2012).

Varanda, M. G., Pinto, G., and Martins, F. (2011). "Life cycle analysis of biodiesel production." *Fuel Process Technol.,* 92(5), 1087-1094.

Vasudevan, P. T., and Briggs, M. (2008). "Biodiesel production-current state of the art and challenges." *J. Ind. Microbiol. Biotechnol.,* 35(5), 421-430.

Villa, A., Tessonnier, J., Majoulet, O., Su, D. S., and Schlogl, R. (2009). "Amino-functionalized carbon nanotubes as solid basic catalysts for the transesterification of triglycerides." *Chem. Commun.,* (29), 4405-4407.

Vunjak-Novakovic, G., Kim, Y., Wu, X., Berzin, I., and Merchuk, J. C. (2005). "Air-lift bioreactors for algal growth on flue gas: Mathematical modeling and pilot-plant studies." *Ind. Eng. Chem. Res.,* 44(16), 6154-6163.

Wang, X., Liu, R., Waje, M. M., Chen, Z., Yan, Y., Bozhilov, K. N., and Feng, P. (2007). "Sulfonated ordered mesoporous carbon as a stable and highly active protonic acid catalyst." *Chem. Mater.,* 19(10), 2395-2397.

Warabi, Y., Kusdiana, D., and Saka, S. (2003). "Reactivity of triglycerides and fatty acids of rapeseed oil in supercritical alcohols." *Bioresour. Technol.,* 91(3), 283-287.

Wassell Jr., C. S., and Dittmer, T. P. (2006). "Are subsidies for biodiesel economically efficient?" *Energ. Policy,* 34(18), 3993-4001.

West, A. H., Posarac, D., and Ellis, N. (2007). "Simulation, case studies and optimization of a biodiesel process with a solid acid catalyst." *Int. J. Chem. React. Eng.,* 5, A37(1-10).

West, A. H., Posarac, D., and Ellis, N. (2008). "Assessment of four biodiesel production processes using HYSYS.Plant." *Bioresour. Technol.,* 99(14), 6587-6601.

Westbrook, C. K., Pitz, W. J., Mehl, M., and Curran, H. J. (2011). "Detailed chemical kinetic reaction mechanisms for primary reference fuels for diesel cetane number and spark-ignition octane number." *Proc. Comb. Ins.,* 33(1), 185-192.

Wicke, B., Dornburg, V., Junginger, M., and Faaij, A. (2008). "Different palm oil production systems for energy purposes and their greenhouse gas implications." *Biomass Bioenergy,* 32(12), 1322-1337.

Wu, F., Wang, J., Chen, W., and Shuai, S. (2009). "A study on emission performance of a diesel engine fueled with five typical methyl ester biodiesels." *Atmos. Environ.,* 43(7), 1481-1485.

Xiao, L., Mao, J., Zhou, J., Guo, X., and Zhang, S. (2011). "Enhanced performance of HY zeolites by acid wash for glycerol etherification with isobutene." *Appl. Catal., A,* 393(1-2), 88-95.

Xing, R., Liu, N., Liu, Y., Wu, H., Jiang, Y., Chen, L., He, M., and Wu, P. (2007a). "Novel solid acid catalysts: sulfonic acid group-functionalized mesostructured polymers." *Adv. Funct. Mater.,* 17(14), 2455-2461.

Xing, R., Liu, Y., Wang, Y., Chen, L., Wu, H., Jiang, Y., He, M., and Wu, P. (2007b). "Active solid acid catalysts prepared by sulfonation of carbonization-controlled mesoporous carbon materials." *Microporous Mesoporous Mater.,* 105(1-2), 41-48.

Yee, K. F., Tan, K. T., Abdullah, A. Z., and Lee, K. T. (2009). "Life cycle assessment of palm biodiesel: Revealing facts and benefits for sustainability." *Appl. Energy,* 86(Supplement1), S189-S196.

Zabeti, M., Wan Daud, W.,Mohd Ashri, and Aroua, M. K. (2009). "Activity of solid catalysts for biodiesel production: A review." *Fuel Process Technol.,* 90(6), 770-777.

Zafiropoulos, N. A., Ngo, H. L., Foglia, T. A., Samulski, E. T., and Lin, W. (2007). "Catalytic synthesis of biodiesel from high free fatty acid-containing feedstocks." *Chem. Commun.,* 35, 3670-3672.

Zamzow, K., Tsukamoto, T. K., and Miller, G. C. (2006). "Biodiesel and bioreactors: waste from biodiesel production as a carbon source for bioreactors treating acid-mine drainage." *Mine Water Environ.*, 25(3), 163-170.

Zhang, Y., Dube, M. A., McLean, D. D., and Kates, M. (2003). "Biodiesel production from waste cooking oil: 1. Process design and technological assessment." *Bioresour. Technol.,* 89(1), 1-16.

Zhao, W., Yang, B., Yi, C., Lei, Z., and Xu, J. (2010). "Etherification of glycerol with isobutylene to produce oxygenate additive using sulfonated peanut shell catalyst." *Ind. Eng. Chem. Res.,* 49(24), 12399-12404.

Zheng, Y., Chen, X., and Shen, Y. (2008). "Commodity chemicals derived from glycerol, an important biorefinery feedstock." *Chem. Rev.,* 108(12), 5253-5277.

Zhou, C., Beltramini, J. N., Fan, Y., and Lu, G. Q. (2008). "Chemoselective catalytic conversion of glycerol as a biorenewable source to valuable commodity chemicals." *Chem. Soc. Rev.,* 37(3), 527-549.

Ziolkowska, J., Meyers, W. H., Meyer, S., and Binfield, J. (2010). "Targets and mandates: Lessons learned from EU and US biofuels policy mechanisms." *AgBioForum,* 13(4), 398-412.

Zong, M. H., Duan, Z. Q., Lou, W. Y., Smith, T. J., and Wu, H. (2007). "Preparation of a sugar catalyst and its use for highly efficient production of biodiesel." *Green Chem.,* 9(5), 434-437.

Appendix A Catalyst characterization

A.1 Procedure for the detection of sulfate ions using precipitation of barium sulfate

During the preparation of the carbon-based catalysts, the final catalyst was washed with plenty of hot water to remove the homogeneous sulfuric acid. The washing was done until the pH of the washed water became neutral and no sulfate ions were detected. The detection of sulfate ions was done by precipitation of barium sulfate according to the standard procedure by APHA (American Water Works Association et al. 1981). In a typical experiment, pH of the washed water (50 mL) was adjusted to pH 4.5 – 5.0 using HCl. 1 – 2 mL of HCl was then added into the washed water sample. The sample was heated to boiling while stirring gently and 0.1 M barium dichloride warm solution was added slowly. White precipitate was formed when sulfate ion was present in the sample.

For the detection of sulfate ions in the product of esterification of oleic acid with methanol (top layer), a slight modification from the procedure described above was made. Since the amount of sample was small (~4 mL) and easily evaporated when heated as it contained methanol, 10 mL of distilled water and 0.2 mL of HCl were added. The same heating and addition of 0.1 M barium dichloride as described above was done.

A.1.1 Handling of hydrofluoric acid (HF)

HF was used in the preparation of carbon-based catalyst for the removal of silica template (Chapters 2 and 3). The MSDS of HF was carefully reviewed for safety precautions to reduce the risk of handling HF which is an extremely hazardous chemical, both in liquid or vapour forms. HF differs from other acids because the fluoride ion readily penetrates the skin, resulting in destruction of deep tissue layers, including bone.

HF was always used with adequate ventilation to minimize inhalation of vapour. Concentrations greater than 5 wt.% was always handled inside a fume hood. A laboratory coat and medium or heavyweight nitrile gloves were worn at all times when working with HF. A second pair of nitrile disposable gloves was worn under the reusable gloves for protection against leaks. Gloves that had not been contaminated with HF were disposed. Contaminated gloves were disposed of as HF waste. HF waste was disposed according to UBC waste disposal procedures.

HF and HF wastes were stored in labeled chemically compatible containers (e.g., polyethylene or teflon). Glass, metal, and ceramic containers were not compatible with HF. Precaution was taken not to store HF with incompatible chemicals such as ammonia or other alkaline materials. HF was placed on a low protected shelf in a secondary container or other location where it would not be accidentally spilled or knocked over.

A.2 Procedure for the porosimetry analysis using the Micromeritics ASAP2020

The degassing program is given below:

Degassing conditions

Evacuation phase	
Temperature ramp rate	= 10.0°C/min
Target temperature	= 120°C
Evacuation rate	= 5.0 mmHg
Unrestricted evacuation from	= 10.0 mmHg
Vacuum set point	= 10 µmHg
Evacuation time	= 120 min
Heating phase	
Ramp rate	= 10°C/min
Hold temperature	= 120°C
Hold time	= 60 min
Evacuation and heating phase	
Hold pressure	= 10 mmHg

A.2.1 Sample preparation and analysis

Approximately 1.0 g of sample was placed inside a BET tube (weight of the sample and the tube was recorded) and degassed according to the condition in Section A.2. After degassing, the sample and the tube was weighed to get the actual sample weight. During the degassing step, moisture and air were removed, leaving only the

pure sample. The analysis condition used was multipoint isotherm. Upon completion of the analysis, the results including the specific surface area, pore volume, and pore diameter distribution were obtained.

The specific surface area of the sample is taken based on the BET value (Brunauer et al. 1938). The BET equation is as follows:

$$\frac{\frac{P}{P_o}}{V\left(1-\frac{P}{P_o}\right)} = \frac{C-1}{V_m C}\left(\frac{P}{P_o}\right) + \frac{1}{V_m C}$$

Equation A-1

where V is the total volume adsorbed (STP) at pressure P, V_m is the volume adsorbed (STP) at monolayer coverage, P_o is the saturation vapor pressure of the adsorbate gas (or vapour), and C is a constant. A plot of $\frac{\frac{P}{P_o}}{V\left(1-\frac{P}{P_o}\right)}$ versus $\frac{P}{P_o}$ should give a linear plot with a slope of $\frac{C-1}{V_m C}$ and an intercept of $\frac{1}{V_m C}$, from which V_m and C can be determined, and surface area can be calculated from V_m. The preferred range of $\frac{P}{P_o}$ for best results is 0.05 to 0.4.

A.3 Procedure for the determination of total acidity of a catalyst

Total acidity was determined using a back-titration method. In a typical analysis, 0.1g of sample was put in a beaker containing 60 mL of 0.008 M NaOH, and stirred for 30 min at room temperature. An excessive amount of NaOH was used in order to completely neutralize all acidic functional groups in the sample. The NaOH solution (containing the sample), as the analyte, was then titrated on an automatic titrator (Metrohm 794 Titrino or 894 Titrino), using 0.02 M HCl as the titrant. The titration was stopped once the analyte pH turned to ~4. Figure A-1 shows an excerpt of a titrator analysis result print out for a back-titration analysis on VPS2 (Replicate #2).

A.3.1 Sample calculation for the determination of total acidity

Number of moles of 60 mL 0.008 M NaOH (titrator)

$$= 0.008\ \frac{\text{mol}}{\text{L}} \times 60\ \text{mL} \times \frac{1\ \text{L}}{1000\ \text{mL}} = 4.8 \times 10^{-4}\ \text{moles NaOH}$$

Number of moles of 3.171 mL 0.02 M HCl (titrant) (data obtained from the titrator analysis)

$$= 0.02\ \frac{\text{mol}}{\text{L}} \times 3.171\ \text{mL} \times \frac{1\ \text{L}}{1000\ \text{mL}} = 6.342 \times 10^{-5}\ \text{moles HCl}$$

In a back titration analysis, the acid functional groups on the sample were neutralized with an excessive 60 mL 0.008 M NaOH to ensure a complete neutralization. Therefore, the total acidity of the sample can be calculated as:

$$= 4.8 \times 10^{-4}\ \text{mol} - 6.342 \times 10^{-5}\ \text{mol} = 0.4166\ \text{mmol}$$

The total acidity per gram of catalyst

$$= \frac{0.41658\ \text{mmol}}{0.1035\ \text{g}} = 4.02\ \text{mmol/g}.$$

The measurement was repeated three times, with the average reported as the total acidity.

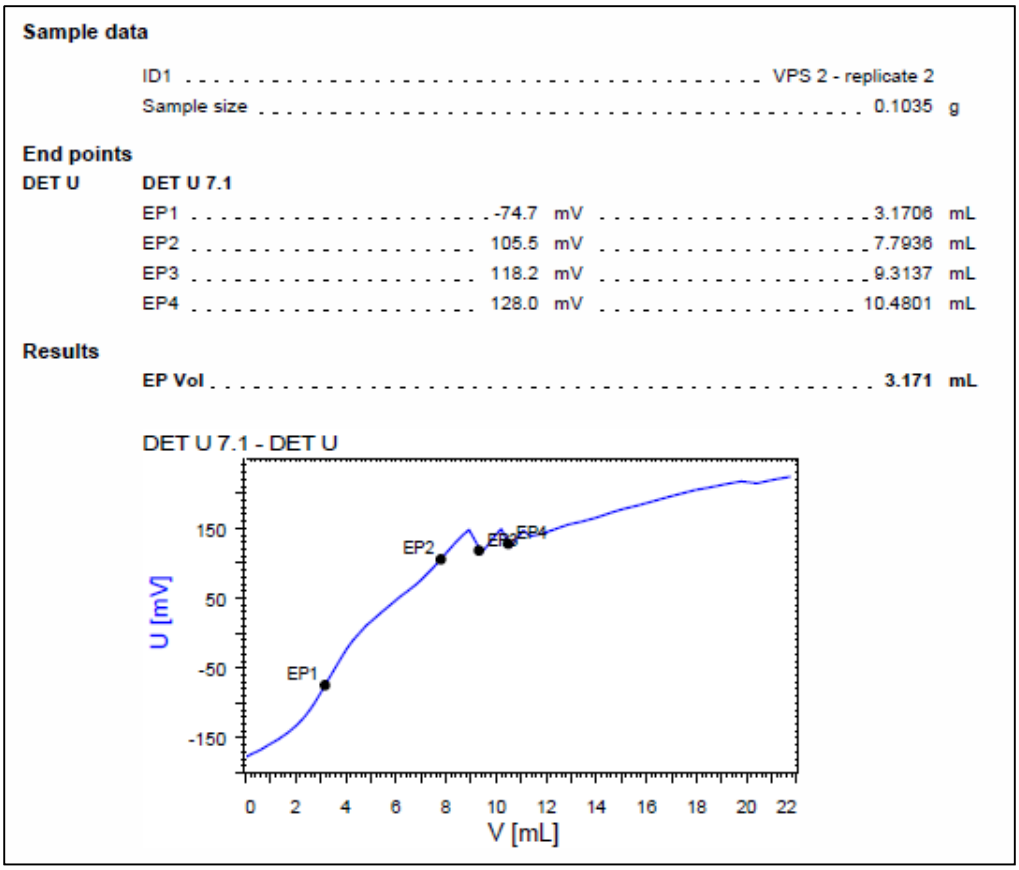

Figure A–1 A titrator analysis print out showing the sample information, end points and the titration curve.

Table A-1 shows the total acidity analysis of three replicates of the carbon-based catalysts.

Table A-1 Data for the total acidity analysis of the carbon-based catalysts.

Catalyst	Total acidity (mmol/g)					
	Replicate 1	Replicate 2	Replicate 3	Average	SD	% SD
VPS 1	3.11	3.19	3.30	3.20	0.10	2.99
VPS 2	3.89	4.02	3.95	3.96	0.07	1.70
VPS 3	4.06	4.08	4.18	4.11	0.07	1.64
Sugar Catalyst	4.19	4.16	4.10	4.15	0.05	1.17

A.4 Sample calculation of SO_3H concentration

Table A-2 shows the elemental analysis of the carbon-based catalyst. Take the mass of sample as 100 g, then, the calculation for VPS1,

Number of moles of C

$$= \frac{63.81}{100} \times 100\ \text{g} \times \frac{1\ \text{mol}}{12.011\text{g}} = 5.313 \text{ moles.}$$

Number of moles of H

$$= \frac{2.2}{100} \times 100\ \text{g} \times \frac{1\ \text{mol}}{1.0079\ \text{g}} = 2.183 \text{ moles.}$$

Number of moles of O

$$= \frac{26.43}{100} \times 100\ \text{g} \times \frac{1\ \text{mol}}{15.9994\ \text{g}} = 1.652 \text{ moles.}$$

Number of moles of S

$$= \frac{2.81}{100} \times 100 \text{ g} \times \frac{1 \text{ mol}}{32.06 \text{ g}} = 0.088 \text{ moles.}$$

Number of moles of SO_3H is similar with the number of moles of S since S is contained only in SO_3H groups.

$$\text{Acidity of } SO_3H = 0.088 \text{ mol} \times \frac{1000 \text{ mmol}}{1 \text{ mol}} \times \frac{1}{100 \text{ gcat}} = 0.88 \text{ mmol/g}$$

Mol ratio to C for H

$$= \frac{2.183}{5.313} = 0.411$$

Mol ratio to C for O

$$= \frac{1.652}{5.313} = 0.311$$

Mol ratio to C for S

$$= \frac{0.088}{5.313} = 0.016$$

Table A-2 Elemental analysis of VPS1.

Catalyst	Element (wt.%)			
	C	**H**	**O**	**S**
VPS 1	63.81	2.20	26.43	2.81

Catalyst	Mol				SO_3H, mmol/g	Mol ratio to Carbon		
	C	**H**	**O**	**S**		**H:C**	**O:C**	**S:C**
VPS 1	5.313	2.183	1.652	0.088	0.88	0.411	0.311	0.016

Appendix B Sulfonation of char

B.1 Calculation of capillary condensation

Physical properties of fuming sulfuric acid (20 wt.% free SO_3) (Muller 2007):

Molecular weight, MW: 98.08 g/mol

Density:

1.925 g/cm^3 at 25°C;

1.81 g/cm^3 at 50^{o}C;

1.80 g/cm^3 at 60^{o}C

Surface tension at 50^{o}C:

25 wt.% H_2SO_4 is 0.070 N/m;

75 wt.% H_2SO_4 is 0.069 N/m;

100 wt.% H_2SO_4 is 0.047 N/m.

Vapour pressure of fuming sulfuric acid (20 wt.% free SO_3):

at 200^{o}C = 700 kPa

at 240^{o}C = 1833 kPa

By assuming linearity and interpolation, vapour pressure of fuming sulfuric acid (20 wt. % free SO_3) at 210^{o}C can be calculated as:

$$\frac{P_{210}- 700}{210-200} = \frac{1833-700}{240-200}$$

P_{210} = 983.25 kPa

In order to find out whether there is a condensation of sulfuric acid vapour in the pores of the particles, Kelvin equation is used to evaluate the capillary condensation, as follows,

$$P = P_o \times e^{\left(-\frac{2\gamma V_m}{rRT}\right)}$$

Equation B-1

where P is the actual vapour pressure, P_o is the saturated vapour pressure, γ is the surface tension, V_m is the molar volume, R is the universal gas constant, r is the radius of the droplet, and T is temperature.

Concentration of sulfuric acid equivalent to fuming sulfuric acid (20 wt.% free SO_3) (oleum) is calculated as (Muller 2007):

% H_2SO_4 = 100 + % oleum/4.444

20% oleum = 104.5% H_2SO_4

Assuming the concentration of sulfuric acid vapour in the sample bed is 45 wt.%, the surface tension of the 45 wt.% sulfuric acid at 50^{o}C is 0.072 N/m (Muller 2007). The capillary condensation at 50^{o}C sample bed temperature can be evaluated as:

$$\therefore \text{Molar volume, } V_m = \frac{\text{Molecular weight}}{\text{Density}} = \frac{98.08\frac{g}{mol}}{1.81\frac{g}{cm^3}} = 54.19\ \frac{cm^3}{mol} = 5.419 \times 10^{-5}\ \frac{m^3}{mol}$$

Radius of the droplet, r = Pore diameter of sample/2 = 4 x 10^{-9} m/2 = 2 x 10^{-9} m

$$P = P_o \times e^{\left(-\frac{2 \times 0.072\frac{N}{m} \times 5.419 \times 10^{-5}\frac{m^3}{mol}}{2 \times 10^{-9}m \times 8.314\frac{J}{Kmol} \times 323\ K}\right)} = P_o \times e^{(-1.453)} = 0.23\ P_o$$

Since P_o > P, the sulfuric acid vapour condenses onto the pores. Similar calculations for 25, 75 and 100 wt.% sulfuric acid vapour were made, with the resulting vapour pressures being 0.24 P_o, 0.25 P_o, and 0.39 P_o, respectively. Hence, it can be concluded that the sulfuric acid vapour, regardless of the concentration, condenses onto the particle pores.

Meanwhile, for an evaluation of the capillary effect for the char sample soaked in the concentrated sulfuric acid at 210^{o}C, the Kelvin equation can be used for a 100 wt.% sulfuric acid (Note: Data for the surface tension of 100 wt. % sulfuric acid at 210^{o}C is not available, hence, in this calculation, surface tension at 50^{o}C is used), as follows:

$$P = P_o \times e^{\left(-\frac{2 \times 0.047\frac{N}{m} \times 5.419 \times 10^{-5}\frac{m^3}{mol}}{2 \times 10^{-9}m \times 8.314\frac{J}{Kmol} \times 483\ K}\right)} = P_o \times e^{(-0.634)} = 0.53\ P_o$$

This shows that the concentrated sulfuric acid easily penetrated into the pores due to the capillary effect.

B.2 Mechanism of sulfonation of benzene

In the catalyst preparation step, the incomplete carbonized sugar was sulfonated using fuming sulfuric acid. The possible sulfonation mechanism is presented as follows (Solomon and Fryhle 2000):

Step 1: $2H_2SO_4 \rightleftarrows SO_3 + H_3O^+ + HSO4^-$
This equilibrium produces SO_3 in concentrated H_2SO_4.

Step 2:

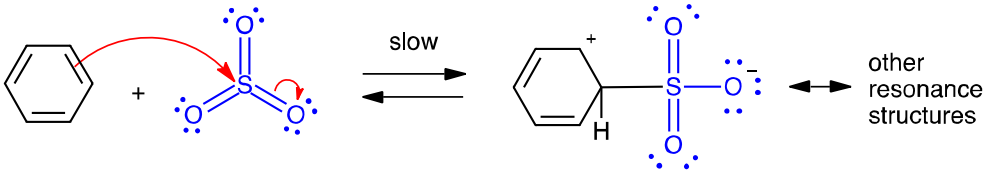

The π electrons of the aromatic C=C act as a nucleophile attacking the electrophilic S, pushing charge out onto an electronegative O atom. This destroys the aromaticity giving the cyclohexadienyl cation intermediate (SO_3 is the actual electrophile that reacts with benzene to form an arenium ion).

Step 3:

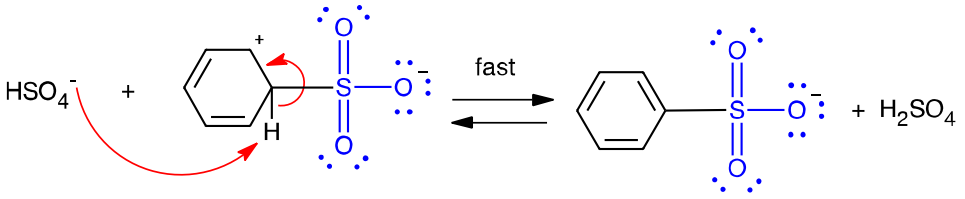

Loss of the proton from the sp^3 C bearing the sulfonyl- group reforms the C=C and the aromatic system (A proton is removed from arenium ion to form the benzenesultonate ion).

Step 4:

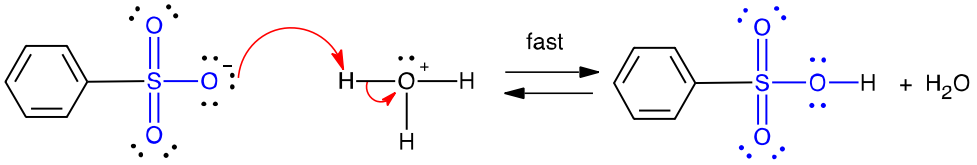

The benzenesulfonate ion accepts a proton to become benzenesulfonic acid.

Figure B–1 Mechanism of sulfonation of benzene.

Under favourable conditions, such as high concentration of water and the presence of dilute sulfuric acid, the equilibrium lies appreciably to the left and desulfonation occurs (Solomon and Fryhle 2000).

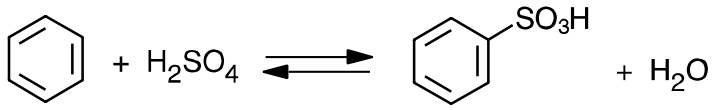

Figure B–2 Sulfonation of benzene showing a reversible reaction. Adapted from Solomon and Fryhle (2000).

B.3 Sample calculation of fuming sulfuric acid concentration in liquid and vapour phases

In order to evaluate the difference between sulfonation in liquid and in vapour phase, the actual concentration of the sulfuric acid at the vicinity of the char particle in each phase is considered. The concentration of 100 wt.% sulfuric acid at 210°C (the data for density at 210°C is not available in the literature; hence, the density at 60°C is used) can be calculated from the following:

$$\frac{\text{Density}}{\text{Molecular weight}} = \frac{1.80\ \text{gcm}^{-3}}{98.08\ \text{gmol}^{-1}} \times \frac{1000\ \text{cm}^3}{1\ \text{L}} = 18.35\ \text{mol/L}$$

Whereas, the concentration of 100 wt.% sulfuric acid vapour at 60°C can be calculated as below:

Vapour pressure of 100 wt.% sulfuric acid vapour at 60°C, $P_{60} = 0.2$ Pa

From the ideal gas law, PV = nRT, the concentration of 100 wt. % sulfuric acid vapour is

$$\frac{n}{V} = \frac{P}{RT} = \frac{0.2\ \text{Nm}^{-2}}{(8.314\ \text{JK}^{-1}\text{mol}^{-1})(333\ \text{K})} = 7.22 \times 10^{-5}\ \frac{\text{mol}}{\text{m}^3} \times \frac{1\ \text{m}^3}{1000\ \text{L}} = 7.22 \times 10^{-8}\ \text{mol/L}$$

The concentration of sulfuric vapour at various wt.% of sulfuric acid vapour at 60 and 80°C are given in Table B-1.

Table B-1 Concentration of sulfuric acid vapour at various vapour pressures and temperatures.

wt.% H_2SO_4	Vapour Pressure, N/m^2		Concentration of H_2SO_4,n/V (mol/L)	
	333 K	353 K	333 K	353 K
25	23000	100000	8.31×10^{-3}	3.41×10^{-2}
45	10000	50000	3.61×10^{-3}	1.70×10^{-2}
75	800	4000	2.89×10^{-4}	1.36×10^{-3}

The calculation shows that the concentration of sulfuric acid in vapour phase is at least 538 fold lower than the concentration of concentrated aqueous sulfuric acid. This gives an insight on the magnitude of reaction between sulfuric acid and carbon; where, the sulfonation of mesoporous char in liquid phase completely destroys the pores, while sulfonation in vapour phase preserves them.

Appendix C Esterification of oleic acid with methanol

C.1 Structure of oleic acid molecule

Figure C-1 shows a simulated molecule size of an oleic acid, with a length of 2.4 nm and a height of 0.3 nm. The geometry of oleic acid molecule was optimized by Accelrays Inc., Dmol^3 module as implemented in the software. It can be inferred that the oleic acid molecules could have easily traveled into the catalyst pores (average pore width being 4 nm). However, the chance of the steric effect occurring is also high especially if the oleic acid molecules agglomerate at the pore mouth. Hence, for the esterification of oleic acid with methanol, the location of active sites is crucial as it affects their accessibility by the long oleic acid molecules.

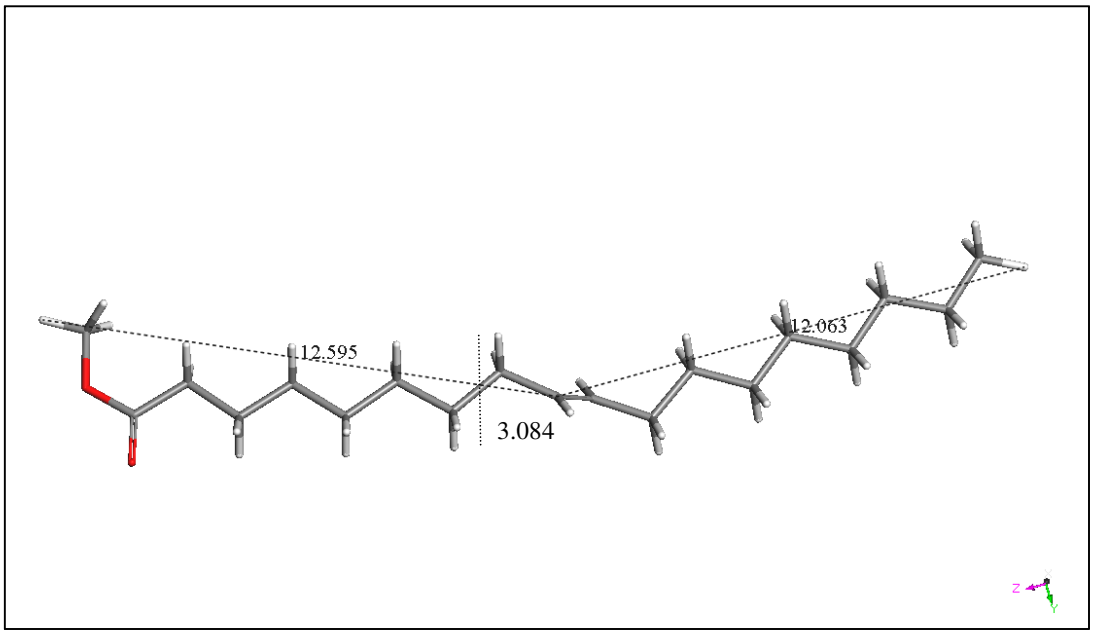

Figure C–1 Simulated molecule size of oleic acid. Unit measurement is in Angstrom.

Figure C-2 shows the mechanism of acid-catalyzed esterification. Esterification reactions proceed very slowly in the absence of strong acid, but they reach the equilibrium within a matter of a few hours when an acid and an alcohol are refluxed with a small amount of concentrated H_2SO_4 (Solomon and Fryhle 2000). In general, oleic acid could undergo hydration reaction under a suitable condition (Mosley et al. 2002).

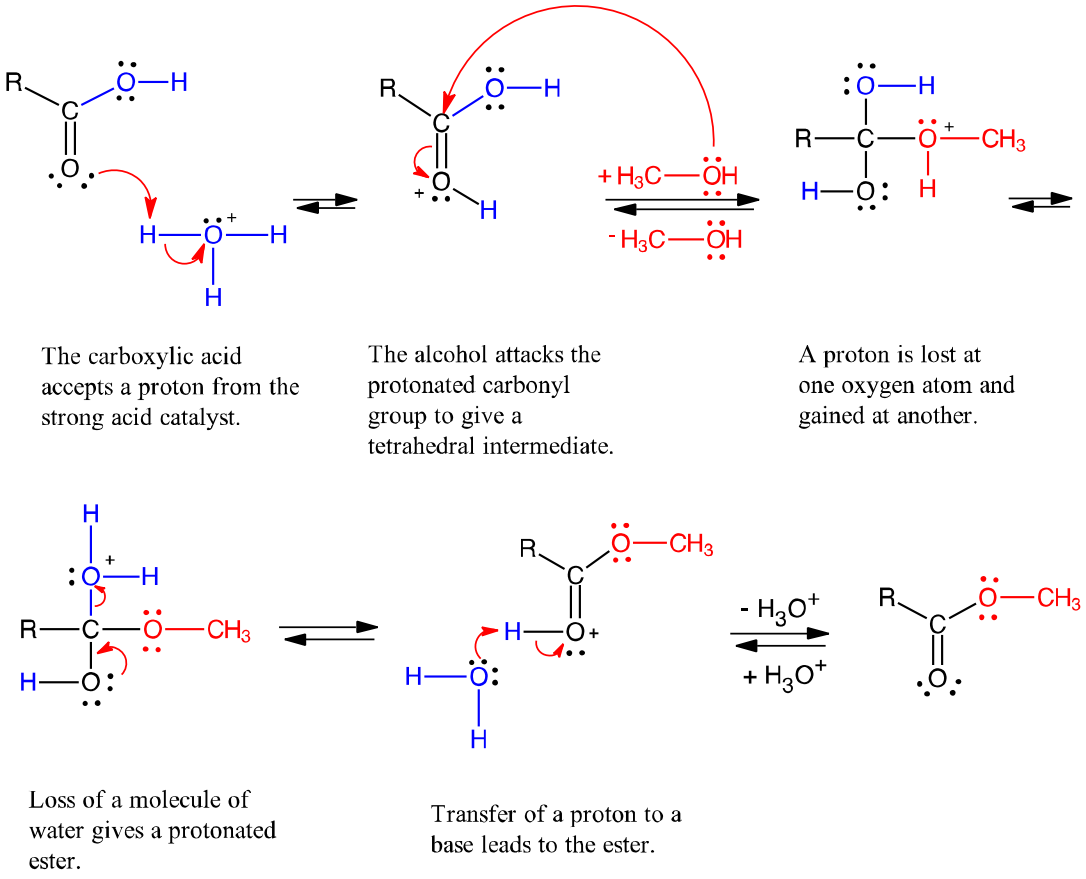

Figure C–2 Mechanism of acid-catalyzed esterification reaction.

C.2 Preparation of methyl oleate calibration curve

A stock solution of methyl oleate was prepared in a 5 mL volumetric flask using heptane as the solvent. One drop of a pure methyl oleate was added into the flask, weighed, and then filled with heptane. The concentration obtained was 540 mg/L methyl oleate. Three methyl oleate standard solutions were then prepared using the stock solutions as indicated in Table C-1.

Table C-1 Concentration of methyl oleate standard solutions.

Volume of stock solution , µL	Methyl oleate standard solution, mg/L	Solution
37	3.996	Standard 1
74	7.992	Standard 2
111	11.988	Standard 3
Volumetric flask volume = 5 mL		

The standard solutions were then analyzed on a GC-MS to generate the methyl oleate calibration curve.

Table C-2 shows the results of the esterification of oleic acid with methanol experiments. There were 4 to 6 trials done for each catalyst.

Table C-2 Data of the esterification of oleic acid with methanol catalyzed by CMK-w-SO_3H, CMK-SO_3H-w, sugar catalyst, and H_2SO_4 reported in Chapter 2.

Time, h	Concentration of methyl oleate (g/mL). Catalyst: CMK-w-SO_3H							
	Trial 1	Trial 2	Trial 3	Trial 4	Trial 5	Trial 6	Ave.	SD
0	0.000	0.000	0.000	0.000	0.000	0.000	0.000	0.000
4	0.272	0.296	0.324	0.384	0.321	0.345	0.324	0.039
10	0.423	0.579	0.353	0.447	0.487	0.469	0.460	0.075
24	0.498	0.470	0.401	0.596	0.530	0.523	0.503	0.065

Time, h	Concentration of methyl oleate (g/mL). Catalyst: CMK-SO_3H-w							
	Trial 1	Trial 2	Trial 3	Trial 4	Trial 5	Trial 6	Ave.	SD
0	0.000	0.000	0.000	0			0.000	0.000
4	0.083	0.083	0.155	0.159			0.120	0.043
10	0.230	0.137	0.186	0.199			0.188	0.039
24	0.251	0.252	0.327	0.365			0.298	0.056

Time, h	Concentration of methyl oleate (g/mL). Catalyst: Sugar catalyst							
	Trial 1	Trial 2	Trial 3	Trial 4	Trial 5	Trial 6	Ave.	SD
0	0.000	0.000	0	0	0		0.000	0.000
4	0.369	0.295	0.274	0.254	0.243		0.287	0.050
10	0.642	0.643	0.340	0.368	0.323		0.463	0.164
24	0.384	0.381	0.388	0.332	0.319		0.360	0.033

Time, h	Concentration of methyl oleate (g/mL). Catalyst: H_2SO_4							
	Trial 1	Trial 2	Trial 3	Trial 4	Trial 5	Trial 6	Ave.	SD
0	0.000	0.000	0.000	0.000	0		0.000	0.000
4	0.453	0.377	0.432	0.373	0.334		0.394	0.048
10	0.551	0.541	0.320	0.340	0.437		0.438	0.108
24	0.343	0.296	0.341	0.479	0.319		0.355	0.072

Table C-3 shows the reproducibility of the GC-MS analysis of three arbitrarily selected samples. The average standard deviation percentage was 3.9%. This indicated that the analysis was reproducible.

Table C-3 Data of the reproducibility of the GC-MS analysis of the esterification samples in Chapter 4.

Sample	Concentration of methyl oleate (mg/L)						
	Trial 1	Trial 2	Trial 3	Trial 4	Average	SD	% SD
SC-8h	2.137	2.289	2.146	-	2.191	0.085	3.9
SC-12h	2.569	2.559	2.450	-	2.526	0.066	2.6
VPS2-12h	2.399	2.416	2.186	2.221	2.306	0.119	5.2

Table C-4 shows the reproducibility of the esterification experiments. There were 2 runs arbitrarily chosen to be carried out three times. The average of the standard deviation percentage was 7.35%.

Table C-4 Data of the reproducibility of esterification experiments in Chapter 4.

Sample	Concentration of methyl oleate (mg/L)					
	Trial 1	Trial 2	Trial 3	Average	SD	% SD
VPS2-2h	1.634	1.390	1.294	1.439	0.175	12.2
H_2SO_4-1h	2.396	2.303	2.412	2.370	0.059	2.5

C.3 Sample calculation of initial formation rate

Figure C-3 shows an activity of VPS1 on the esterification of oleic acid with methanol.

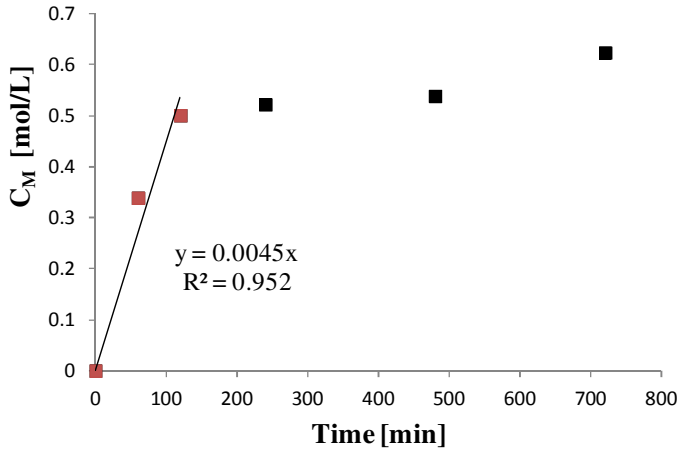

Figure C–3 Concentration of methyl oleate versus time in the VPS1 catalytic system.

Initial formation rate is the tangent of the curve at the origin. Hence, the initial formation rate for VPS1 catalytic system in this example is 4.5 mmol/L.min.

C.4 Calculation of equilibrium constant and equilibrium conversion of esterification reaction

Table C-5 Thermodynamic properties of methanol, oleic acid, methyl oleate, and water

	Gibbs free energy of formation, kJ/mol at 80°C
Methanol (CAS# 67-56-1)	- 153.2
Oleic acid (CAS# 112-80-1)	- 98.97
Methyl Oleate (CAS#112-62-9)	- 21.31
Water (CAS#7732-18-5)	-237.19 (Liquid)

(Source: Knovel database)

Esterification reaction:
Oleic acid + Methanol ⇆ Methyl oleate + Water
The equilibrium constant at temperature T can be calculated from the change in the Gibbs free energy using
$-RT\ln[K(T)] = \Delta G^{o}Rx(T)$

Equation C-1

$\Delta G^{o}Rx(80^{o}C)$ $= \Delta G^{o}$Methyl oleate + ΔG^{o}water $-\Delta G^{o}$Oleic acid - ΔG^{o}Methanol
$= (-21.31) + (-237.19) - (-153.2) - (-98.97)$
$= -6.33$ kJ/mol.

$$\ln K(80^{o}C) = \frac{-\frac{6.33\ \text{kJ}}{\text{mol}} \times 1000\ \text{J/kJ}}{-8.3145\ \frac{\text{J}}{\text{Kmol}} \times 353.15\ \text{K}}$$

$\ln K(80^{o}C) = 2.1558$

Equilibrium constant, $K_e(80^oC) = e^{2.1558} = 8.63$

The concentration equilibrium constant K_e is

$$K_e = \frac{[\text{Methyl oleate}][\text{water}]}{[\text{Oleic acid}][\text{Methanol}]} = \frac{C_m \times C_w}{C_A \times C_o}$$

Equilibrium conversion can be related with the equilibrium constant for an equal molar feed as

$$K_e = \frac{C_{A,0}.X_e \times C_{A,0}.X_e}{C_{A,0}.(1-X_e) \times C_{A,0}.(1-X_e)} = \frac{X_e^2}{(1-X_e)^2} = 8.6348$$

$$\frac{X_e}{1-X_e} = \sqrt{8.6348} = 2.9385$$

$$X_e = \frac{2.9385}{3.9385} = 0.7461 = 75\ \%$$

Table C-6 shows the data for the samples used to generate the plot in Figure 3-20.

Table C-6 Data of the porosity analysis of the chars and functionalized chars in the multiple vapour phase sulfonation (Chapter 3).

Sample	Sulfonation Temp., ^oC	Sulfonation time, h	Micropore Area (m^2/g)	BET SA (m^2/g)	Micropore volume (cm^3/g)	Pore size (nm)
Sample 1	120	24	141	822	0.058	5.80
Sample 2	120	24	132	790	0.055	5.88
Sample 3	120	24	152	856	0.063	5.75
Sample 5	160	5	138	588	0.060	4.86
Sample 6	22	24	15	100	0.006	3.40
Sample 7	22	24	110	565	0.046	5.17
Sample 8	60	24	79	453	0.033	5.06
Sample 9	60	24	27	177	0.011	3.48
Sample 10	60	1	125	485	0.055	3.79
Sample 11	80	1	111	418	0.049	3.39
Sample 12	40	1	160	531	0.071	3.43
Sample 13	60	0.5	119	584	0.05	4.38
Sample 15	60	4	110	569	0.05	4.24
Sample 16	80	4	102	526	0.04	3.66
Sample 17	60	1	42	121	0.02	2.42
Sample 18	60	1	2.3	2.6	0.0011	1.46
Sample 19	60	24	107	511	0.05	3.62
VPS 1	80	4	74	403	0.03	5.02
VPS 2	60	1	24	106	0.01	3.54
VPS 3	60	1	12	40	0.01	3.18
CMK-w[a]	-	-	140	872	0.06	6.34
CMK-w[b]	-	-	131	827	0.05	6.28

[a]Batch 2
[b]Batch 3

Figures C-4 and C-5 show the nitrogen sorption and pore size distribution of three different batches of CMK-w. The variation among batches was nominal, which was 3.3% with respect to the BET surface area (Table C-7).

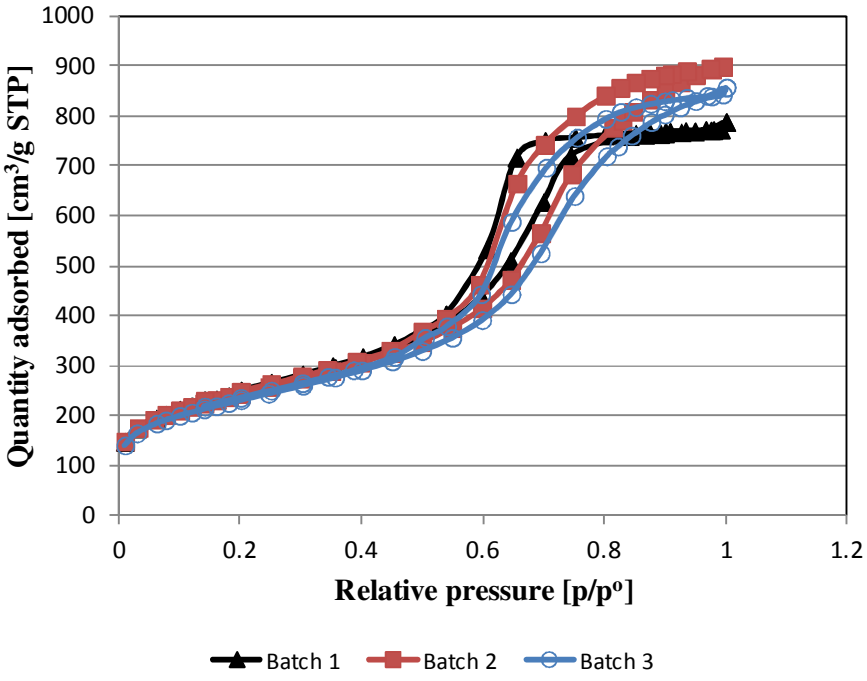

Figure C–4 Nitrogen sorption isotherm of three different batches of CMK-w measured at -196°C.

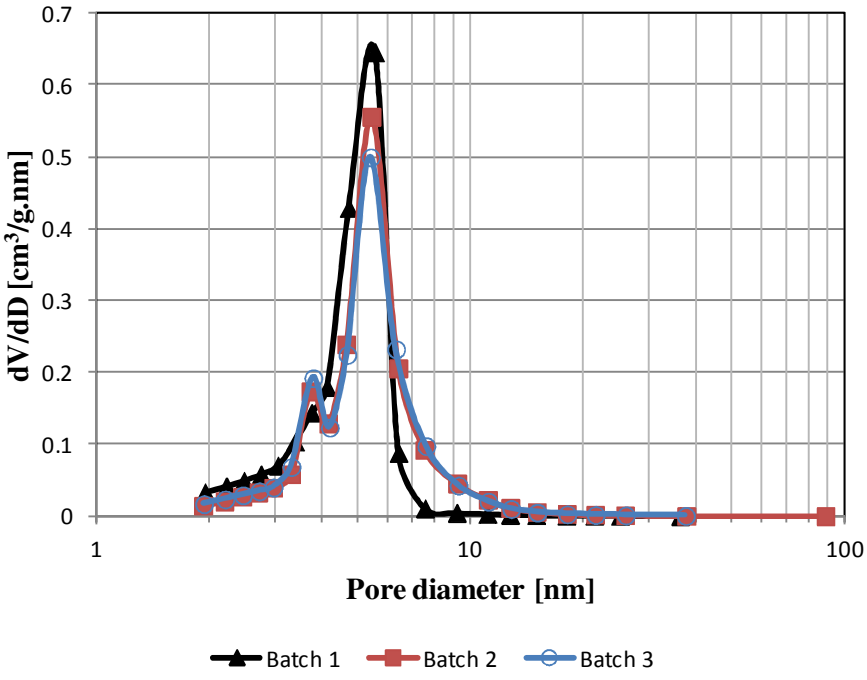

Figure C–5 BJH (desorption) pore size distribution plots of three different batches of CMK-w.

Table C-7 Analysis of the reproducibility of the preparation of CMK-w.

CMK	BET Surface area (m^2/g)
Batch 1	880
Batch 2	872
Batch 3	827
Average	860
SD	29
% SD	3.32

C.5 Results of TGA and DTA of VPS2, VPS3, and sugar catalyst spent catalysts.

Figures C-6 through C-11 show the results of TGA and DTA of VPS2, VPS3, and sugar catalysts. Results for VPS1 are given in Figures 4-6 and 4-7.

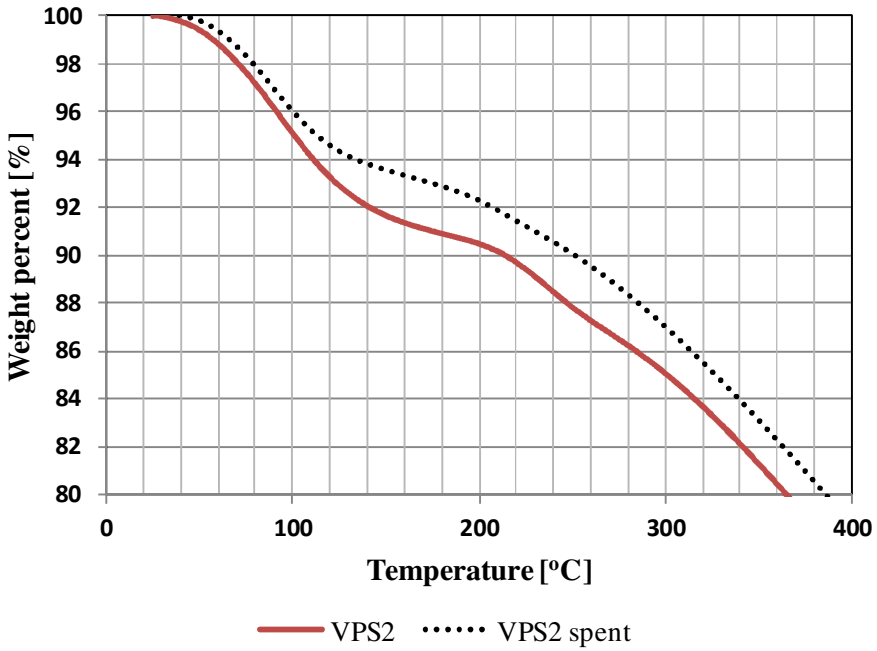

Figure C–6 TGA of fresh and spent VPS2 under N_2.

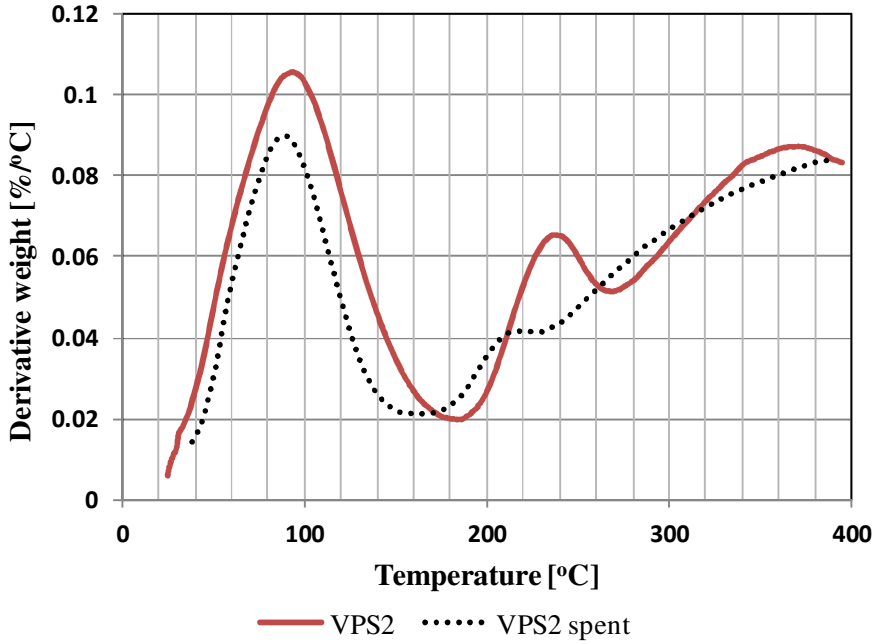

Figure C–7 DTA of fresh and spent VPS2 under N_2.

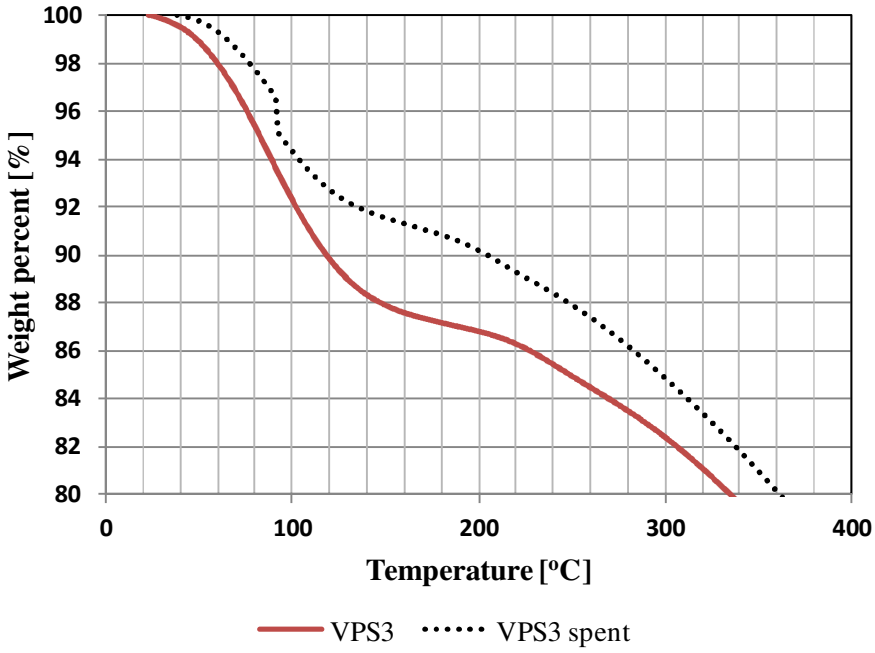

Figure C–8 TGA of fresh and spent VPS3 under N_2.

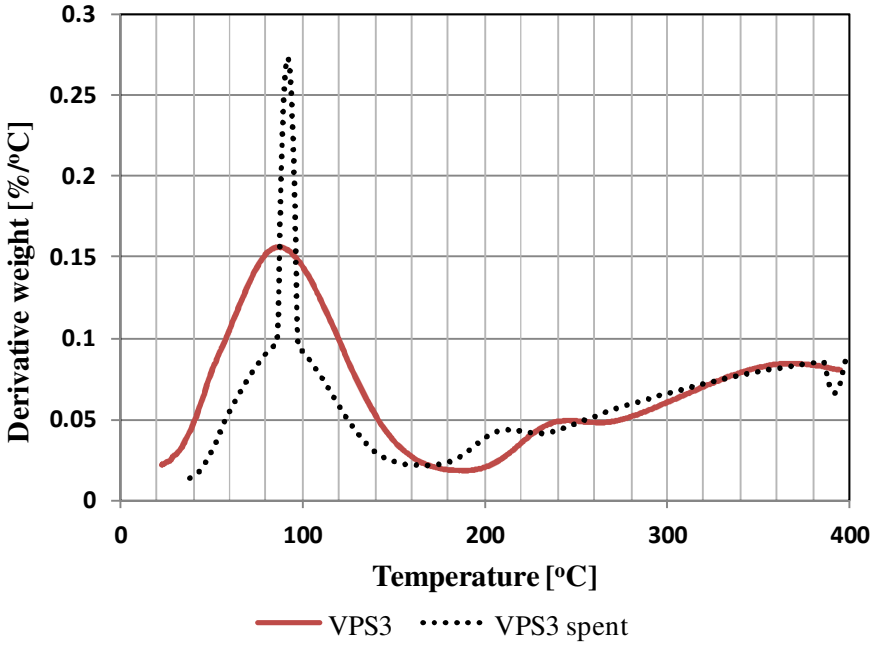

Figure C–9 DTA of fresh and spent VPS3 under N_2.

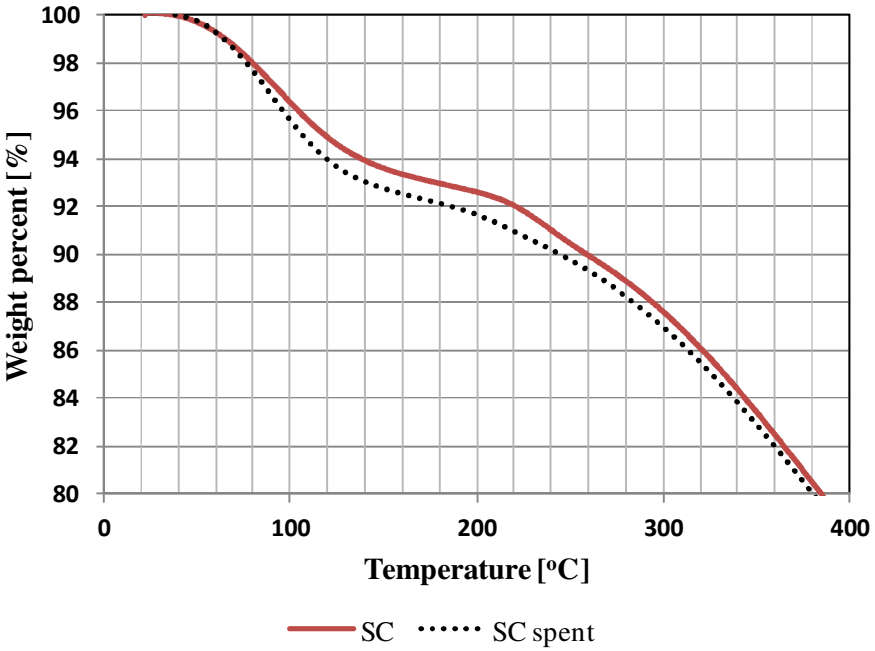

Figure C–10 TGA of fresh and spent sugar catalyst under N_2.

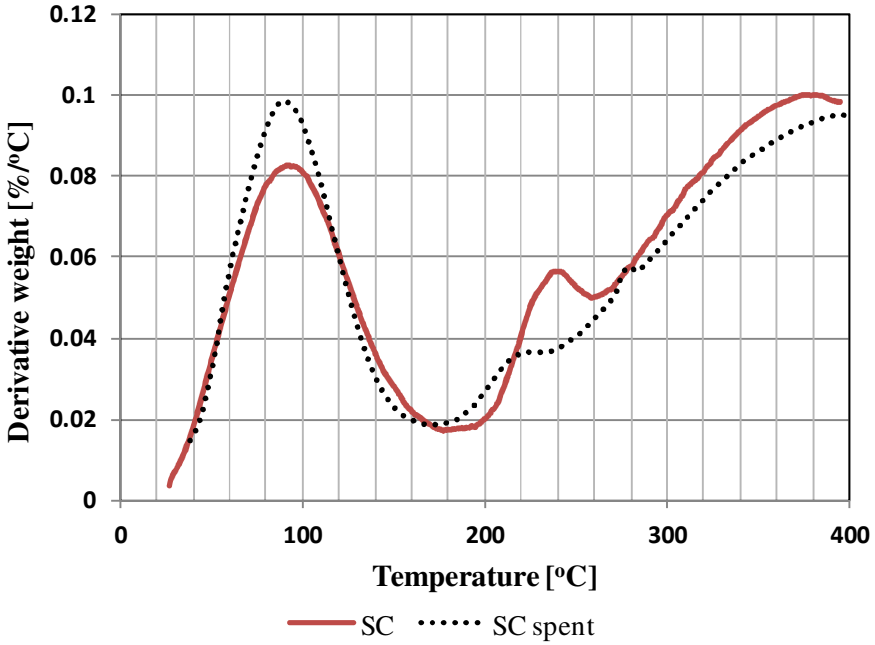

Figure C–11 DTA of fresh and spent sugar catalyst under N_2.

C.6 Determination of reaction order

Reaction order was evaluated with respect to oleic acid using first and second order equations.
First order reaction:

$$\frac{dC_A}{dt} = kC_A$$

Equation C-2

Integration gives

$$\int_{C_{Ao}}^{C_A} \frac{dC_A}{C_A} = k\int_0^t dt$$

$$\ln\frac{C_{Ao}}{C_A} = kt$$

Equation C-3

A plot of $\ln\frac{C_{Ao}}{C_A}$ versus t gives a linear curve for a first order reaction. Figure C-12 shows the curve fit of first order equation for all catalytic systems.

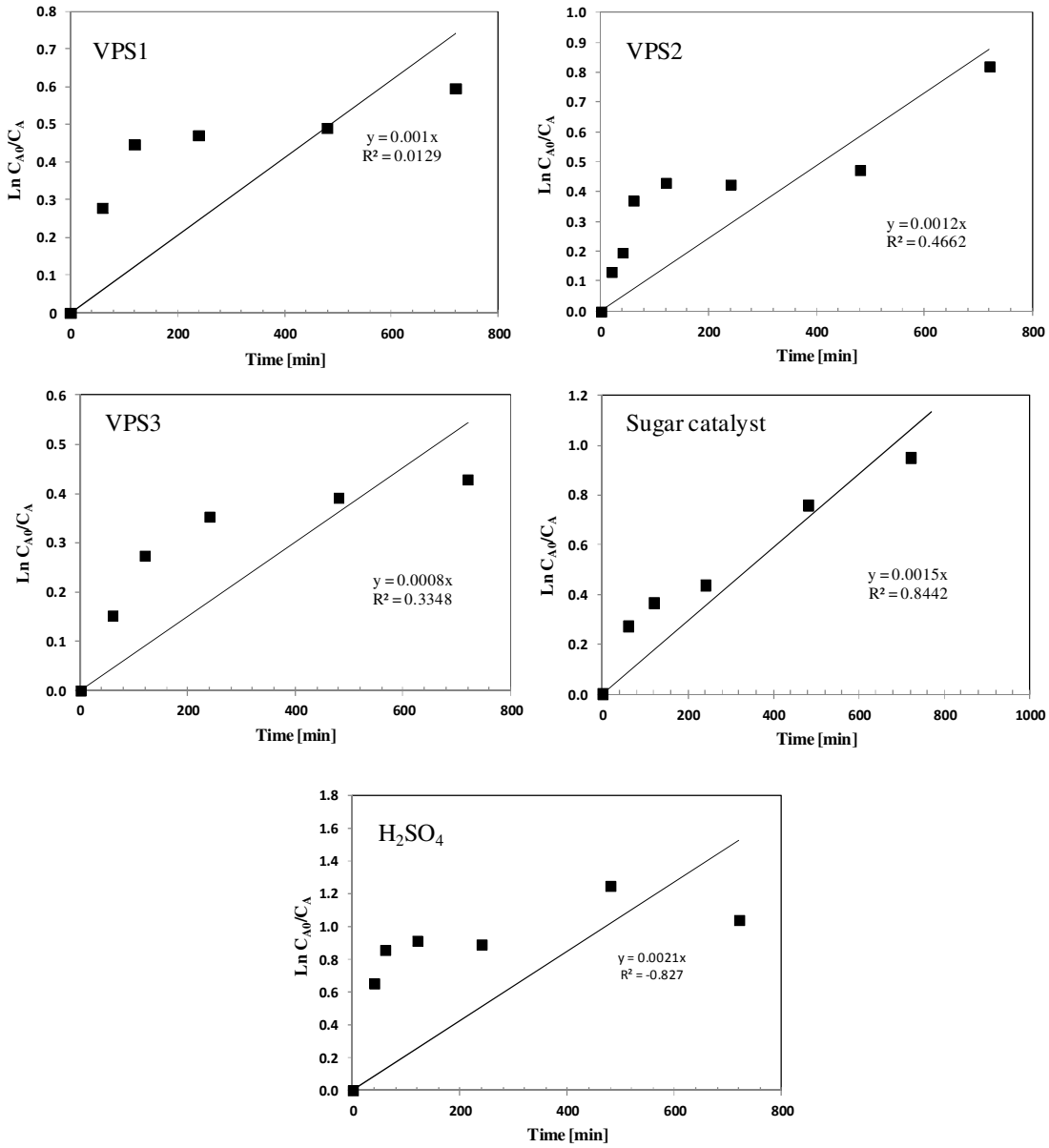

Figure C–12 Curve fit using first order reaction model for the esterification of oleic acid with methanol catalyzed by VPS1, VPS2, VPS3, sugar catalyst or H_2SO_4.

For a second order reaction, the kinetic expression is:

$$\frac{dC_A}{dt} = kC_A^{\,2}$$

Equation C-4

Integration gives

$$\int_{C_{Ao}}^{C_A} \frac{dC_A}{C_A^{\,2}} = k\int_0^t dt$$

$$\frac{1}{C_A} - \frac{1}{C_{Ao}} = kt$$

$$\frac{1}{C_A} = \frac{1}{C_{Ao}} + kt$$

Equation C-5

A plot of $\frac{1}{C_A}$ versus t gives a linear curve with an intercept of $\frac{1}{C_{Ao}}$ for a second order reaction. Figure C-13 shows the plot for second order equation for all catalytic systems.

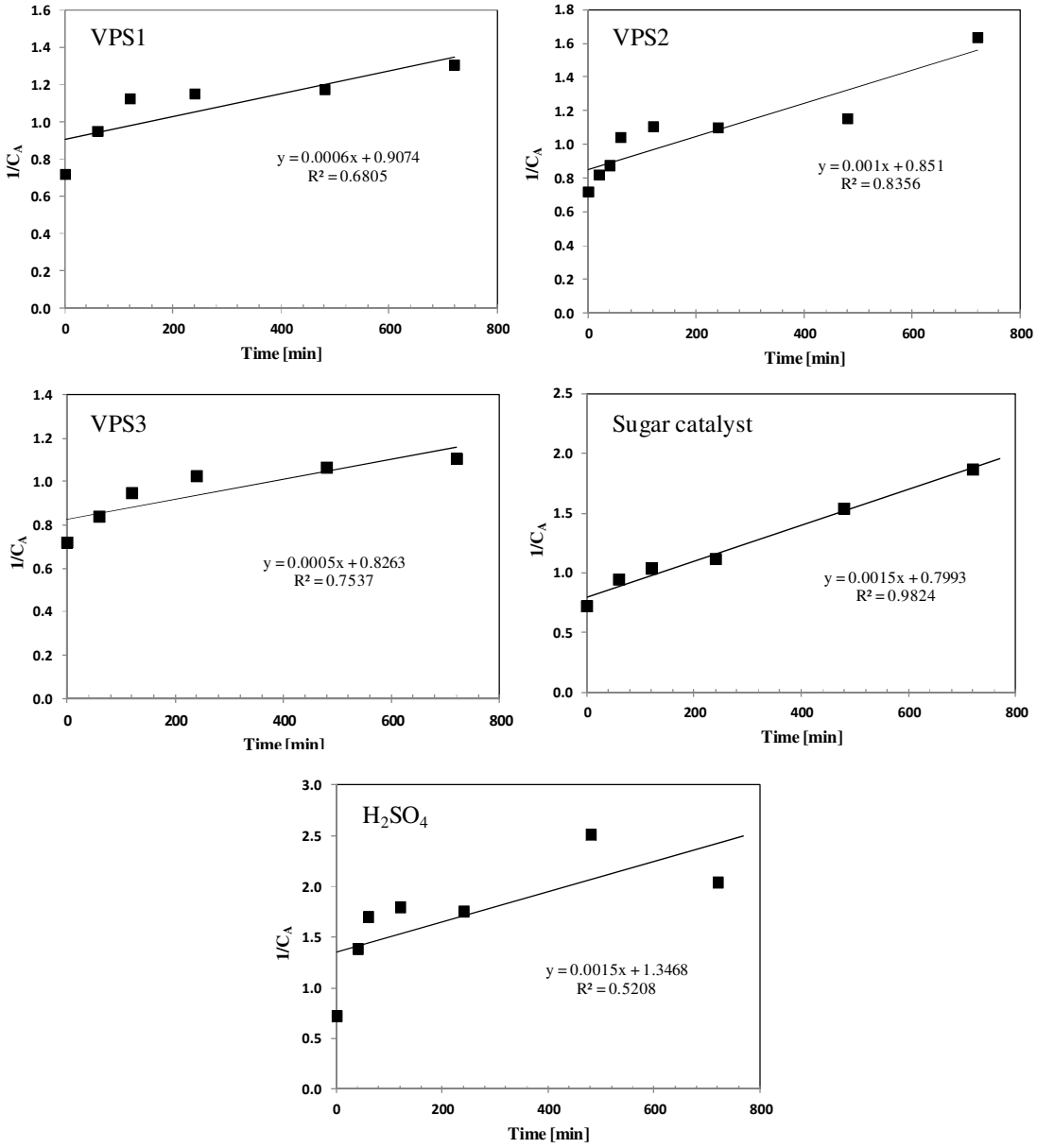

Figure C–13 Curve fit using second order reaction model for the esterification of oleic acid with methanol catalyzed by VPS1, VPS2, VPS3, sugar catalyst, or H_2SO_4.

Figure C-14 shows the comparison of experimental and first and second order simulations of the oleic acid conversion. As shown in Figure C-14, the goodness of fit, R^2, of the second order reaction for all catalytic systems are larger than that of the first order reaction. This implies that the second order reaction kinetics fits the data better than the first order reaction kinetics. However, the values of R^2 of the second order reactions are relatively low. This suggests that the catalytic systems undergo catalyst deactivation, which contributes to the poor fit when using second order reaction kinetic alone. Hence, a mathematical model has been developed to incorporate deactivation term into the second order kinetic expression, as shown in Section 4.3.3.

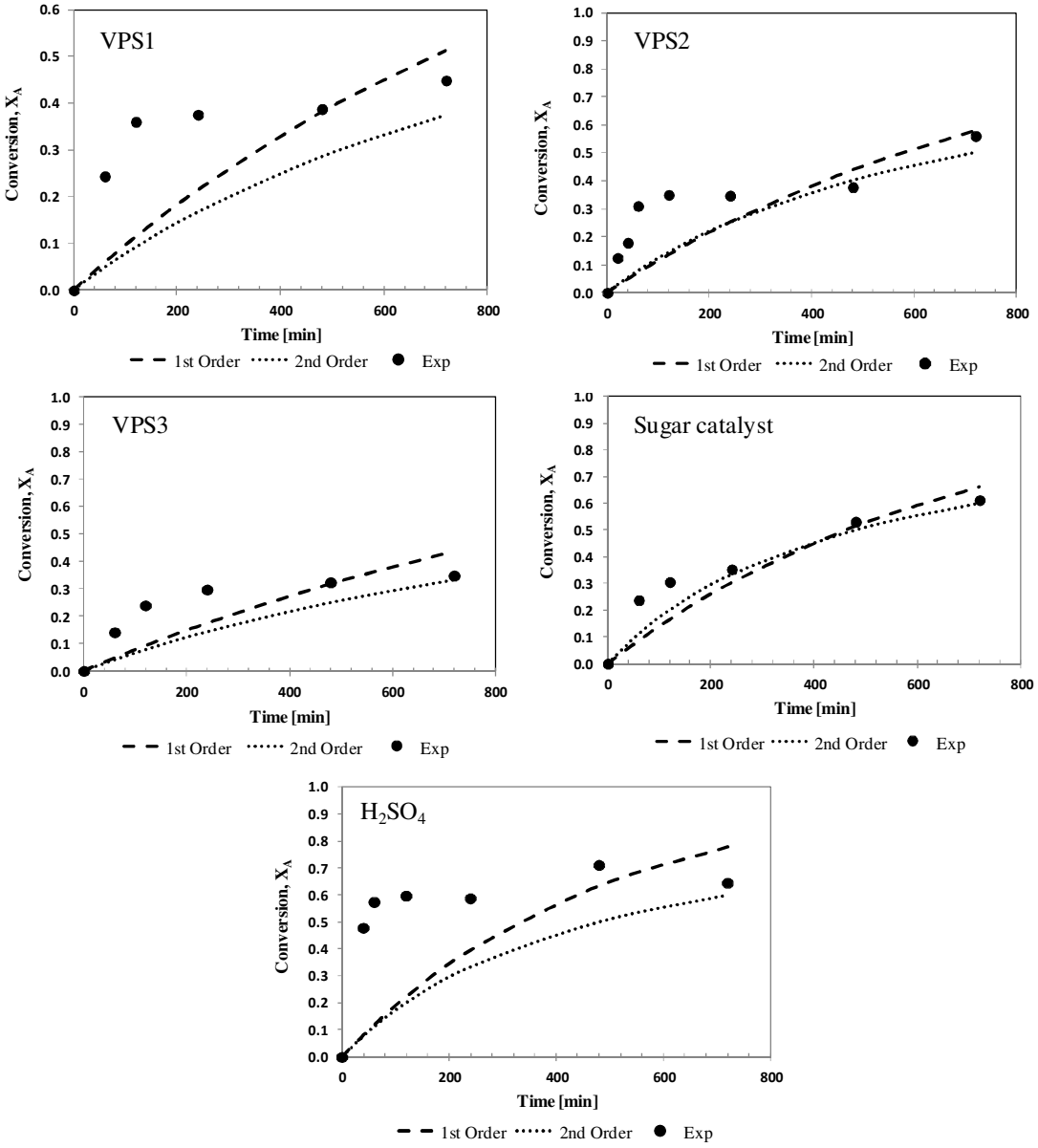

Figure C–14 Comparison of experimental, first order and second order simulations of the oleic acid conversion catalyzed by VPS1, VPS2, VPS3, sugar catalyst, or H_2SO_4.

C.7 Calculation of effectiveness factor

The low conversion of the esterification of oleic acid with methanol catalyzed by the carbon-based catalysts was associated with catalyst deactivation. In order to estimate the influence of internal pore diffusion on the reaction rates in the carbon-based catalysts, the Weisz – Prater criterion is used. The Weisz - Prater criterion (C_{WP}) uses measured values of the rate of reaction, $-r_A'$ (obs), to determine if internal diffusion is limiting the reaction, as shown in the following equation (Fogler 2006):

$$C_{WP} = \frac{-r_A'(obs)\rho_c R^2}{D_e C_{As}}$$

Equation C-6

where

$-r_A'$ (obs)	Rate of reaction observed (mol/L.s.gcat)
ρ_c	Specific density of catalyst (g/m^3)
R	Catalyst particle radius (m)

D_e Effective diffusivity (m^2/s)

C_{As} Concentration of A at the surface (mol/L or M)

All the terms in Eq. C-7 are either measured or calculated, as shown in the following sections. Consequently, C_{WP} can be calculated. If

$$C_{WP} << 1$$

there are no diffusion limitations and consequently no concentration gradient exists within the pellet. If

$$C_{WP} >> 1$$

internal diffusion limits the reaction severely.

To the best of author's knowledge, effective diffusivity, D_e, for the esterification of oleic acid with methanol is not available in the literature. Therefore, this value is estimated using the correlations available in the literature as shown in the following step-by-step calculation.

C.7.1 Calculation of effective diffusivity of oleic acid – methanol

Effective diffusivity in porous solids can be calculated as (Fogler 2006)

$$D_e = \frac{D_{AB}\phi_p\sigma_c}{\tilde{\tau}}$$

Equation C-7

where

$$\tilde{\tau} = \text{tortuosity} = \frac{\text{Actual distance a molecule travels between two points}}{\text{Shortest distance between those two points}}$$

$$\phi_p = \text{catalyst porosity} = \frac{\text{Volume of void space}}{\text{Total volume (voids and solids)}}$$

σ_c = Constriction factor

D_{AB} = Mutual diffusivity (m^2/s)

The values of the tortuosity and constriction factor for the carbon-based catalyst are not known, and are therefore estimated based on the typical values reported in the literature (Fogler 2006): $\tilde{\tau} = 3.0$ and $\sigma_c = 0.40$, respectively.

Likewise, to the best of author's knowledge, the mutual diffusion for oleic-methanol at 80°C, D_{AB}, is also not available in the literature. This value is estimated using the correlations available in the literature. For the calculation of effective diffusivity of oleic acid – methanol, their individual properties are given in Table C-8.

Reaction condition of esterification oleic acid with methanol:

Methanol = 250 mmol (MW = 32.04 kg/kmol)

Oleic acid = 25 mmol (MW = 282.467 kg/kmol)

Reaction temperature = 80°C (353K)

Table C-8 Properties of oleic acid and methanol for the calculation of mutual diffusivity.

	Density, ρ (kg/m^3)	Viscosity, μ (cP)	Mole fraction, x_i	Molar Volume, V (m^3/kmol)	Critical temperature, T_c (K)	Critical pressure, P_c (Pa)	Assoc. factor, φ
Oleic acid (A)	853.7	6.556	0.09	0.3309	781	1.39×10^6	1
Methanol (B)	725.8	0.2917	0.91	0.0441			1.9

(Source: Knovel database)

Mutual diffusion of oleic acid in methanol is calculated according to Siddiqi-Lucas correlation (Knudsen et al. 1997)

$$D^o_{AB} = \frac{9.89 \times 10^{-8}\, V_B^{0.265}\, T}{V_A^{0.45}\, \mu_B^{0.907}}$$

Equation C-8

where

D^o_{AB} Mutual diffusivity at infinite dilution of A (oleic acid) in B (methanol) (m^2/s or cm^2/s)

V_A, V_B Molar volume of A (oleic acid) and B (methanol) at its normal boiling point (m^3/kmol or cm^3/mol)

μ_A, μ_B Viscosity of pure A and B (methanol) (cP)

T Temperature (K)

Hence,

$$D^o_{AB}=\frac{9.89\times10^{-8}\times0.0441^{0.265}\times353}{0.3309^{0.45}\times0.2917^{0.907}}$$

$$\therefore D^o_{AB}=7.6769\times10^{-5}\ m^2s^{-1}$$

In a similar fashion, mutual diffusion of methanol in oleic acid can be calculated as

$$D^o_{BA}=\frac{9.89\times10^{-8}\ V_A^{0.265}\ T}{V_B^{0.45}\ \mu_A^{0.907}}$$

$$D^o_{BA}=\frac{9.89\times10^{-8}\times0.3309^{0.265}\times353}{0.0441^{0.45}\times6.556^{0.907}}$$

$$\therefore D^o_{BA}=1.9275\times10^{-5}\ m^2s^{-1}$$

Cladwell-Babb correlation (Knudsen et al. 1997) for mutual diffusivity, D_{AB},

$$D_{AB}=(x_A\ D_{BA}{}^o+x_B\ D_{AB}{}^o)\ \beta_A$$

Equation C-9

where

$$\beta_A=\frac{M_A^{1/2}\times P_c^{1/3}}{T_c^{5/6}}=\frac{282.467^{0.5}\times\left(1.39\times10^6\right)^{1/3}}{781^{5/6}}=7.2881$$

hence,

$$D_{AB}=\left(0.09\times1.9275\times10^{-5}+0.91\times7.6769\times10^{-5}\right)7.2881$$

$$=5.2155\times10^{-4}\ m^2s^{-1}.$$

The value of catalyst porosity, ϕ_p, of the carbon-based catalysts is measured in the laboratory as discussed in the succeeding section.

C.7.1.1 Determination of catalyst porosity

Catalyst porosity, ϕ_p, can be calculated using the following equation

$$\phi_p=\frac{V_{pore}}{V_{pore}+\frac{1}{\rho_s}}$$

Equation C-10

where

V_{pore} Total pore volume (cm^3/g)

ρ_s Catalyst specific density (g/cm^3)

Total pore volume of the catalyst sample was measured using a porosimeter (Micromeritics ASAP 2020); whereas, catalyst specific density was measured using a pycnometer (Quantachrome Instruments).

In a typical pycnometry analysis, a helium gas was used, as opposed to nitrogen gas, because helium gas could better penetrate into the carbon-based catalyst particles. A micro cup type was used in the measurement (Table C-9).

Table C-9 Cup and reference volumes for pycnometer measurement.

Standard volumes (Cup type: Micro)	
Cup volume, Vc (cm^3)	12.1829
Reference volume, Vr (cm^3)	6.0925

Below is a sample calculation for sample VPS1:

Measured values: Weight of VPS1, w = 1.5695 g

P1 = 17.137 kPa

P2 = 5.982 kPa

Volume of the particulate sample (V_p) is calculated from,

$$V_p = V_c - V_r\left(\frac{P1}{P2} - 1\right) = 12.1829 - (6.0925)\left(\frac{17.137}{5.982} - 1\right) = 0.8218 \text{ cm}^3$$

The catalyst specific density, ρ_s is calculated from

$$\rho_s = \frac{W}{V_p} \times 1000 = \frac{1.5695}{0.8218} \times 1000 = 1909.73 \text{ kgm}^{-3} = 1.91 \text{ gcm}^{-3}$$

From the porosimetry analysis, the total volume of pores, $V_{pore} = 0.51$ cm^3/g

The catalyst porosity (ϕ_p) can be calculated as:

$$\phi_p = \frac{V_{pore}}{V_{pore} + \frac{1}{\rho_s}} = \frac{0.51}{0.51 + \frac{1}{1.91}} = 0.492$$

The measurement of the solid density of the carbon-based catalyst was done in triplicate (Table C-10), their average porosities are presented in Table C-11.

Table C-10 Data of the measurement of specific density of VPS1, VPS2, and VPS3.

Sample	Specific density, ρ (g/cm^3)					
	Trial 1	Trial 2	Trial 3	Average	SD	% SD
VPS1	1.9097	2.0290	1.7157	1.8848	0.1581	8.39
VPS2	1.8496	1.5790	1.4363	1.6216	0.2099	12.95
VPS3	1.0350	1.0302	1.3320	1.1324	0.1729	15.27

Table C-11 Characteristics of VPS1, VPS2, and VPS3.

Catalyst	Specific density, ρ_s, 10^6 g/m^3	Porosity, ϕ_p	Total pore volume V_{pore}, cm^3/g	Particle radius, R, μm
VPS1	1.885 ± 0.129	0.488	0.51	38.0
VPS2	1.622 ± 0.171	0.132	0.09	30.5
VPS3	1.132 ± 0.141	0.035	0.03	27.0

Effective diffusivity in porous solid (VPS1) can now be calculated as

$$D_e = \frac{D_{AB}\phi_p\sigma_c}{\tilde{\tau}} = \frac{0.000521554 \times 0.492 \times 0.4}{3.0} = 3.4214 \times 10^{-5} \text{m}^2\text{s}^{-1}$$

The data below were obtained experimentally,

Reaction rate, $-r_A'$ (obs) = 3.567 x 10^{-4} M/s.gcat

Finally, once all the required terms are obtained, the Weisz – Prater criterion can be calculated using the correlation

$$C_{WP} = \frac{r_A \rho_s R^2}{D_e C_{As}}$$

Equation C-11

For example, for VPS1, with $C_{AS} = 1.388$ M,

$C_{WP} = \frac{3.567\times10^{-4}\times1.885\times10^{6}\times0.000038^2}{3.4214\times10^{-5}\times1.388} = 0.02 \ll 1$ - there is no diffusion limitation.

Realistically, the concentration at the surface, C_{AS}, cannot be measured by standard techniques. Table C-12 shows the Weisz – Prater criterion for various C_{AS} values. All catalysts show no diffusion limitation up to 0.092 mol/L. In the esterification experiment, the lowest concentration of oleic acid at maximum conversion was 0.5 mol/L. This implies that, for all the catalytic systems tested, there were no diffusion limitations.

Table C-12 Weisz - Prater criterion for VPS1, VPS2, and VPS3 at various C_{AS} values.

Concentration of oleic acid at the surface, C_{AS} (mol/L)	Weisz – Prater criterion, C_{WP}		
	VPS1	VPS2	VPS3
1.388	0.02	0.07	0.06
0.200	0.14	0.46	0.39
0.092	0.31	0.99	0.85
0.080	0.36	1.14	0.98
0.060	0.48	1.53	1.30
0.020	1.43	4.58	3.90

Appendix D Etherification of glycerol with isobutylene

D.1 Structure of glycerol molecule

Figure D-1 shows a simulated molecule size of a glycerol, indicating a molecule length of 0.63 nm and a height of 0.34 nm. The size of glycerol is relatively very small compared with the pore diameter of VPS1, VPS2 and VPS3 (~4 nm). This suggests that glycerol molecules can easily access the active sites in the pores without steric effect as opposed to the circumstance in the esterification of oleic acid.

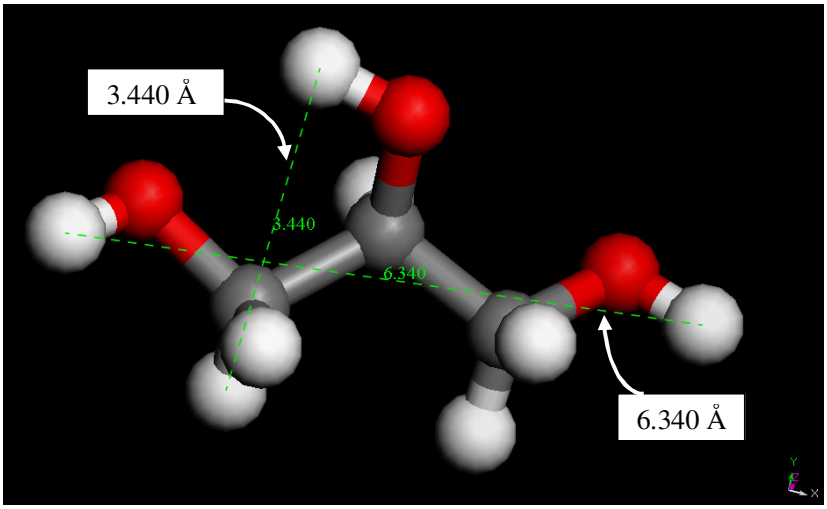

Figure D–1 Simulated molecule size of glycerol.

D.2 Detailed procedures for the etherification of glycerol with isobutylene experiment

Figure D-2 shows the dimension of the 50 mL autoclave reactor. The volume of reactor below the mechanic stirrer level is

$$= \frac{\pi D^2}{4} H = \frac{\pi(33.02\ \text{mm})^2}{4} \times (58.42\ \text{mm} - 52\ \text{mm}) = 4544\ \text{mm}^3 = 4.5\ \text{mL}$$

The volume of glycerol has to be at least 4.5 mL in order to reach the level of the mechanic impeller. Without the impeller switched on, glycerol does not mix with isobutylene, but settles at the bottom of the reactor together with the solid catalyst. A good mixing of glycerol, isobutylene, and the catalyst is achieved once the impeller is switched on with the glycerol level is above the level of the mechanic impeller, as shown in Figure D-2. If a reaction was performed with the volume of glycerol below the level of the mechanic impeller, the mixing would not happen immediately because of immiscibility of glycerol and isobutylene. Hence, in this study, an isobutylene to glycerol molar ratio of 2:1 was used, where the volumes of glycerol and isobutylene were 13 and 33 mL, respectively.

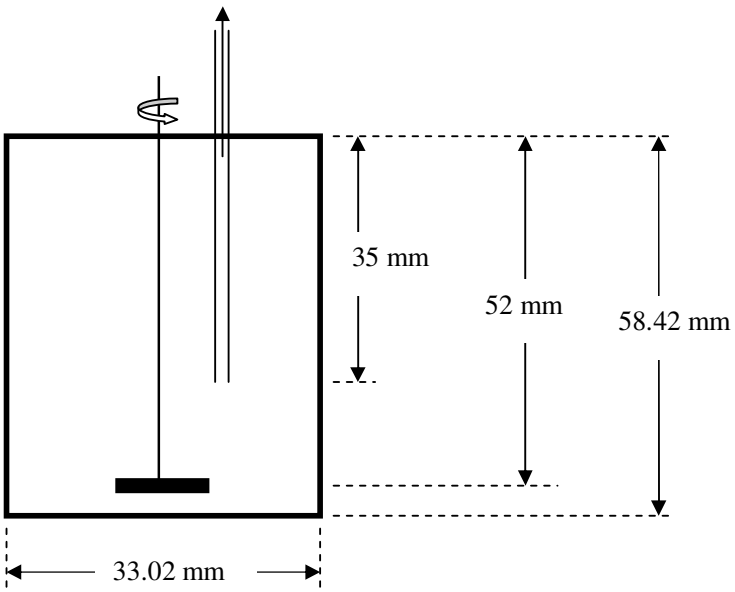

Figure D–2 Dimension of a 50 mL autoclave reactor showing the height of the mechanic 4-blade impeller and sampling tube (not to scale).

A list of chemicals used in the experiment is presented in Table D-1.

Table D-1 Properties of chemicals used in the etherification of glycerol with isobutylene experiment.

Compound	MW (g/mol)	Density, g/mL	Purity, %
Glycerol	92.09	1.262	98.57
MTBG	148.20	1.44	99.08
DTBG	204.31	0.9223[1]	72.96
TTBG	260.41	0.8000[2]	87.88
DIB	112.21	0.708	
1,3-propanediol	76.09	1.053	93.53
Isobutylene	56.11	0.59	
MSTFA	199.25	1.075	
Pyridine	79.10	0.978	100

[1,2] Experimentally measured in the lab by taking the weight of 100 and 10 µL for DTBG and TTBG, respectively (Table D-2). The measurement was repeated 3 times, and the data reported are the average. The errors of the DTBG and TTBG densities are 3.9 and 4.5%, respectively.

Table D-2 Data of the measurement of the density of DTBG and TTBG.

Sample	Volume (uL)	Density (g/mL)					
		Trial 1	Trial 2	Trial 3	Average	SD	% SD
DTBG	100	0.9040	0.9250	0.9380	0.9223	0.0172	1.86
TTBG	10	0.7600	0.8100	0.8300	0.8000	0.0361	4.51

D.2.1 Procedure for analysis of glycerol etherification with isobutylene product

D.2.1.1 Preparation of calibration curves using Internal Standard technique

0.0304 g of 1,3-propanediol used as internal standard was dissolved in 972 µL pyridine. Concentration of the internal standard (IS) can be calculated as:
Volume of 0.0304 g 1,3-propanediol

$$= \frac{0.0304\ \text{g}}{1.053\ \frac{\text{g}}{\text{mL}}} \times \frac{1000\ \mu\text{L}}{1\ \text{mL}} = 29\ \mu\text{L}.$$

Concentration of IS

$$= \frac{\frac{0.0304\ \text{g}}{76.09\ \frac{\text{g}}{\text{mol}}} \times 0.9353}{(972+29\ \mu\text{L}) \times \frac{1\ \text{mL}}{1000\ \mu\text{L}} \times \frac{1\ \text{L}}{1000\ \text{mL}}} = 373.35\ \frac{\text{mmol}}{\text{L}}$$

A stock solution containing glycerol, MTBG, DTBG, and TTBG was prepared in a 5 mL volumetric flask, using 1,4-dioxane as solvent, as shown in Table D-3.

Table D-3 Stock solution for the preparation of calibration curves.

Analyte	Weight, g	Moles, mmol	Concentration, mmol/L
Glycerol	0.0040	0.0428	8.56
MTBG	0.0050	0.0335	6.69
DTBG	0.0080	0.0286	5.72
TTBG	0.0040	0.0135	2.70

Sample calculation:

Concentration of glycerol

$$= \frac{\frac{0.0040\ \text{g}}{92.09\ \text{g/mol}} \times 0.9857 \times \frac{1000\ \text{mmol}}{1\ \text{mol}}}{5\ \text{mL} \times \frac{1\ \text{L}}{1000\ \text{mL}}} = 8.56\ \text{mmol/L}$$

Standard solutions were prepared from the stock solution and the internal standard solution in 1 mL glass vials as shown in Table D-4.

Table D-4 Preparation of the stock solutions with the internal standard and derivatizing agents.

Standard Solution	Volume, µL			
	Stock	**IS**	**MSTFA**	**TOTAL**
Standard solution 1	10	10	10	30
Standard solution 2	50	10	10	70
Standard solution 3	100	10	10	120

The standard solutions were rigorously mixed using a vortex mixer at 3000 rpm for 10 s. The solutions were left in a fume hood for 30 min at ambient condition for a complete derivatization reaction. 800 µL heptane was added to each standard solution. In order to get a more dilute sample without using a large quantity of solvent, a serial dilution technique was adopted. All standard solutions were further diluted 1000 folds using heptane. The final concentration is shown in Table D-5.

Table D-5 Final concentration of the standard solutions.

Standard Solution	Analyte concentration, nmol/L					
	Glycerol	**MTBG**	**DTBG**	**TTBG**	**IS**	**MSTFA**
Standard solution 1	103	81	69	33	4498	65000
Standard solution 2	492	384	328	155	4291	62000
Standard solution 3	931	727	621	293	4058	59000

Sample calculation:

For Standard solution 1, concentration of glycerol

$$= \left(\frac{10}{30+800}\right)\left(\frac{1}{1000}\right) 8.56\ \frac{\text{mmol}}{\text{L}} = 1.031 \times 10^{-4}\ \frac{\text{mmol}}{\text{L}} \times 10^{6}\ \frac{\text{nmol}}{\text{mmol}} = 103\ \frac{\text{nmol}}{\text{L}}$$

The standard solutions were then analyzed with a GC-MS using internal standard quantitative analysis technique to generate the calibration curves.

Samples were withdrawn from the reactor during the reaction at the interval of 3, 5, 8, 12 and 22 h. Approximately, a volume of ~300 μL of sample was withdrawn in every sampling. Samples were centrifuged at 12000 rpm for 10 min to separate the catalyst. 10 μL of the clear supernatant was carefully transferred into a 5 mL volumetric flask. The flask was then filled with 1,4-dioxane to dilute the sample. The samples were then derivatized by mixing 50 μL of the diluted samples with 10 μL of each IS solution and MSTFA. Further derivatization steps were similar to the procedures described previously.

Overall sample dilution factor can be calculated as follows:

Sample dilution with 1,4-dioxane, DF_a

$$= \frac{\text{Total volume}}{\text{Sample volume}} = \frac{5000\ \mu L}{10\ \mu L} = 500$$

Sample dilution with derivatization solutions, DF_b

$$= \frac{70+800}{50} = 17.4$$

Sample dilution with heptane, DF_l

$$= \frac{1000}{1} = 1000$$

Overall sample dilution factor, $DF = DF_a \times DF_b \times DF_l = 500 \times 17.4 \times 1000 = 8{,}700{,}000$

Actual concentration of samples = DF x GC-MS quantitative analysis.